UCRL-19446
c.2

CHARGE ASYMMETRY IN THE MUONIC DECAY OF THE K_2^0

Michael Anthony Paciotti
(Ph.D. Thesis)

December 1969

AEC Contract No. W-7405-eng-48

LAWRENCE RADIATION LABORATORY
UNIVERSITY of CALIFORNIA BERKELEY

UCRL-19446

DISCLAIMER

CHARGE ASYMMETRY IN THE MUONIC DECAY OF THE K_2^o

Contents

CHARGE ASYMMETRY IN THE MUONIC DECAY OF THE K_2^0

Michael Anthony Paciotti

Lawrence Radiation Laboratory
University of California
Berkeley, California

December 1969

ABSTRACT

The charge asymmetry $R \equiv \frac{\Gamma(K_L^0 \to \pi^- \mu^+ \nu_\mu)}{\Gamma(K_L^0 \to \pi^+ \mu^- \bar{\nu}_\mu)}$ is measured to be $1.0098 \pm .0032$.

Separation of muons from pions is achieved by passage through 230 grams/cm^2 of aluminum and 870 grams/cm^2 of lead. Positive and negative muons are spatially separated behind the pion filter by application of a magnetic field preceeding the aluminum and lead absorber.

Data is taken with scintillation counters, and optical thin-plate and thick-plate spark chambers are used for calibration of systematic effects.

I. INTRODUCTION

In 1954 Gell-Mann and Pais[1] proposed a model of the K^o, $\bar{K}^o$ complex in which the particle K_2^o was an equal mixture of K^o and $\bar{K}^o$. It was ten years later, when Christenson, Cronin, Fitch, and Turlay[2] found that this same K_2^o meson decayed into $\pi^+\pi^-$, before there was reason to believe that K_2^o might not be strictly $K^o + \bar{K}^o$ (or $K^o - \bar{K}^o$). At that time one might have given even odds as to whether the apparent CP violation was due to an effect in the decaying process or due to K_2^o itself being a mixture of CP odd and even states.

The discussions will remain within the comprehensive phenomenology written down by several authors[3,4,5,6,7]. In this framework the parameter ε is the amount of the old K_1 of Gell-Mann and Pais mixed in with the old K_2 to make up the K_L^o we see in nature. In the summer of 1967, when this project was proposed at Stanford Linear Accelerator Center (SLAC), an upper limit for $\mathrm{Re}\,\varepsilon$[8] based on existing experimental data was smaller than the measured limits on $\mathrm{Re}\,\varepsilon$[9]. This paper concerns measurement of the real part of ε. More precisely, we determine the charge ratio

$$R \equiv \frac{\Gamma(K_2^o \to \pi^- \mu^+ \nu)}{\Gamma(K_2^o \to \pi^+ \mu^- \bar{\nu})} \quad .$$

The connection of R with T non-invariance (assuming CPT symmetry) was indicated even before parity violation was found[10].

The experiment is basically a counter experiment with spark chambers used to make checks and study effects. The technique is to separate the muonic mode from the others with a thick lead wall that filters out pions, electrons, and γ-rays while allowing passage of muons. The sign of the muon is found with a large magnet that separates spatially the positive muons from negative muons.

II. PHENOMENOLOGY

A. Relation of Charge Asymmetry to the K^o, $\bar{K}^o$ Composition of K_L^o

The relationship between the charge asymmetry measured in this experiment and the composition of K_L^o into K^o and $\bar{K}^o$ which was first pointed out by Lee, Oehme, and Yang in 1957 [10] will be developed.

The discussion assumes the validity of CPT symmetry. In doing so, the number of equations is considerably reduced, and as long as the CP data is consistent with the theory with CPT valid nothing essential is lost.

The Gell-Mann and Pais model builds the K^o and $\bar{K}^o$ out of states with definite CP numbers. The states are

$$|K_1\rangle = \frac{1}{\sqrt{2}}(|K^o\rangle + |\bar{K}^o\rangle) \quad \text{and}$$

$$|K_2\rangle = \frac{1}{\sqrt{2}}(|K^o\rangle - |\bar{K}^o\rangle)$$

with the convention that CPT $|K^o\rangle = +|\bar{K}^o\rangle$. Then

$$|K^o\rangle = \frac{1}{\sqrt{2}}(|K_1\rangle + |K_2\rangle) \quad \text{and}$$

$$|\bar{K}^o\rangle = \frac{1}{\sqrt{2}}(|K_1\rangle - |K_2\rangle) \quad .$$

As written the $|K_1\rangle$ has even CP for a spin zero Kaon and is therefore associated with the decays $\pi^+\pi^-$ and $\pi^o\pi^o$.

The $|K_2\rangle$ state is then predicted to have CP odd with decay modes such as $3\pi^o$. The $3\pi^o$ system is required to have an even spatial wave function under interchange of any two π^o's due to bose statistics. Hence the relative orbital angular momentum between two π^o's contains only even components and the total space parity is even ($SPIN_K = 0$). The overall parity is odd because of the intrinsic parity of the pions. The C operation on π^o's is even, and hence CP $\psi(3\pi^o) = -\psi(3\pi^o)$.

A basis for the apparent CP violation discovered in 1964 is that the state $|K_L^o\rangle$ seen in nature decays readily into a strictly odd CP $3\pi^o$

state and also decays into a strictly CP even $\pi\pi$ state. Perhaps the $|K_L^o>$ state in nature is not exactly $|K_2>$ as proposed by Gell-Mann and Pais but some combination

$$|K_L^o> = \frac{|K_2> + \epsilon|K_1>}{\sqrt{1 + |\epsilon|^2}} \quad \text{where } \epsilon \text{ is small.}$$

Maybe the $|K_2>$ actually decays to $\pi^+\pi^-$ and thereby violates CP symmetry; or perhaps both situations occur. The first possibility is investigated here.

Substituting for $|K_1>$ and $|K_2>$, $|K_L^o> = \frac{(1+\epsilon)|K^o> - (1-\epsilon)|\bar{K}^o>}{\sqrt{2(1+|\epsilon|^2)}}$

Let A = Amplitude $(K^o \to \pi^- \mu^+ \nu_\mu)$. CPT symmetry has already been assumed, and if the $\pi^-\mu^+$ electromagnetic interaction is neglected, A^* = Amplitude $(\bar{K}^o \to \pi^+ \mu^- \bar{\nu}_\mu)$.

For now assume that the $\Delta S = -\Delta Q$ amplitudes

Amplitude $(\bar{K}^o \to \pi^- \mu^+ \nu_\mu)$ and

Amplitude $(K^o \to \pi^+ \mu^- \bar{\nu}_\mu)$ are zero.

The empirical $\Delta S = \Delta Q$ selection rule says that in leptonic strangeness non-conserving decays of hadrons the change in strangeness of the hadronic part is equal to the change in charge of the hadronic part (maybe vacuum in final state).

$$R \equiv \frac{\Gamma(K_L^o \to \pi^- \mu^+ \nu_\mu)}{\Gamma(K_L^o \to \pi^+ \mu^- \bar{\nu}_\mu)}$$

$$R = \frac{\int_{\text{average Dalitz area detected in experiment}} |(1+\epsilon)A|^2}{\int |(1-\epsilon)A^*|^2} = \left|\frac{1+\epsilon}{1-\epsilon}\right|^2 \cong 1+4\,\mathrm{Re}\epsilon$$

In the approximations made the asymmetry R is the same in all regions of the Dalitz plot. The real part of the parameter ϵ is measured in this experiment. The possibility of non-zero $\Delta S = -\Delta Q$ amplitudes can be

included in the derivation of Reε from R. Let

$$\text{Amplitude } (K^0 \to \pi^- \mu^+ \nu_\mu) = F \quad \Delta S = \Delta Q$$

$$\text{Amplitude } (\bar{K}^0 \to \pi^+ \mu^- \bar{\nu}_\mu) = \bar{F} \quad \Delta S = \Delta Q$$

$$\text{Amplitude } (K^0 \to \pi^+ \mu^- \bar{\nu}_\mu) = G \quad \Delta S = -\Delta Q$$

$$\text{Amplitude } (\bar{K}^0 \to \pi^- \mu^+ \nu_\mu) = \bar{G} \quad \Delta S = -\Delta Q$$

F is the complete amplitude for a kinematic arrangement of $\pi\mu\nu$. It contains the strangeness changing vector current between K and π which has the form

$$f_+(q^2)\ (P_\lambda + Q_\lambda) + f_-(q^2)\ (Q_\lambda - P_\lambda)\ .$$

P_λ is the π momentum, Q_λ is the K momentum, and $q^2 = (Q_\lambda - P_\lambda)^2$ is the momentum transfer. The amplitude G contains the form factors

$$g_+(q^2)\ (P_\lambda + Q_\lambda) + g_-(q^2)\ (Q_\lambda - P_\lambda)\ .$$

CPT is assumed so that $\bar{F} = -F^*$ and $\bar{G} = -G^*$.

The following definitions are usually made:

$$X_+(q^2) = -g_+^*(q^2)/f_+(q^2)$$

$$X_-(q^2) = -g_-^*(q^2)/f_-(q^2)$$

For K_{e3} decays where the minus form factor contributes very little to the decay rate,

$$R \cong 1 + 4\ \mathrm{Re}\epsilon\ \frac{(1-|X_+(q^2)|^2)}{|1-X_+(q^2)|^2}$$

It is the charge ratio for any particular point on the Dalitz plot. The same formula results for $K_{\mu 3}$ if $X_+(q^2) = X_-(q^2)$. The factor multiplying Reε in the above equation is measured in K_{e3} decays by Bennett, Nygren, Saal, Sunderland, and Steinberger[11] to be $.96 \pm .05$. The result can be thought of as an average over the Dalitz plot or simply the answer for constant form factors. The apparatus for the $K_{\mu 3}$ experiment has equal detection efficiency over the whole surface of the Dalitz plot. Also the variation in the factor $\dfrac{(1-|X_+(q^2)|^2)}{|1-X_+(q^2)|^2}$ due to the introduction of

$X_-(q^2)$ for $K_{\mu 3}$ decays can only be small. The measured value of .96 ± .05 for the factor is included in the determination of Ree from the value of the charge asymmetry R found in this experiment.

B. Bearing of Experiment on Theories Outside the Usual Phenomenology

This experiment together with the K_{e3} asymmetry experiments done at Brookhaven have bearing on two possible explanations of the apparent CP violating effects. Neither of the theories require CP violation, and both have the characteristic that the charge asymmetry can depend on the original fraction of K^o's and $\bar{K}^o$'s produced at the target. They are

1) the introduction of additional neutral K mesons in an effort to fit experimental data as mentioned in the literature in 1965[12,13] and recently re-asserted by Lipkin[14] and

2) the suggestion by Lalović[15] that there might be troubles with the quantum mechanics used in the usual formalism. To date the SLAC experiment is the only one completed or in progress in which a large fraction of $\bar{K}^o$'s is produced.

Figure 1 gives the relative yields of K^+ and K^- as a function of momentum at 3° from a 18 GeV/c electron beam[16]. K^+/K^- varies from about 1.5 at 2.0 BeV/c to about 2.5 at 10.0 BeV/c.

No one single mechanism is responsible for Kaon production[17]. The Drell mechanism, pictured below, predicts that the K^+/K^- ratio is about 1.3[18]; the $K^o/\bar{K}^o$ production ratio is similar since it depends only on the relative cross sections of $\bar{K}^o$ and K^o on beryllium. The Drell mechanism does not dominate production, but when it does contribute it produces $\bar{K}^o$'s in quantity comparable to K^o.

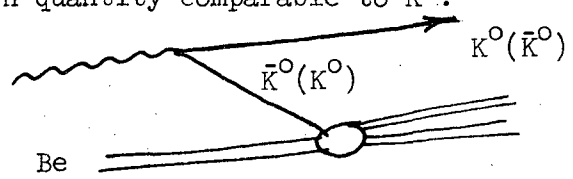

Fig. 1

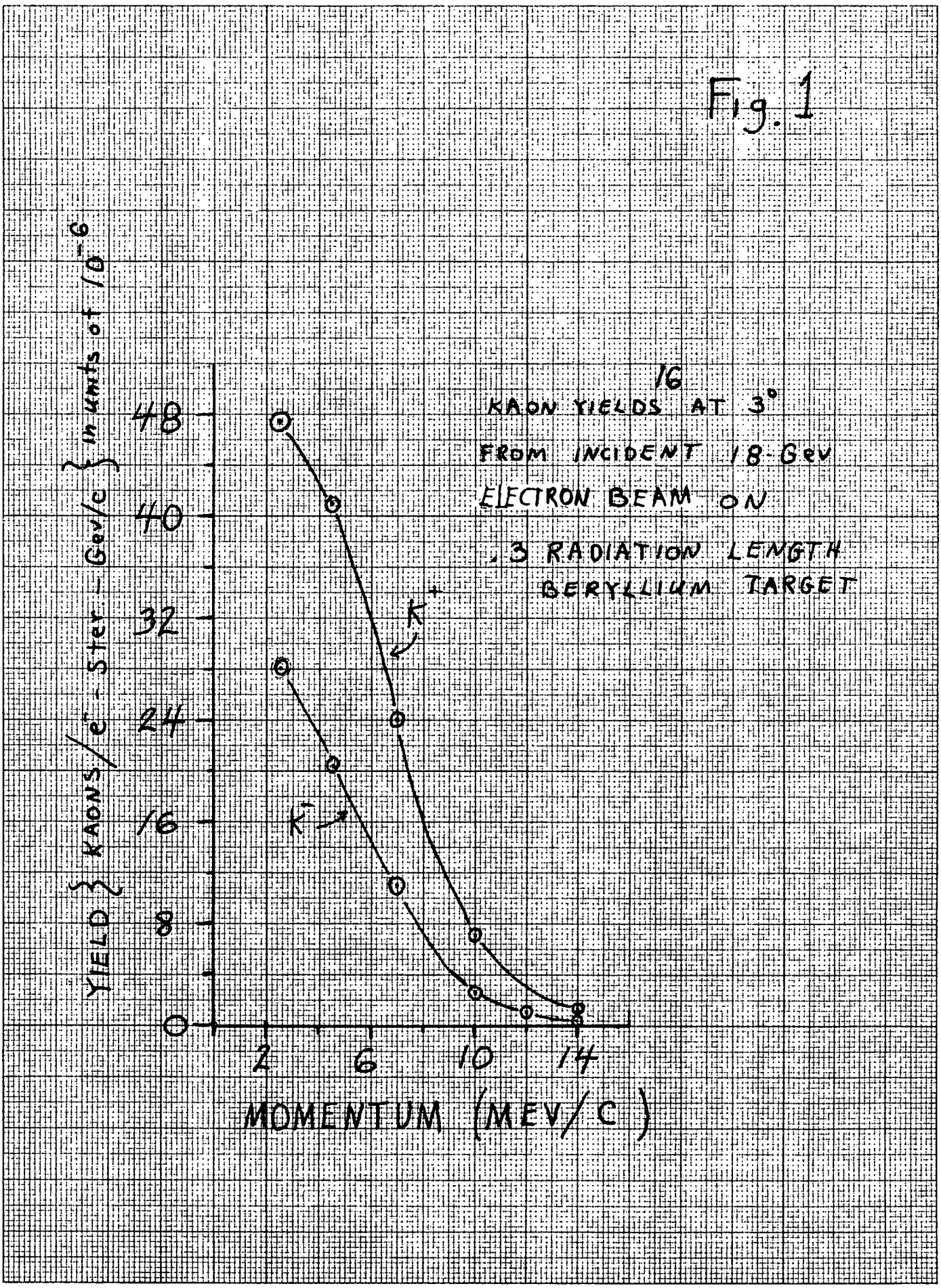

Production of ϕ's[19] and their subsequent decay to Kaons implies that K^+/K^- and $K^o/\bar{K}^o$ equal 1.45. K^* production is another possible mechanism with decay to Kaons. K^*'s should be produced in much the same ways as K's with similar ratios for $K^*/\bar{K}^*$. Kaon production by the pions in the target which are associated with the Drell mechanism could well be a big contributor to the total K flux. Roughly speaking, production from pions would give $K^+/K^- \approx 2$ and $K^o/\bar{K}^o \approx 2$[20].

The associated production two-body reactions imply that only K^+ and K^o would be produced.

$$\gamma + n \rightarrow K^+ + \Sigma^-$$

$$\gamma + p \rightarrow K^+ + \Lambda^o \ (\Sigma^o)$$

$$\gamma + p \rightarrow K^o + \Sigma^+$$

$$\gamma + n \rightarrow K^o + \Lambda^o \ (\Sigma^o)$$

$$\gamma + N \rightarrow K^* + Y$$

$$\hookrightarrow K$$

However the fact that there is a large number of K^- in the SLAC beam means that these above reactions certainly do not dominate the production but could contribute to the large K^+/K^- ratios at higher momentum.

Associated production processes dominate Kaon production in the proton accelerators. Therefore K_L^o's in the Brookhaven neutral beam originate primarily with K^o and not $\bar{K}^o$. One can compare the SLAC result for K_2^o charge asymmetry with the results from Brookhaven.

III. EXPERIMENTAL TECHNIQUE

A. Method

The charge asymmetry data are taken with scintillation counters. Spark chambers are used only for checks and calibrations of systematic effects in the experiment. Figures 2 and 3 display the apparatus. A neutral beam of K_L^o's and neutrons 6-inches high and 9 inches wide enters the apparatus at a distance of about 230 feet from a Be target. A decay volume is defined by an anti-counter at the upstream end and a bank of counters called "S-counters" at the downstream end. The anti-counter is a 20" x 20" counter and shields the decay volume from charged particles, most of which come from K decays in the 20 foot free flight path from the last sweeping magnet.

The S-bank presents an area of 20 inches horizontally and 16 inches vertically to the K_L beam; there are 8 counters each 2 inches high. At least 2 out of the 8 counters are required as part of an event trigger. So the coincidence (2S) $\bar{A}$, i.e. $(S_i\ S_j)\ \bar{A}$, represents a charged K_L^o decay. The detection efficiency for decays in the volume, except for the muon range cut-off imposed by the pion filter, is almost entirely determined by the acceptance of the S bank. For $K_{\mu 3}$ decays where the muon has momentum greater than 1.6 BeV/c the probability for the muon and pion to fire separate S counters is about 50%. Decays are missed due to both particles hitting the same S counter or to one of the particles (usually the pion) missing the S-bank entirely.

From the S-bank on the pion from $K_L \to \pi\mu\nu$ events is disregarded; the lead wall is intended to remove them while allowing the muons to pass. The sign of the muon is determined in the following manner: Located 2 feet after the S-bank is the "ATLAS" H magnet whose gap is 16.5 inch. The field is horizontal, deflecting particles up and down. The field

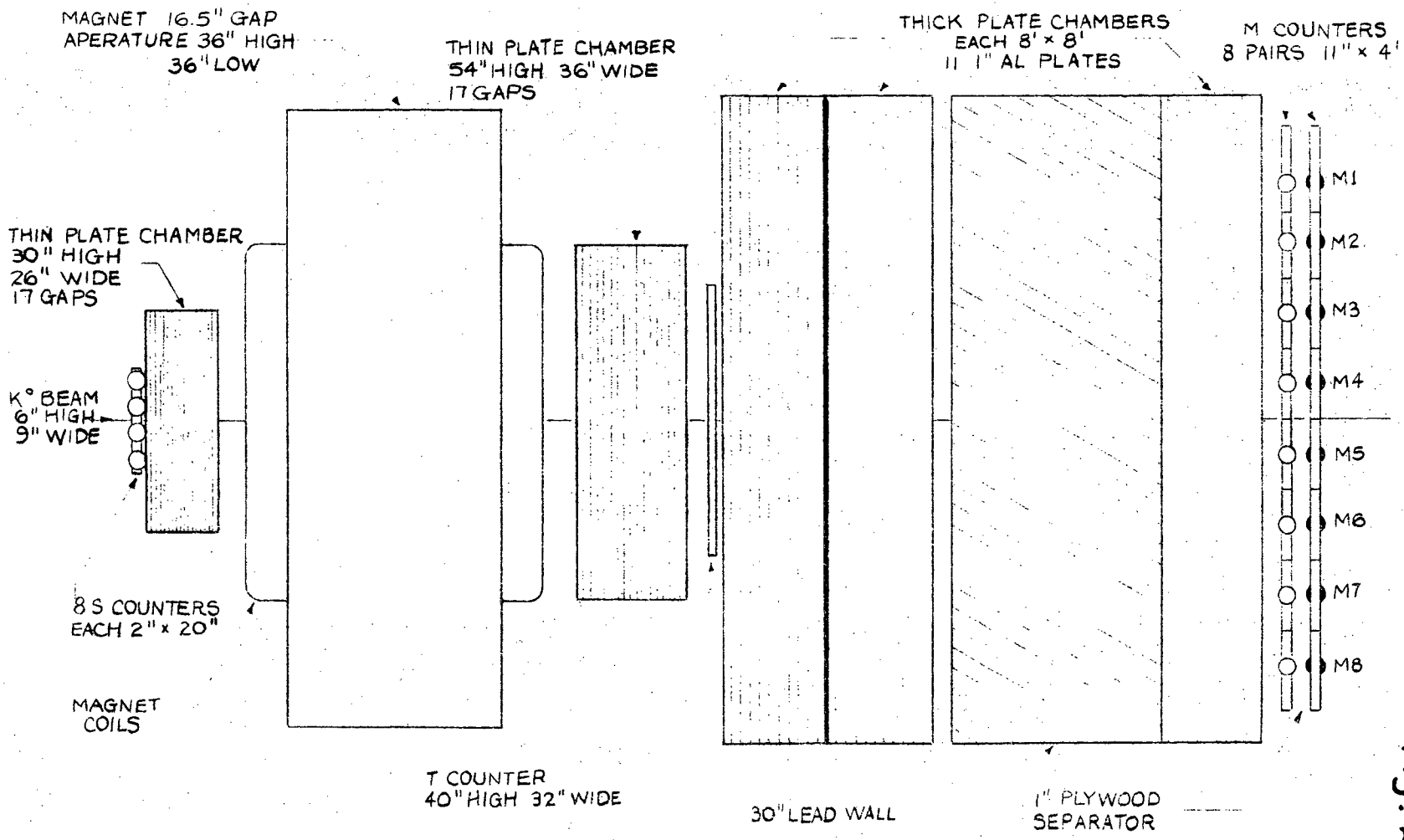

Fig. 2

FRONT VIEW K° ASYMMETRY EXPERIMENT

Fig. 3

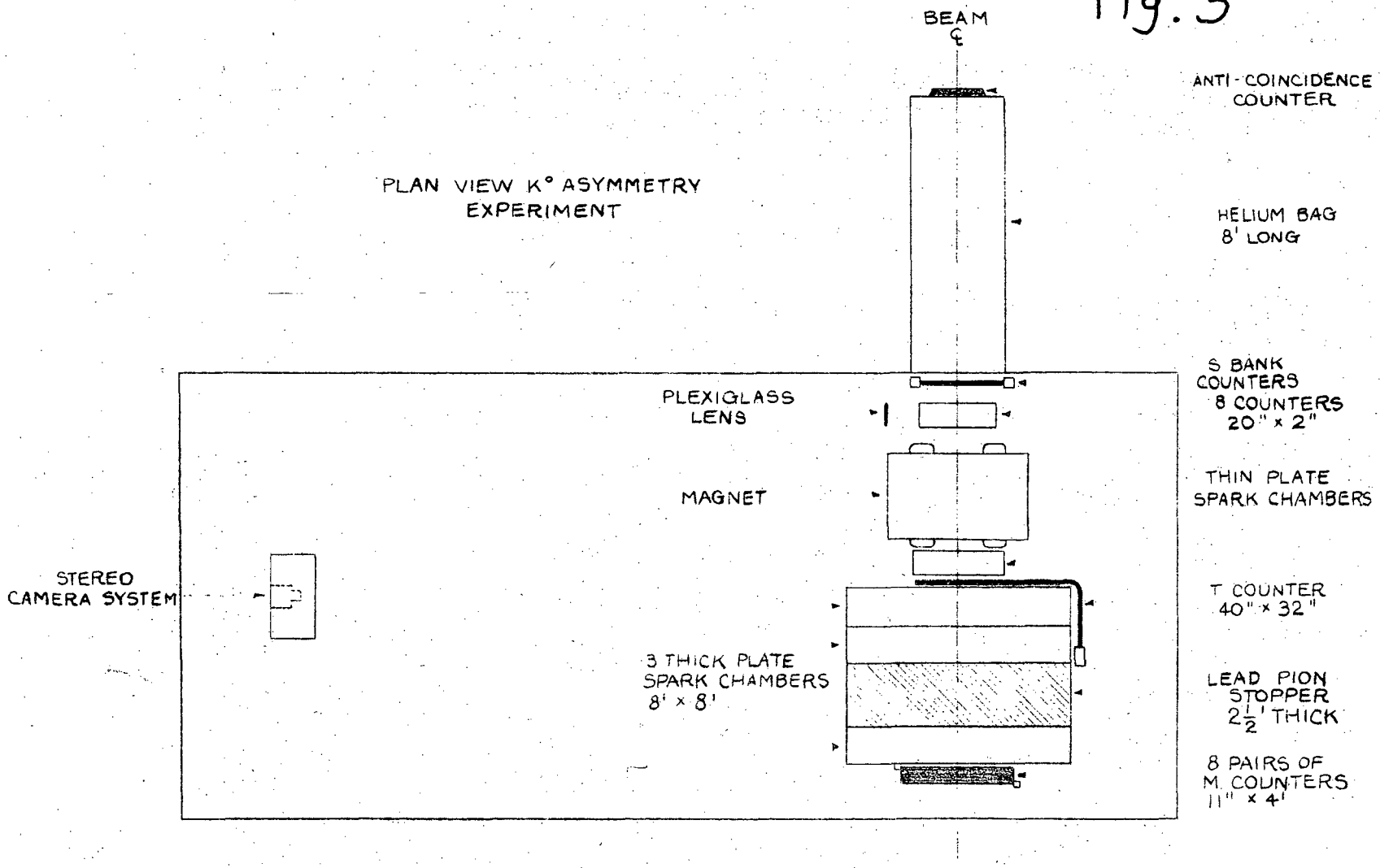
BEAM
℄
ANTI-COINCIDENCE COUNTER
PLAN VIEW K° ASYMMETRY EXPERIMENT
HELIUM BAG 8' LONG
S BANK COUNTERS 8 COUNTERS 20" x 2"
PLEXIGLASS LENS
MAGNET
THIN PLATE SPARK CHAMBERS
STEREO CAMERA SYSTEM
T COUNTER 40" x 32"
3 THICK PLATE SPARK CHAMBERS 8' x 8'
LEAD PION STOPPER 2½' THICK
8 PAIRS OF M. COUNTERS 11" x 4'

integral is sufficient to produce a deflection which is greater than that due to the maximum transverse momentum of the muon in the K decay itself. Positive and negative muons from $K_L^o \rightarrow \pi\mu\nu$ are angularly separated by the magnet. Spatial separation occurs at a point 10 feet behind the middle of the magnet; depending on field direction muons above the beam centerline are counted as positive (negative) and those below the centerline are counted as negative (positive).

The hodoscope which detects the muons and thereby establishes a sign for each event exposes an area of 4 feet by 7.3 feet to the incident muons. The magnet disperses the muons in the long dimension which is broken up into 8 counter bins each 11-inches high. The counters are called M's. M1 through M4 catch all the muons above the beam centerline and M5 through M8 catch all the ones below the centerline. The region between the magnet and the M bank contains pion absorbing material. The bulk of the absorber is a 30-inch lead wall; the remainder is composed of 3 aluminum spark chambers each having 11 one inch plates for a total thickness of 33-inches of aluminum.

B. Beam

The experiment was carried out at "END STATION B" at SLAC. Figure 4 shows the targeting arrangement, the shielding and sweeping magnets within the end station, and the experimental apparatus located just outside the building.

A primary 15 BeV/c electron beam is directed onto a cylindrical beryllium target 1 foot long and 1-1/2 inches in diameter. The beam continues on into a 20 KW water-cooled beam dump. The target is observed at an angle of 3^o from the primary beam, and this secondary beam passes through a 3 inch square channel through the 12 foot steel wall that

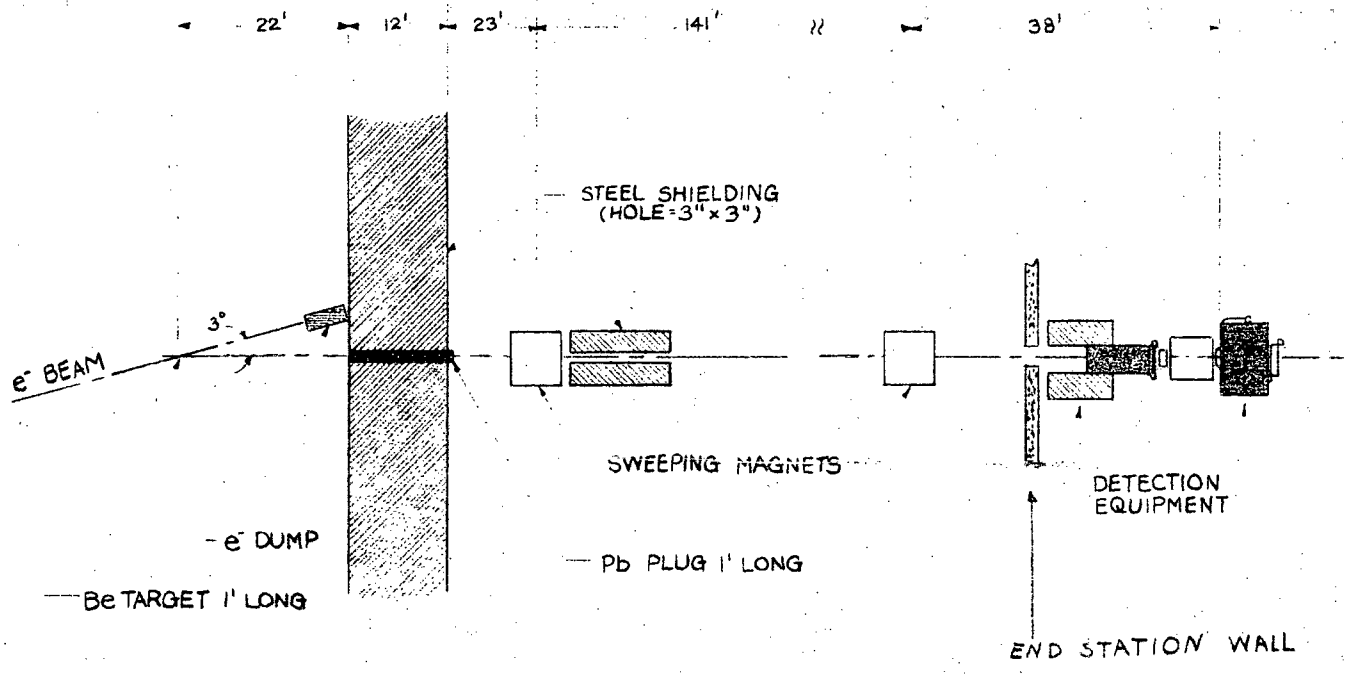

K° BEAM LAYOUT

Fig. 4

separates the beam dump area from the end station. This wall contains most of the radiation produced in the dump. The range of 15 BeV muons is about 33 feet of steel, and at least this much steel was placed behind the dump area in the direction of the apparatus. This dumping arrangement is sufficiently clean that no increase is observed in any singles counting rates above the cosmic ray level with the target out of the beam and 20 KW of beam power into the dump.

Two sweeping magnets are located inside the end station; they are 18" x 72" x 6" gap magnets run at 20 kilogauss. The first one follows a lead converter 12" thick which caps the end of the beam hole into the end station. The electrons from the converted gamma rays as well as the other charged products in the secondary beam are swept into steel muon shielding.

The second sweeping magnet sweeps out charged decay products from neutral K-decays in the 140 foot distance from the first magnet. At this point the size of the neutral beam is defined, vertically by the 6" pole tips and horizontally by lead blocks in the gap with a 9-inch separation.

The primary electron beam time average current for data runs was normally 1.5μa when the accelerator was delivering all of its 360 pulses per second into our channel. This rate corresponds to a little over 20 KW of beam power.

C. Equipment

1. Counters

There are a total of 26 scintillation counters in the experiment. The anti-counter is a 20-inch by 20-inch by 1/4 inch thick piece of pilot B scintillating material with a twisted light pipe. It uses a 5-inch diameter photomultiplier. The anti was 110 inches from the S-counter bank. This 110 inch decay region was filled with a He bag whose width

and height are very much greater than the lateral dimensions of the neutral beam.

The 8 S-counters are each 2-inch by 20-inch pilot B scintillator 1/4 inch thick with 56 AVP photo tubes. No change in gain of the tubes was detected when the field was reversed; however two studies are made to determine that the sign of the muon is almost entirely uncorrelated with the efficiency of any S-counter. One is experimental and the other uses the Monte Carlo; these checks are in Section IV-B.

Another counter (called "T") was inserted to reduce the accidental event rate. It is located behind the exit aperture of the Atlas magnet. Data was taken at three field integrals, 392 kilogauss-inches, 468 kilogauss-inches, and 540 kilogauss-inches. The data will be labeled by its field integral. The higher the field the larger the T counter must be in the vertical direction in which the magnet is dispersing the various momentum muons. So for 392 and 468 Kg-in. runs a T counter 30 inches in the vertical direction by 32 inches wide was used. It is 1/2 inch PILOT B scintillator with eight 56 AVP tubes, 4 on the top and 4 on the bottom. The pulses were added before the "T" discriminator. At 540 Kg-in. where half of the data was taken a larger T counter was used. It's vertical height is 40 inches, and the extra height insured that at the higher field nearly all of the muons would be intercepted by T.

The insertion of the T counter into the circuit reduces the accidental rate by about a factor of 3 and was essential to maintain a reasonable data taking rate. The predominant accidental triggers are due to a real K^{o} decay which fires the 2ST coincidence in time with an M count due to a neutron or K^{o} induced secondary which penetrates the lead. The point is that the real 2S rate is three times the real 2ST rate.

The M counter bank is a hodoscope of 8 double counters. For example

a count in M1 is really a coincidence between M1A and M1B. The two members of an M pair are separated by the 1-inch plywood board on which they are mounted. This arrangement was necessary because (2ST) (M accidental) rate is proportional to the singles counting rate in the M bank. That singles rate is substantially reduced by requiring a double in each M. Multitudes of soft γ-rays can fire a single counter but not a double separated by an inch of wood. The 16 individual counters in the M bank are 11" wide, 48' long and 1/2 " thick PILOT B scintillating material with a 56 AVP on one end. In the pair setup the tubes were placed on opposite ends so that the broader coincidence of the two tubes more accurately reflects an average time for the muon. The very tight coincidence obtained by tubes on the same end of the scintillator did not reduce accidentals any more than the opposite end arrangement and was more difficult to time with the (2ST) signals.

Each of the M-counters was checked with a pulse height analyser to see that the tail of the spectrum for muons was well above the discriminator threshold and that the position of the peak did not change with field. It was concluded that the efficiency for straight through muons was virtually 100%.

2. Spark Chambers

The chambers are pictured in Figs. 2 and 3. The chambers before and after the magnet are thin-plate construction. The one near the S-bank is 30 inches high, 26 inches wide, and 11 inches thick. The one behind the magnet is larger to catch particles diverging from the decay point; it is 54 inches high, 36 inches wide, and also 11 inches thick. Except for the lateral dimensions these thin plates have the same construction. They each have 17 gaps which are 3/8-inch. The plates are constructed by gluing and vacuum pressing 2 mil hard aluminum onto prepared polyurethane foam 1/4-inch thick. The result is 1.5 grams/ cm^2 in the beam line for each

chamber. The front chamber could easily hold 5 and 6 tracks. This characteristic is necessary to be able to see a K^o or n interaction in the S counter bank in the presence of other tracks from a K decay.

The 3 thick plate chambers, all of the optics in this experiment, and the camera system was used in an earlier experiment[21]. The large chambers have an active area 91" x 91". They are each built out of 11 one inch aluminum plates. All of the chambers are viewed through their front face by a 30^o stereo camera system.

3. Electronics

The event trigger is (2S) ($\bar{A}$) (T) (M). In addition to forming "event" signals, the circuitry also recorded various accidental event signals in each of the M-channels. When the spark chambers were running the system set a latch for each counter that fired; the latch was then used to turn on the counter light visible in the picture.

The schematic diagram is shown in Fig. 5. Every counter enters through a LeCroy 121 Discriminator. The output widths of the S-counter discriminators are set at 7 ns, and all 8 signals are then fed into an 8-channel mixer. A 2S coincidence is then detected by a variable threshold discriminator set to go on double pulse height. The anti-counter signal is also put into the 2S discriminator; it is 35 ns wide and covers the very narrow 2S coincidence.

As discussed earlier, the function of the T-counter is to reduce accidental triggers. But it is important that the T requirement does not offer restriction for real events. The T is a large counter, and its input into the (2S) (T) coincidence is set accordingly at a liberal 12 ns. The (2S) (T) output pulse is fanned out to each of the M coincidence circuits and is 10 ns wide. The M coincidence must be broad because tubes are on opposite ends of an M pair. (2S) (T), M_iA, and M_iB go into a

Fig. 5

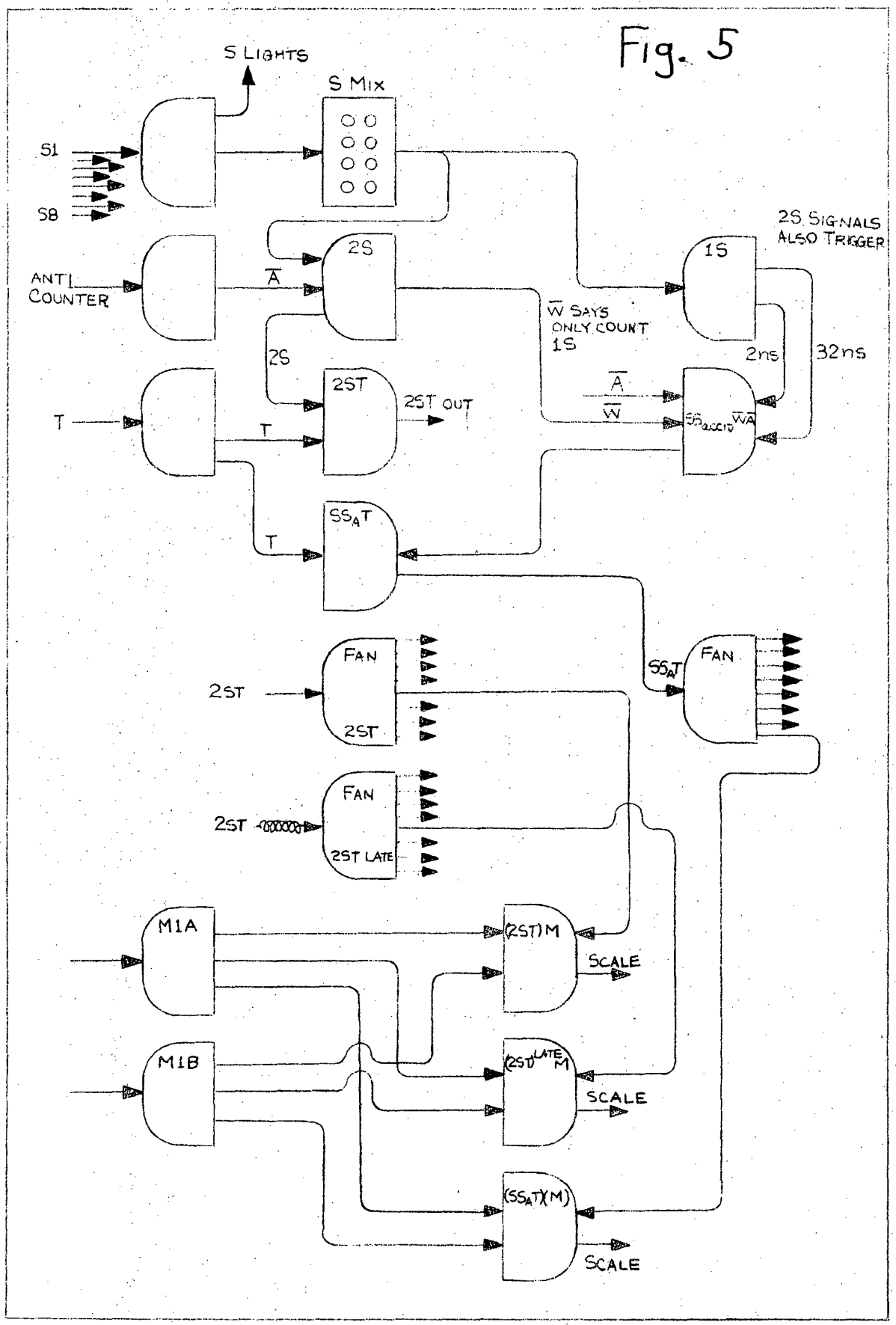
S LIGHTS
S MIX
S1
S8
ANTI COUNTER
$\overline{A}$
2S
1S
2S SIGNALS ALSO TRIGGER
$\overline{W}$ SAYS ONLY COUNT 1S
2ns
32ns
T
2ST
2ST OUT
$\overline{A}$
$\overline{W}$
$SS_A\overline{WA}$
SS_AT
FAN
2ST
2ST LATE
M1A
M1B
(2ST)M
(2ST)^{LATE}M
SCALE
$(SS_AT)(M)$

LeCroy 122 coincidence unit, and the overall width of this 4 fold coincidence is about 22 ns. A very tight $M_i A$, $M_i B$ coincidence could be made with the tubes on the same end, but a large jitter is present with respect to the (2S) (T) pulse, and nothing is gained by a tighter $M_i A$, $M_i B$ coincidence.

The 2 dominant sources of accidentals were monitored. "Events" induced by accidental coincidences of charged K_L^o decays in the front of the apparatus with unrelated particles in the M-counters comprise about 15% of the event triggers at the beam rate used. This in fact was the limit on the beam power used. The random M-triggers are caused by the absorber allowing products from neutrons and K's to penetrate. A delayed (2S) (T) signal was fanned out to eight 122 units wired identically to the real M-coincidence units. These accidentals were scaled concurrently with data throughout the entire experiment.

A second kind of accidental was monitored by the scheme pictured in the diagram. It arises by accidental coincidence of a muon from $K_{\mu 3}$ traversing the entire apparatus with a charged track from a separate decay firing another S-counter. About 55% of the $K_{\mu 3}$ events with a sufficiently energetic muon to pass through the lead fail to register as events because the pion either hits the same S-counter as the muon or misses the S-bank entirely; this group of muons comprises the candidates for (S) ($S_{accidental}$) (T) (M) triggers. Single S-counts from the S-mixer are fed from a discriminator into a 122 unit by two cables. The non-delayed one has the same timing as a normal 2S signal, and because (2S) ($S_{accidental}$) is unwanted, an anti cable called $\bar{W}$ eliminates (2S) counts. The rest of the system is similar to the circuitry for real events, giving (S) (S_A) (T) (M) accidentals for each of the 8 M-channels. It should be noted the time resolutions of the accidental channels were carefully checked to match the "real" channels.

IV. DATA

The complete data are given in Table I. The "up" runs are shown separately from the "down" runs. During the experiment the magnetic field was reversed every 6 or 8 thousand events. With this procedure any geometric or detection differences between the down and up halves of the apparatus cancel out in the asymmetry when the average of the up and the down run is made. The only effects not cancelled out are counter efficiency changes with field or real behaviorial differences between μ^+ and μ^- or π^+ and π^-.

The ratio of μ^+/μ^- for the raw triggers is

$$\frac{\mu^+}{\mu^-} = \frac{\text{Up}(M1 \to M4) + \text{Down}(M5 \to M6)}{\text{Up}(M5 \to M6) + \text{Down}(M1 \to M4)}$$

$$= 1.0089 \pm .0021$$

The corresponding asymmetry in the (2ST) (M accidental) data is $1.004 \pm .0066$ and in the (STM) (S accidental) data it is $1.001 \pm .014$.

The individual M counter asymmetries after accidental subtraction are found by normalizing the Up and Down runs to the same number of total events. For the Up runs, M1 through M4 contain μ^+, and M5 through M8 contain μ^-. For Down runs M1 through M4 contain μ^-, and M5 through M8 contain μ^+. The individual M counter asymmetries along with the accidental asymmetries in each M are given in Table II. Correction for measured wrong decisions, the only effect whose counter dependence is known, is also shown. Again, these numbers depend on the reversing of the magnetic field so that μ^+ and μ^- are counted in each counter under idential conditions. Geometric solid angle or detection efficiency of each counter cancels out in the asymmetry. And again, field dependent efficiencies or different behavior for μ^+ and μ^- or π^+ and π^- do not cancel out, and a large difference would be evident in the deviation of any counter from the average asymmetry after accidental

Table I

Atlas bends μ^+ up

	Raw M Counts	(2ST) with $M_{Accidental}$	STM with $S_{Accidental}$	Accidentals Subtracted	
M1	22718	7236	982	14500	μ^+
M2	45122	2190	791	42141	
M3	80642	4888	1566	74188	
M4	78987	10700	2385	65902	
M5	79820	13656	2458	63706	μ^-
M6	80779	5016	1545	74218	
M7	45266	1464	666	43136	
M8	14867	857	199	13811	
Totals	448201	46007	10592	391602	

Atlas bends μ^- down

M1	22472	7369	978	14125	μ^-
M2	44710	2071	758	41881	
M3	80714	4776	1638	74300	
M4	79086	10497	2372	66217	
M5	80597	13502	2496	64599	μ^+
M6	82608	5115	1639	75854	
M7	46035	1450	646	43939	
M8	14975	807	214	13954	
Totals	451197	45587	10741	394869	

Table II.

	Asymmetry in (STM) $S_{Accidental}$	Asymmetry in (2ST) $M_{Accidental}$	Asymmetry in data after accidentals subtracted	Percentage of wrong decisions	μ^+/μ^- after correction for wrong decisions
M1	1.018 ±.045	.973 ±.017	1.0351 ± .0174	0	1.0351 ± 0.0174
M2	1.058 ±.050	1.048 ±.031	1.0146 ± .0074	0	1.0146 ± 0.0074
M3	.963 ±.035	1.014 ±.020	1.0068 ± .0056	0.6 ± 0.2	1.0069 ± 0.0056
M4	1.019 ±.029	1.010 ±.014	1.0036 ± .0065	7.8 ± 0.7	1.0041 ± 0.0070
M5	1.001 ±.028	.998 ±.012	1.0056 ± .0068	8.8 ± 0.6	1.0065 ± 0.0074
M6	1.045 ±.035	1.029 ±.020	1.0136 ± .0056	0.6 ± 0.2	1.0137 ± 0.0056
M7	.956 ±.055	1.000 ±.037	1.0102 ± .0071	0	1.0102 ± 0.0071
M8	1.060 ±.098	.950 ±.050	1.0020 ± .0129	0	1.0020 ± 0.0129

subtraction of 1.0094 ± .0026. The numbers in the last column of Table II should fluctuate around the average asymmetry, and each one alone is a measure of the charge asymmetry. Only 7 of the 8 numbers are independent since the total counts are constrained to be equal for Up and Down runs.

However, we will not do an error analysis for each of the 7 measurements. Each counter division would have to be treated in the way that the wrong decision line between M4 and M5 is handled. See Section VI-B and E. The agreement of the individual counter asymmetries indicates that momentum dependent effects do not exist to the accuracy of the individual asymmetries. For example the M counters toward the top and bottom handle much lower momentum muons on the average than the M counters nearer the center. Hence momentum dependent scattering differences between μ^+ and μ^- would show up non-uniformly over the M surface. Many more stopping muons are at the top and bottom edges so that a range difference would appear faster in the outside counters. There is some K-momentum dependence on M counter, but the correlation is not large.

V. RECONSTRUCTION OF A SAMPLE OF EVENTS

A. Measurement and Calculation of Parameters from Spark Chamber Film

A total of 1457 events recorded on spark chamber film are measured and completely reconstructed. The μ direction and position in the S, T, and last M chamber are recorded. The π direction and position in the S chamber and T chamber whenever it appeared is also recorded. Angles are measured with a mechanical protractor with respect to the vertical fiducials at the large chambers. The coordinates are taken with a graph paper template.

Measurements are recorded for both views of a 30° stereo pair. All measurements are referenced to a set of fiducials on the front of the thick plate chambers. The reconstructed coordinates are found in real space with respect to the fiducials and then transformed to a rectangular system with origin at the beam axis. The origin is fixed in the vertical direction at the height of the electron beam. The second sweeping magnet which acts as the 6" vertical collimator is accurately positioned at e^{-} beam height. The horizontal origin transverse to the beam is set on the 3° beam line, as is the horizontal collimator inside the second sweeping magnet.

Correction for optical distortion is necessary at the S-chamber. It is found that 90° angles at the S-position are mapped into 89° angles on the scan table. The scan machine itself accounts for only $.08^{\circ}$ of the 1° rotation. The $.08^{\circ}$ was constant during the entire measurement period. The rotation is most accurately made using the charge asymmetry data. The centroid of the combined μ and π S-angle distribution can be located and centered about zero degrees from the beam axis to better than 0.05°. The available horizontal reference at the S-chamber can be measured with the protractor to only $\pm.2^{\circ}$. All information agrees with the 1° rotation found from the S-data. Accordingly the vertical slopes at the S-position are all reduced by 1°. (Positive slope is defined upward moving downstream.) The

horizontal slope resolution is broader than the vertical due to the stereo angle. But the average horizontal angle is only 1.4° or half the average vertical angle and has correspondingly less contribution to transverse momentum. Centering the horizontal distribution takes a uniform reduction of $.6^{\circ}$ in horizontal angle. (Positive angles are defined to be toward camera in Fig. 3). There is no reason known why the vertical angles could be skewed. The slight offset of the S-bank (see Section VIII-A) is not visible in the S-angle distribution in the program. Horizontally the apparatus is completely symmetric.

Twenty percent of the events were remeasured to establish resolutions.

	S-chamber	T-chamber	Last M-chamber
angles (degrees)	.16	.21	.23
coordinates (inches)	.10	.08	.14

Measurement resolutions based on 300 rescanned events

B. Monte Carlo

A computer simulation of $K_{\mu 3}$ events has been made for comparison with the sample of measured decays. The coordinates of these Monte Carlo events are converted to film coordinates where the gaussian measurement errors of the previous section are introduced. The events are then analysed with the same reconstruction program as used for the measured data.

$K_{\mu 3}$ decays are generated in the center of mass using formulas found in Okun[22]. From the function $dP\ (E_{\mu})$, E_{μ}, the total muon energy, is picked. Then E_{π} is picked from the probability $dP\ (E_{\pi}, E_{\mu})$. From the energies and the K mass, the angles are calculated. Then the π, μ plane is picked uniformly from 0 to 2π around the neutrino axis. The neutrino direction in space is the radius vector to a point picked randomly over the surface of a sphere. Then the π and μ momenta are Lorentz transformed to the lab with a K momentum picked from the K^{+} shape shown in Fig. 1.

on page 6. The K momentum is weighted by the probability of decay in the 110 inch decay region 230 feet from the target.

Pions and muons are tracked in the horizontal component of the fringe field until reaching the S bank. Vertical focusing of the magnet is not considered and its effects are discussed in Section VI-C. Two separate S counters are required to fire; if not the event is terminated. Particles are tracked until the T counter is reached. Many of the π's curl in the field or hit the pole tips and are lost. Either the π or μ can trigger the T counter; 99% of the time it is the μ.

The field was mapped with a coil on a zip track and the integral recorded on an xy recorder. The curve on the median plane is fit with a polynomial, and the integral of the polynomial normalized to a long coil measurement of the field integral.

Once in the absorber the muon is stepped through in uniform steps along the beam axis. The diagonal path length is found for a step and energy is lost according to calculation from a polynomial fit to the range-energy table of Barkas and Berger [23].

The energy is gaussian straggled around the computed value with a formula in Rossi[24], page 31.

$$\sigma_E^2 = 2C\ M_e C^2\ E'm\ \frac{1-\beta^2/2}{\beta^2}\ X$$

X is the pathlength in the material.

$\beta = v/c$ is the velocity.

C is a constant depending on material.

E'm is the maximum delta ray energy for muons of momentum P.

$$E'm = \frac{(2\ M_{electron}C^2)\ (P^2C^2)}{M^2_{electron}\ C^4+M^2_{\mu}C^4+2\ M_{electron}C^2(P^2C^2+M^2_{muon}C^4)^{1/2}}$$

A multiple scattering angle from the actual direction is picked for each step from the gaussian distribution with width

$$\sigma_\theta = \frac{21}{V\,P}\sqrt{\frac{X}{X_{rad}}} \quad .$$

P is momentum in MeV/c.

V is particle velocity.

X is the pathlength.

X_{rad} is radiation length of the material.

The large angle scattering is underestimated by the gaussian distribution, but the large angles are so infrequent that their effect on the total scattering distribution for a thick absorber is minimal. See Section VI-E for complete treatment of large scattering. Figure 6 compares the measured scattering angle distribution through the absorber with the program.

C. Comparison of Measured Data and Monte Carlo

1. Transverse momentum plots

Since the Kaon momentum is not known for each event the transverse momentum of the particles is a good check that the events are consistent with $K_{\mu 3}$ decays. The original decay vectors are found by tracking the π and μ S-tracks back through the fringe field until a vertex is made. Since the target is 200 feet from the collimator it is assumed that the beam is parallel.

Figure 7 and 8 compare muon and pion transverse momentum with the program. There are more events for muons than pions due to the π's lost in the magnet. The ratio π/μ in data is 68% compared to 64% in the program, due to complete absorbtion of π's in the program when the pole tip is hit.

The transverse momentum of the neutrino is a sensitive thing to look at.

Fig 6.

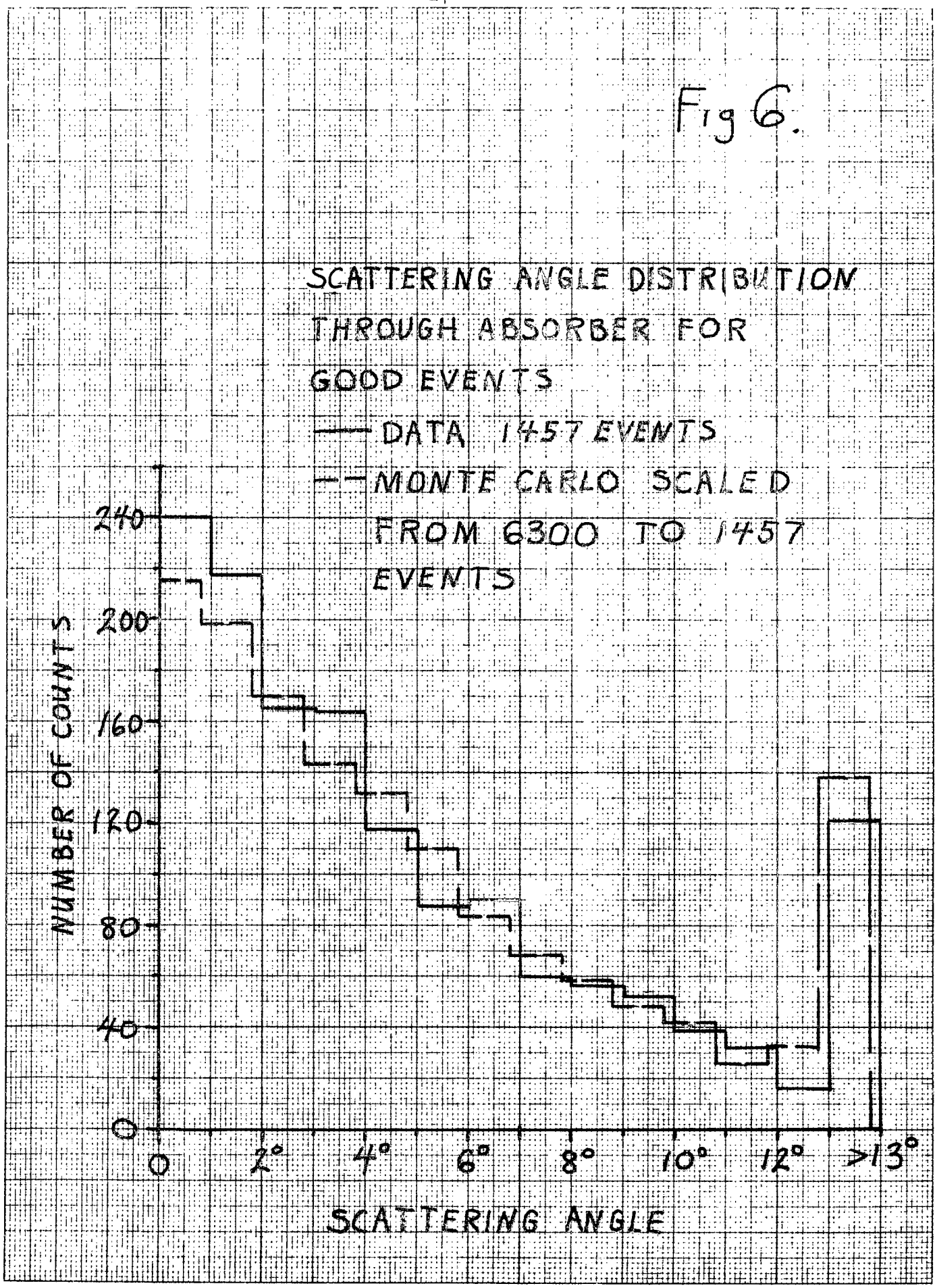
SCATTERING ANGLE DISTRIBUTION
THROUGH ABSORBER FOR
GOOD EVENTS
— DATA 1457 EVENTS
-- MONTE CARLO SCALED
FROM 6300 TO 1457
EVENTS
NUMBER OF COUNTS
240
200
160
120
80
40
0
0
2°
4°
6°
8°
10°
12°
>13°
SCATTERING ANGLE

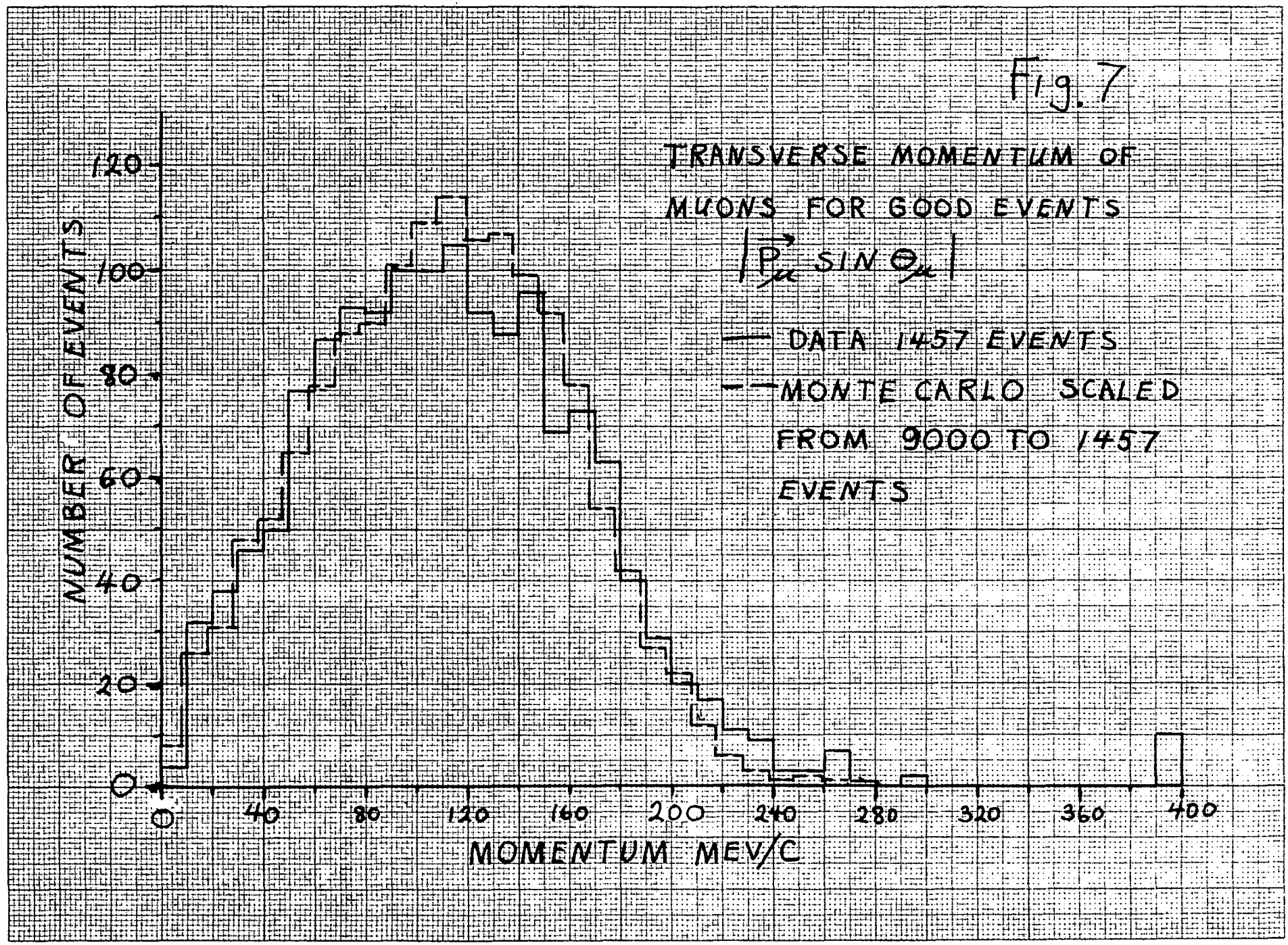

Fig. 7

TRANSVERSE MOMENTUM OF MUONS FOR GOOD EVENTS

$|\vec{P}_\mu \sin\theta_\mu|$

— DATA 1457 EVENTS

– – MONTE CARLO SCALED FROM 9000 TO 1457 EVENTS

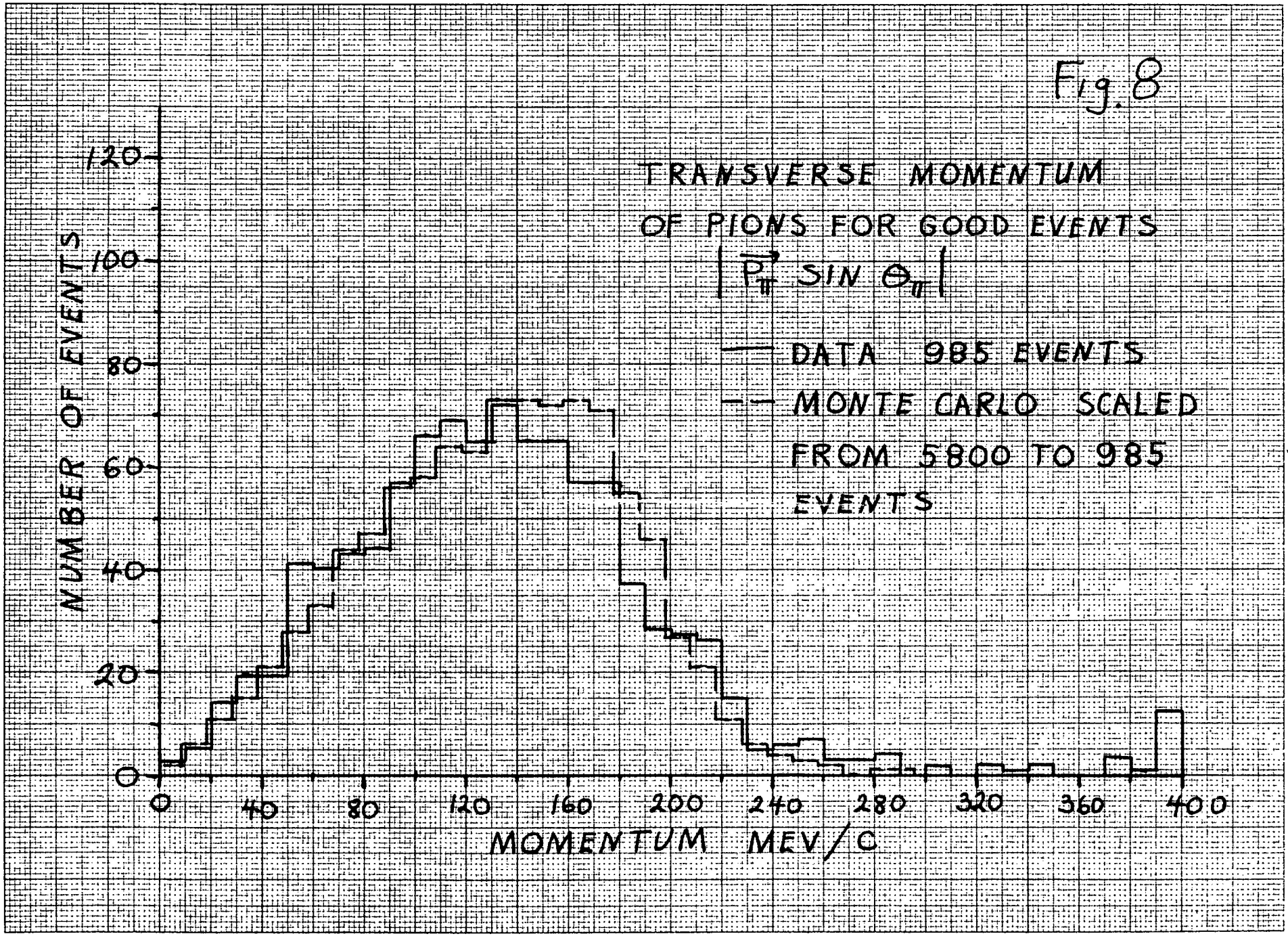
Fig. 8
TRANSVERSE MOMENTUM
OF PIONS FOR GOOD EVENTS
$|\vec{P}_T \sin \theta_\pi|$
— DATA 985 EVENTS
-- MONTE CARLO SCALED
FROM 5800 TO 985
EVENTS
NUMBER OF EVENTS
0
20
40
60
80
100
120
0
40
80
120
160
200
240
280
320
360
400
MOMENTUM MEV/C

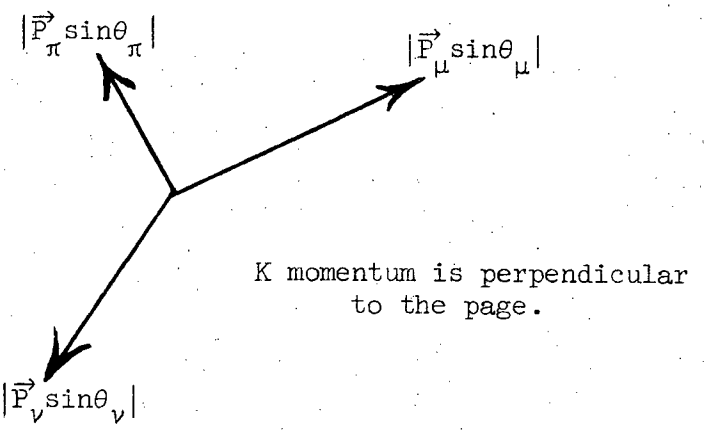

Looking along the axis of the K^o beam, conservation of momentum in the transverse directions gives $|\vec{P}_\nu \sin\theta_\nu|$. The quantities $|\vec{P}_\nu \sin\theta_\nu|$ and $(|\vec{P}_\pi \sin\theta_\pi|+|\vec{P}_\mu \sin\theta_\mu|+|\vec{P}_\nu \sin\theta_\nu|)$ depend on the 3 dimension reconstruction of events. However a different variable is plotted as it gives a better insight into the reconstruction.

$$"P_{tran}" = \sqrt{|\vec{P}_\pi \sin\theta_\pi|^2+M_\pi^2}+\sqrt{|\vec{P}_\mu \sin\theta_\mu|^2+M_\mu^2}+|\vec{P}_\nu \sin\theta_\nu|$$

is analagous to a "transverse four momentum". If all three particles in the center of mass of the K left exactly transversely to the beam axis, "P_{tran}" would equal M_K. Whatever "P_{tran}" is called, it is an invariant and has physical limits.

$$M_\pi + M_\mu < "P_{tran}" < M_K$$

Figure 9 displays the distribution of "P_{tran}". The data shows a greater fraction above M_K than the program. It is possible to have the center of mass energy of $\pi\mu\nu$ greater than M_K with "P_{tran}" still within limits. That situation occurs when π and μ have very different actual momenta so that no Lorentz system can be found where both π and μ are slow enough to fall within a K mass in energy and $\vec{P}_\pi$ and $\vec{P}_\mu$ are comparatively colinear with the beam axis. The tail of Fig. 9 gives the mass resolution of K^o although

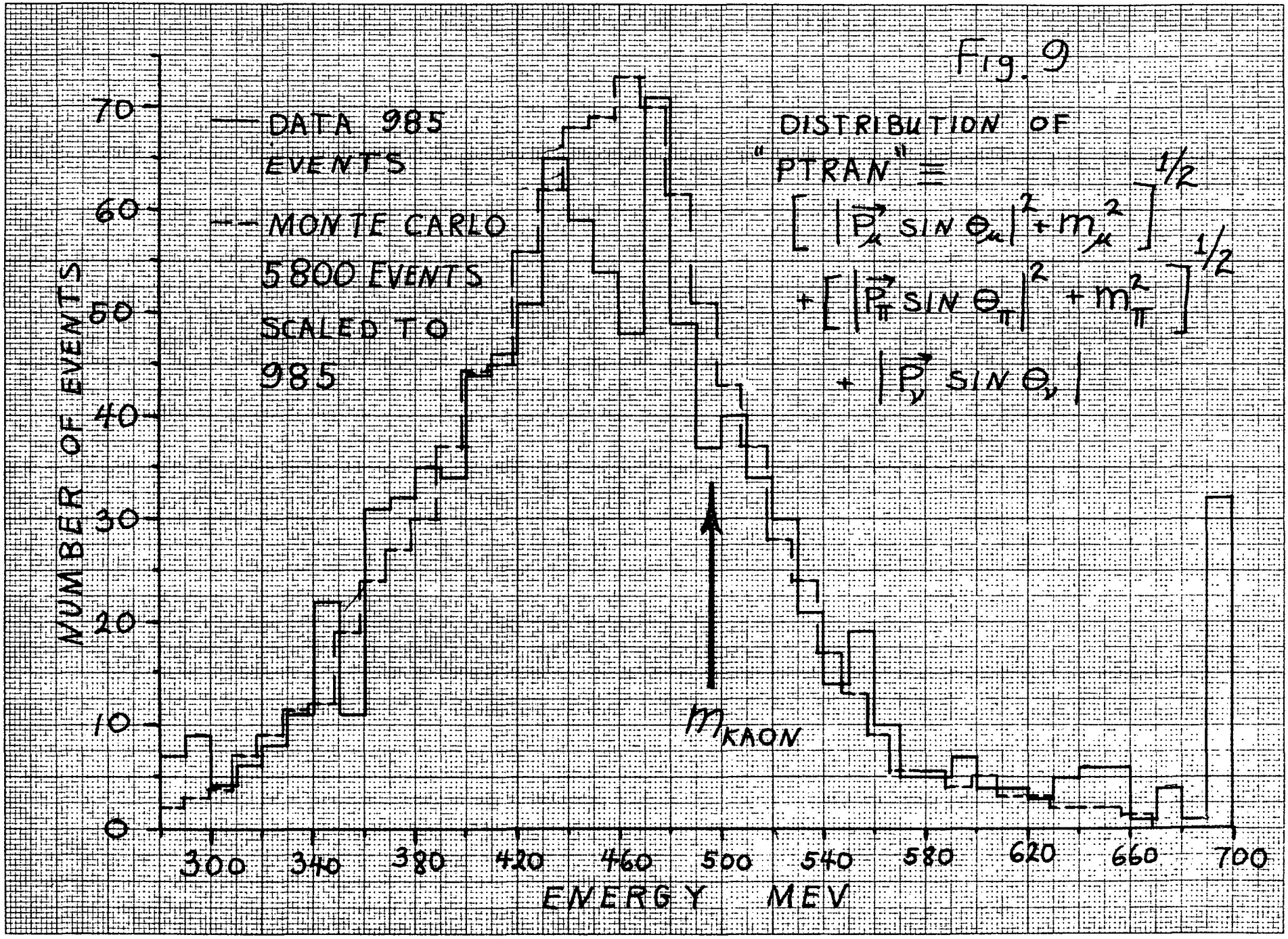
Fig. 9
DISTRIBUTION OF
"PTRAN" ≡
$\left[|\vec{P}_\mu \sin\theta_\mu|^2 + m_\mu^2\right]^{1/2}$
$+\left[|\vec{P}_\pi \sin\theta_\pi|^2 + m_\pi^2\right]^{1/2}$
$+|\vec{P}_\nu \sin\theta_\nu|$
— DATA 985 EVENTS
-- MONTE CARLO 5800 EVENTS SCALED TO 985
NUMBER OF EVENTS
0
10
20
30
40
50
60
70
300
340
380
420
460
500
540
580
620
660
700
ENERGY MEV
m_{KAON}

underestimated due to the above effect. The fraction of events with "P_{tran}" > M_K in data is 26% and in program is 22%. Zero constraint fits to the events find 37% "nonphysical" in data and 34% "nonphysical" in program. "Nonphysical" is defined in the next section.

2. Kinematic fit of events

By measuring $\vec{P}_\pi$ and $\vec{P}_\mu$ a zero constraint fit to the K energy in the lab is possible, assuming the beam is parallel. Two solutions for K energy arise due to the uncertainty as to whether the neutrino went forward or backward in the center of mass.

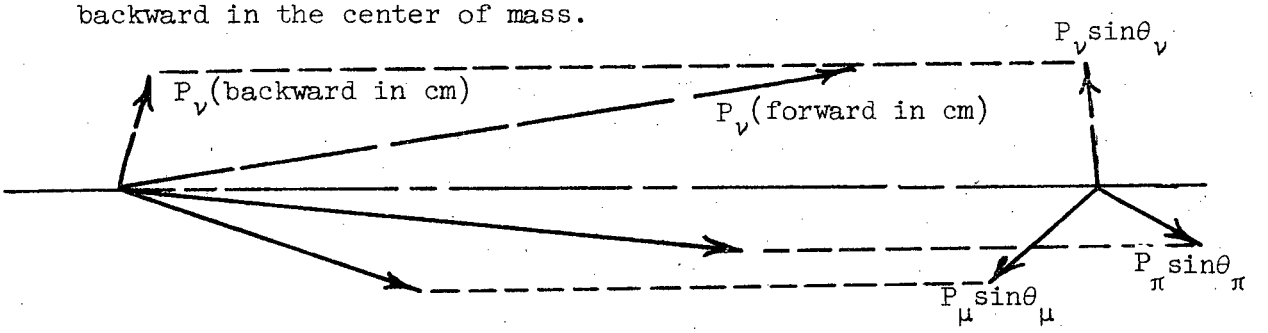

When the neutrino comes out almost laterally in the C.M. the two solutions are nearly equal. The two solutions are found by solution of a quadratic; "nonphysical" situations occur when the radical goes negative. In this case the square of the total four momentum of $\pi\mu\nu$ is greater than M_K^2.

Figure 10 and 11 are two dimensional arrays of the two solutions for P_K from data and Monte Carlo. The "nonphysical" solutions for data amount of 37 percent (34 percent for Monte Carlo) of the events available for study, i.e. where P_π is known. The "nonphysical" ones cannot be plotted, but Monte Carlo events that went "nonphysical" after measurement errors were added nearly all had the two solutions equal to within 150 MeV/c, that is the "nonphysical" ones have a small radical. To display the effect the K mass is increased for "nonphysical" solutions until the

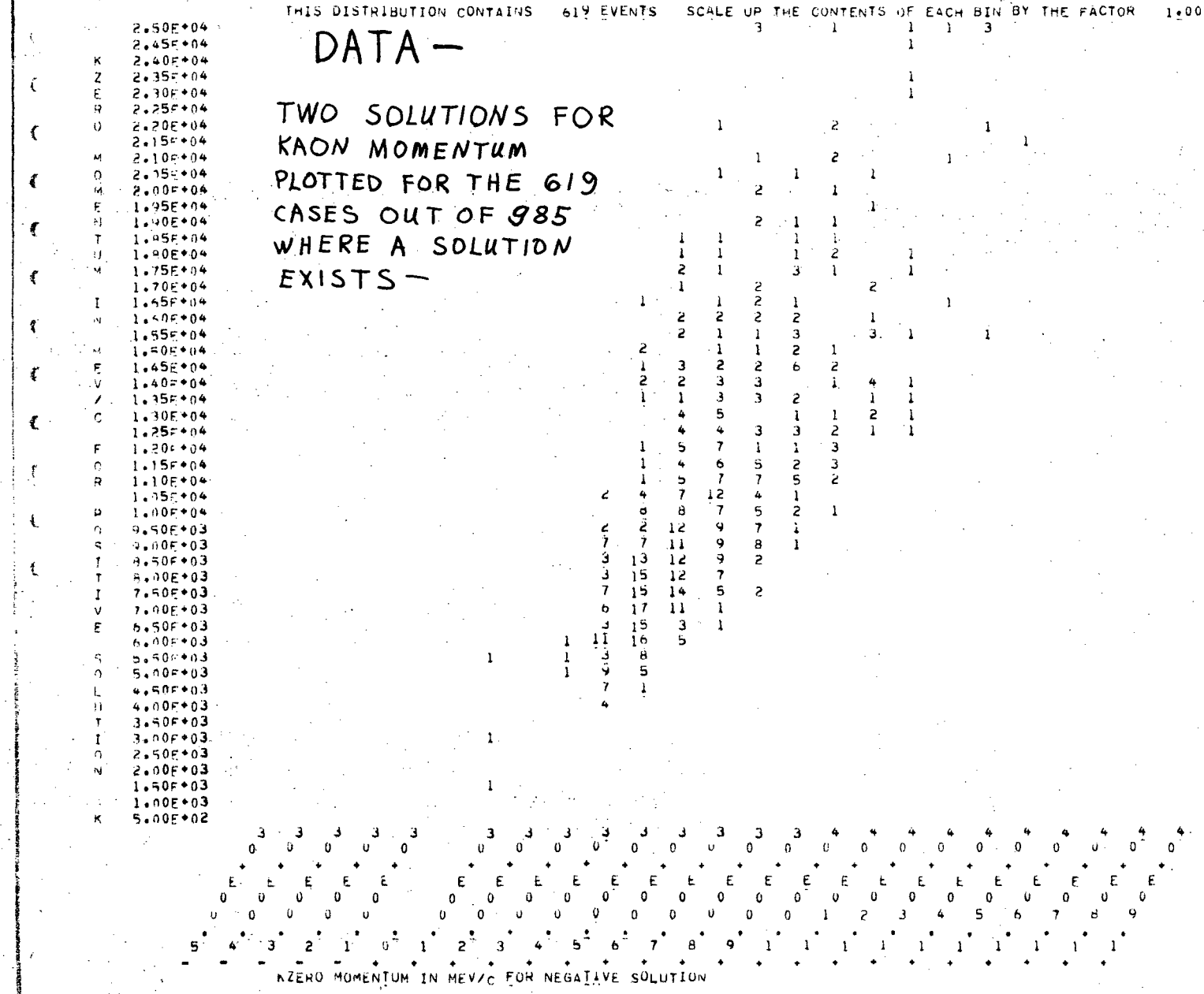
THIS DISTRIBUTION CONTAINS 619 EVENTS SCALE UP THE CONTENTS OF EACH BIN BY THE FACTOR 1.00
DATA —
TWO SOLUTIONS FOR KAON MOMENTUM PLOTTED FOR THE 619 CASES OUT OF 985 WHERE A SOLUTION EXISTS —
KZERO MOMENTUM IN MEV/C FOR NEGATIVE SOLUTION

Fig. 10

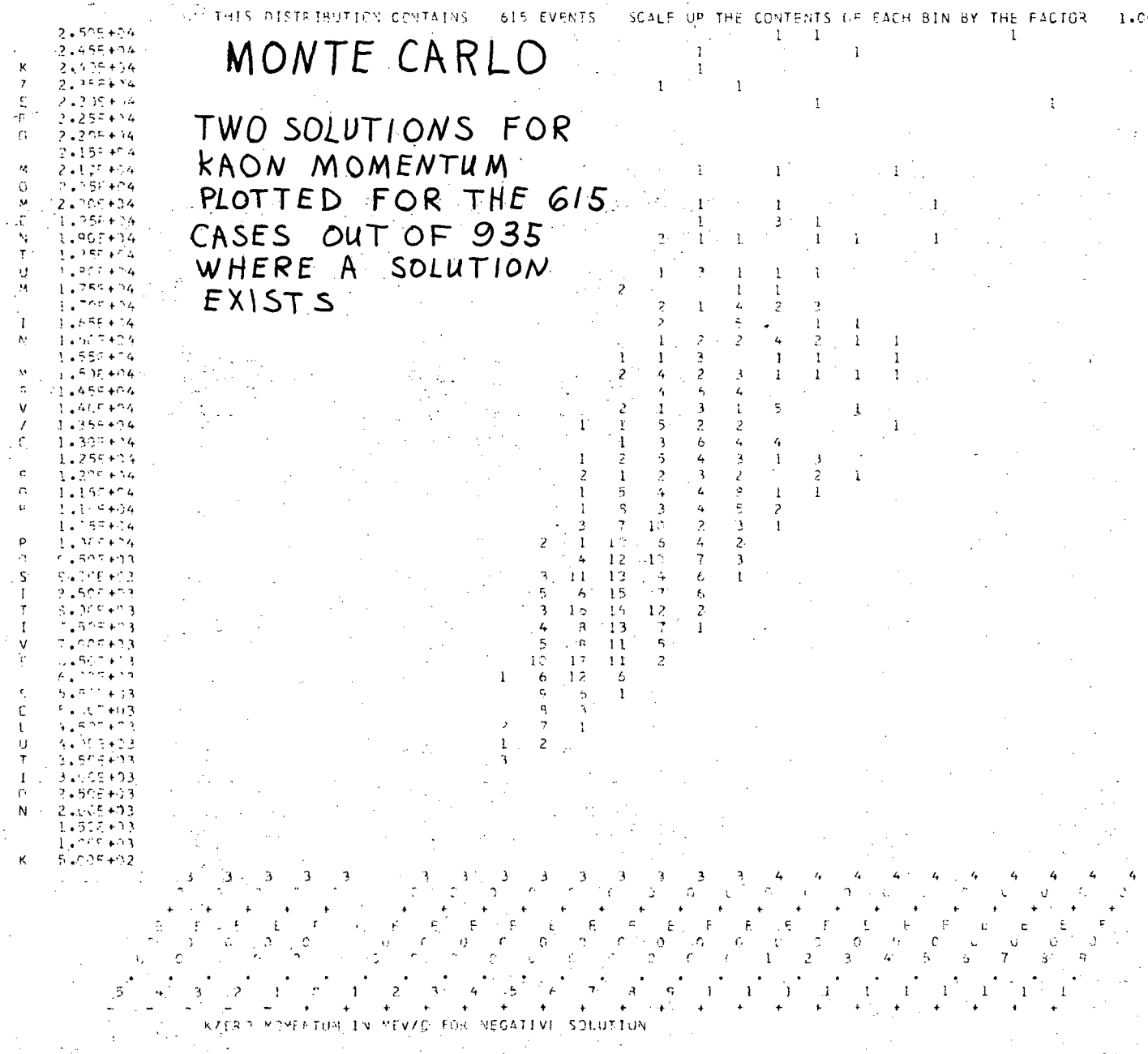
THIS DISTRIBUTION CONTAINS 615 EVENTS SCALE UP THE CONTENTS OF EACH BIN BY THE FACTOR 1.00
MONTE CARLO
TWO SOLUTIONS FOR KAON MOMENTUM PLOTTED FOR THE 615 CASES OUT OF 935 WHERE A SOLUTION EXISTS
KAON MOMENTUM IN MEV/C FOR NEGATIVE SOLUTION

Fig. 11

radical goes positive. That plot is shown in Fig. 12. The data has more events in the tail; however some of them are deserved. Twenty-five percent of the $K_{\mu 3}$ data are "nonphysical". 1.6% of the π's decay in the decay volume and in the magnet. Roughly 3% of the π's interact in material up to and including the first thin plate chamber. In addition many pions glancing off of the pole tips will give an incorrect momentum in the reconstruction. These effects account for some but not all of the data events in the tail of Fig. 12.

3. Distribution of decay vertices

The distribution of decay vertices shows that the events originated inside the helium decay region.

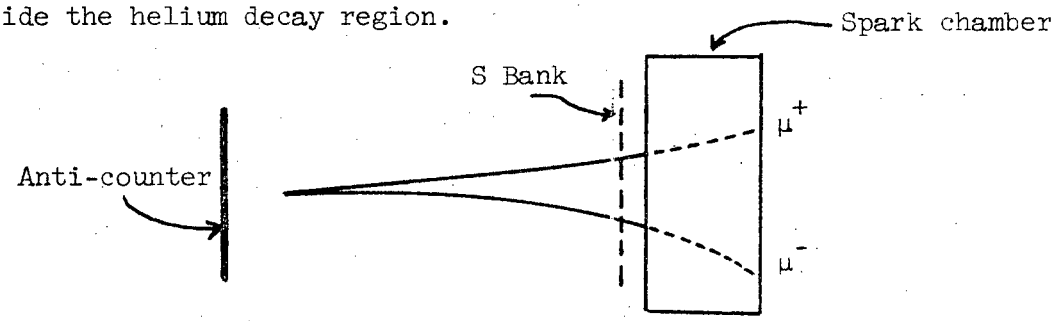

Vertex reconstruction by tracking through fringe field

The program predicts that field tracking can find the vertex to ± 8" for about 80% of the cases. The other 20% are the type indicated in the sketch where the particles are converging far from the S-bank. For those case the resolution is ± 20 inches. The rescanned events verify the conclusions from the program.

Figure 13 shows the distribution of decay vertices along the beam direction for data and program. The horizontal and vertical beam distributions found from data are given in Figs. 14 and 15. Recall that the beam was collimated to a 6" height and 9" width. The 1/2 inch shift in the vertical distribution is due to optical distortion rather than beam

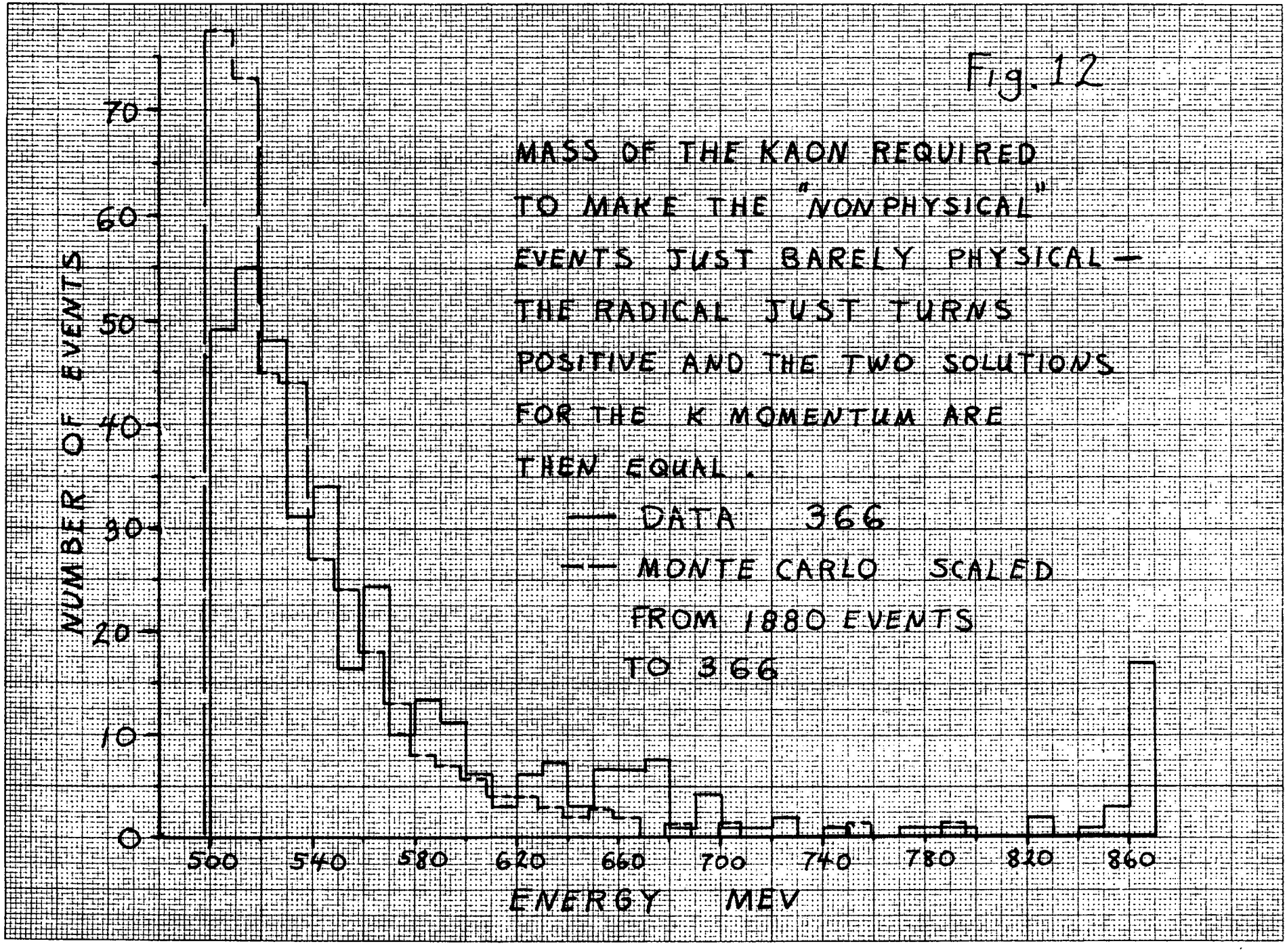

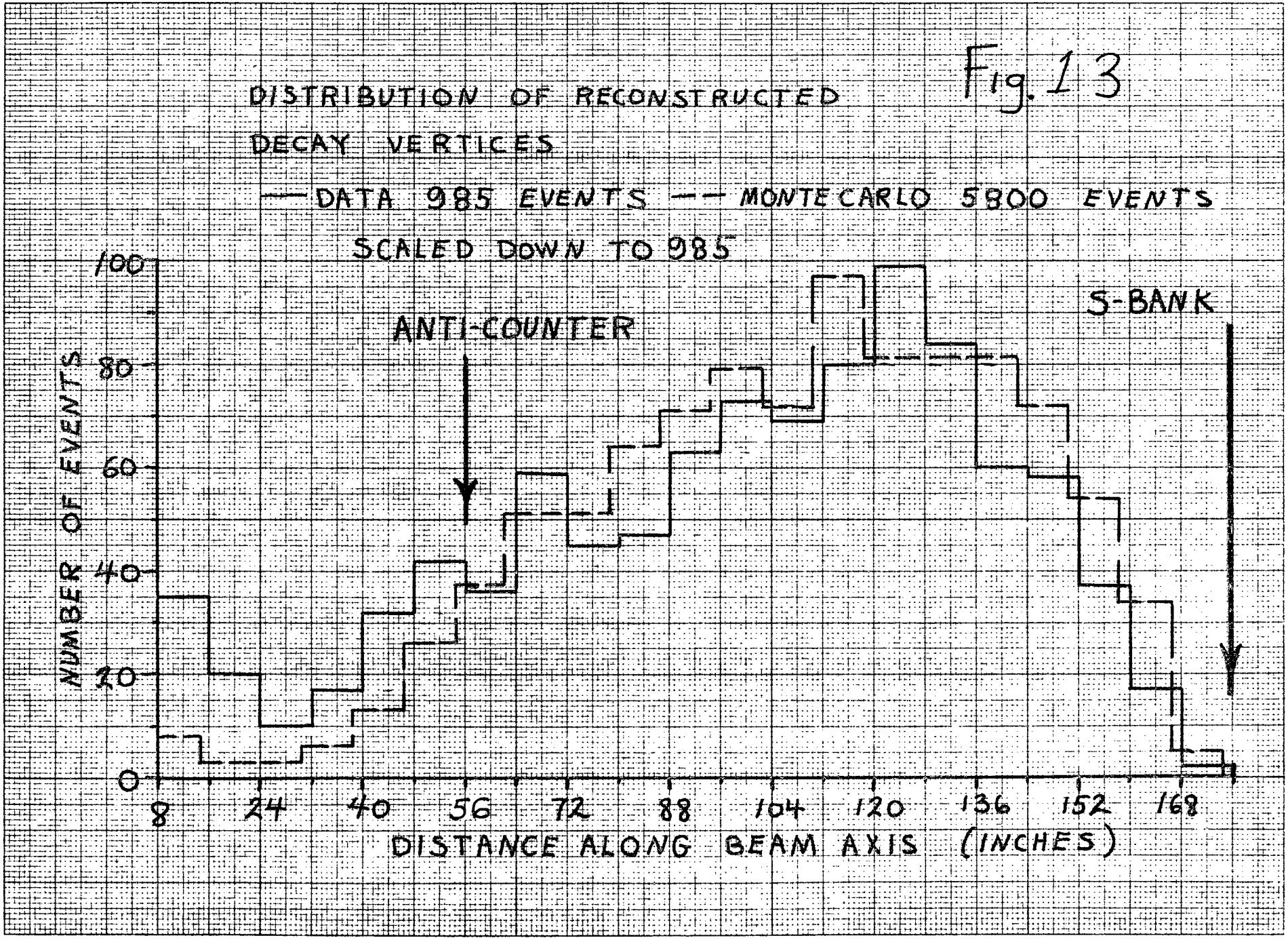
DISTRIBUTION OF RECONSTRUCTED
DECAY VERTICES
—— DATA 985 EVENTS -- MONTE CARLO 5800 EVENTS
SCALED DOWN TO 985
ANTI-COUNTER
S-BANK
NUMBER OF EVENTS
100
80
60
40
20
0
8
24
40
56
72
88
104
120
136
152
168
DISTANCE ALONG BEAM AXIS (INCHES)

Fig. 13

Fig. 14

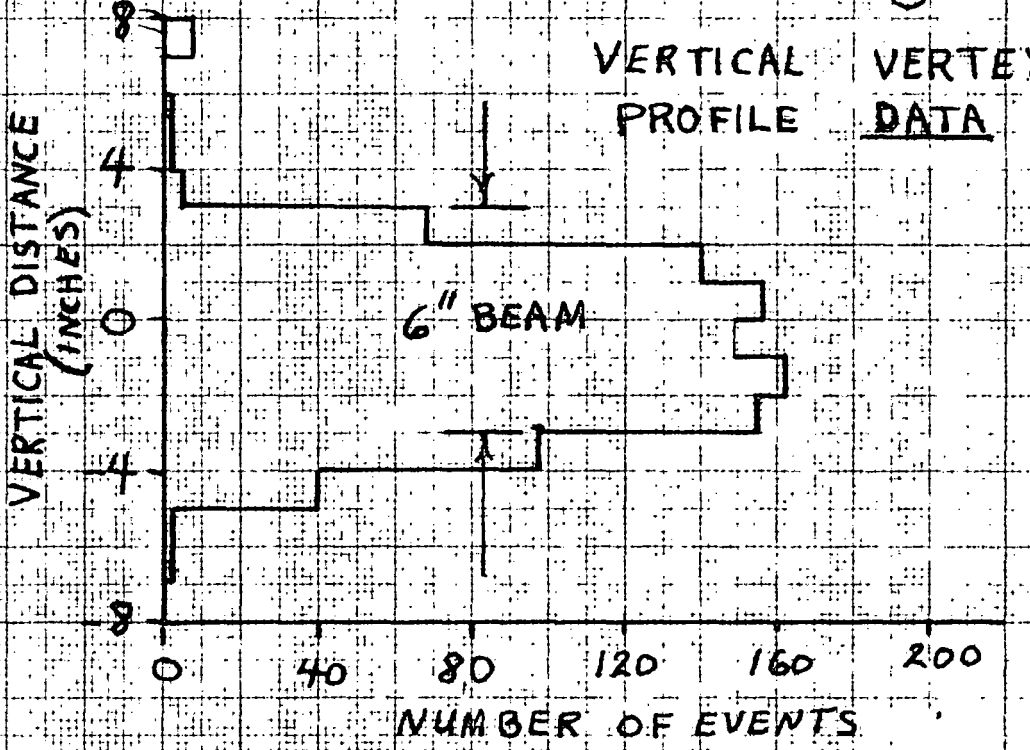
VERTICAL VERTEX PROFILE DATA
VERTICAL DISTANCE (INCHES)
8
4
0
4
8
6" BEAM
0
40
80
120
160
200
NUMBER OF EVENTS

Fig. 15

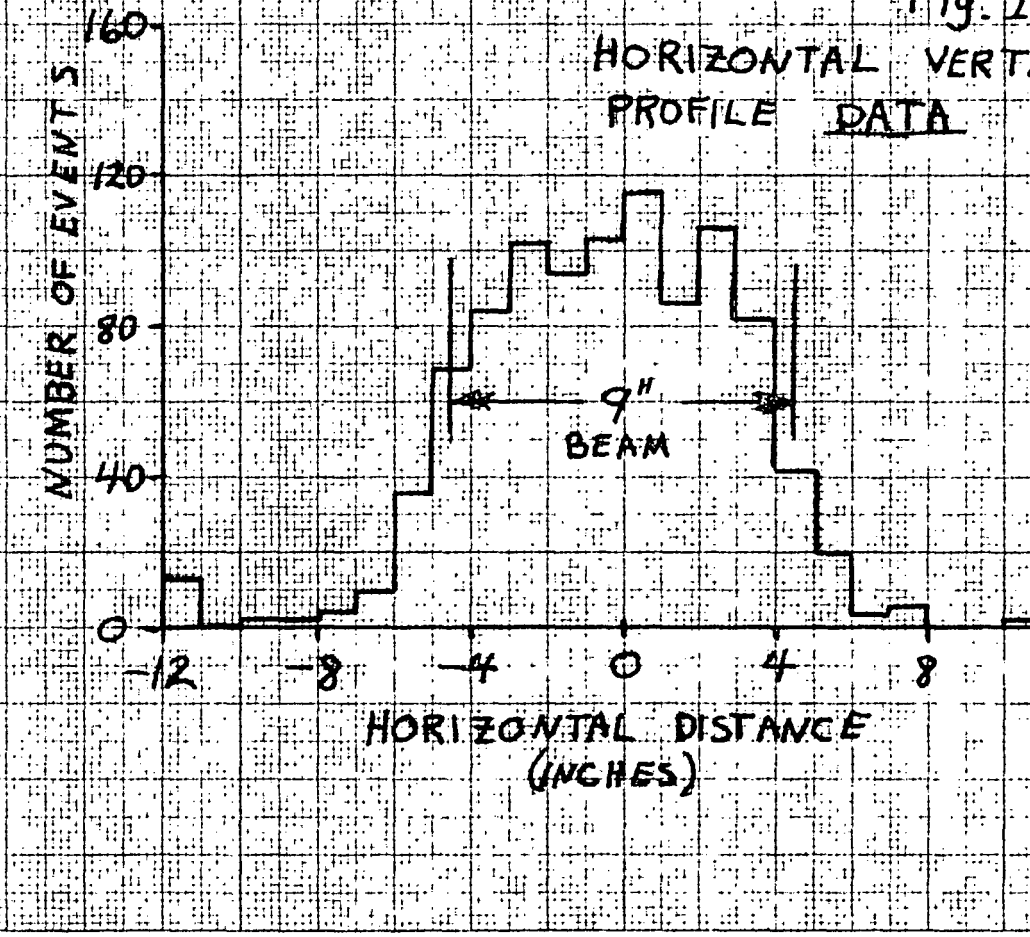
HORIZONTAL VERTEX PROFILE DATA
NUMBER OF EVENTS
160
120
80
40
0
9" BEAM
-12
-8
-4
0
4
8
12
HORIZONTAL DISTANCE (INCHES)

misalignment.

4. Other Distributions

The only counter distributions available for comparison with Monte Carlo are the M-counter distribution, Fig. 16 and the S-counter distribution, Fig. 17. Things which contribute to the extra width of the S-distribution are π decays in the decay volume and delta ray effects which are discussed in Section VIII-C.

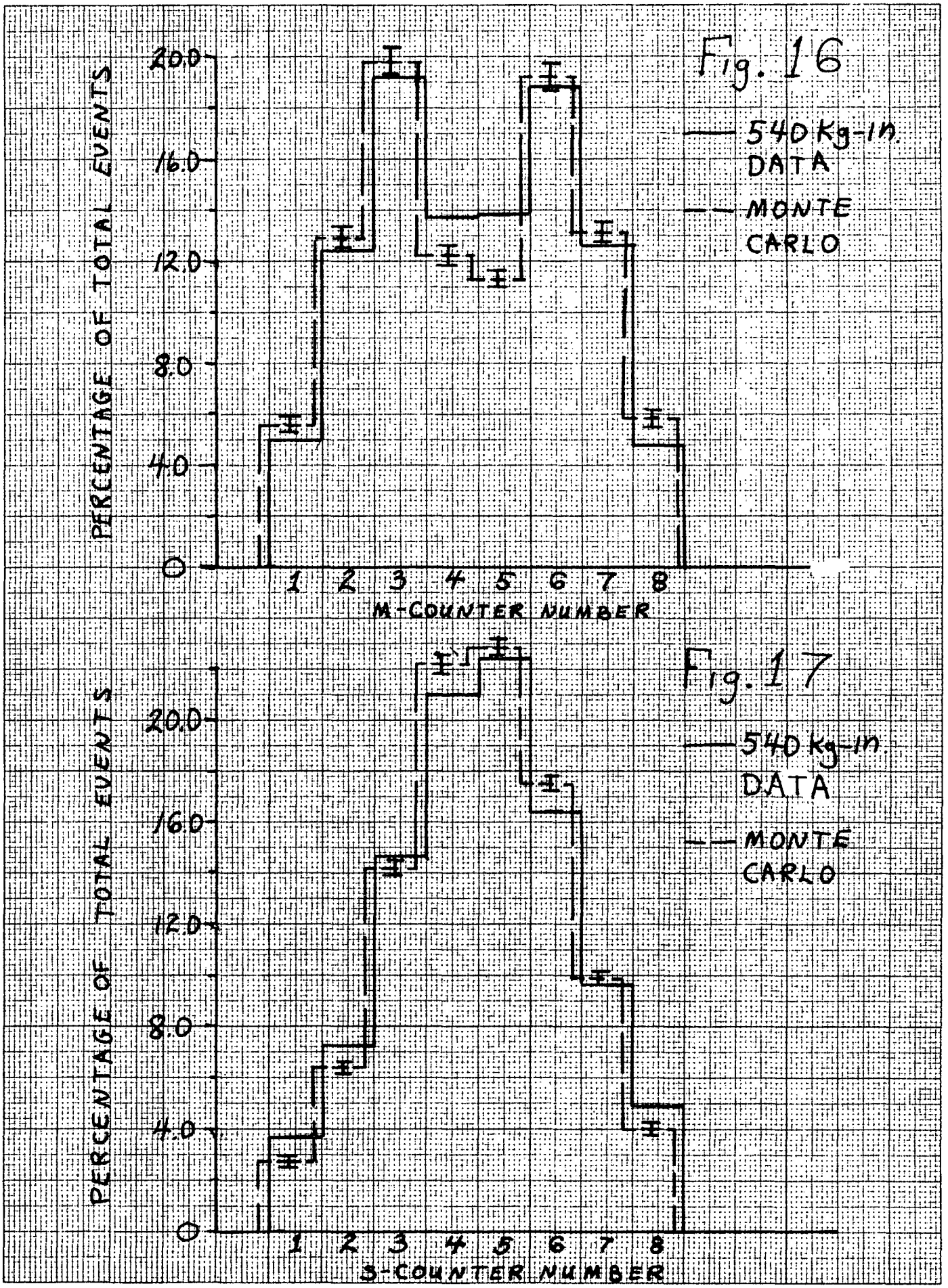

Fig. 16

Fig. 17

VI. ANALYSIS OF CUTS IN THE TRIGGER

A. Introduction

The equipment is designed so that there are no cuts made in the data after the S-bank other than the muon momentum cut-off imposed by the absorber. Since the magnetic field is only 7 Kg-in. in the decay region, the cut made with the S-counter bank is charge independent. The S-counters and the lead almost entirely determine the detection efficiency of the system because to a high percentage, for all of the events triggering the S-bank the muons with sufficient energy will count in the T and M counters. Hence to the order that will be discussed below the trigger is charge independent in detection of $K_{\mu 3}$ events. There are many small effects which might modify this charge independent trigger. They are as follows:

1) Leakage of muons from sides and top of M-counters and spaces between counters--The source of asymmetry in this group of leaking muons comes from a difference in multiple scattering between μ^+ and μ^- or S-counter efficiency change with field reversal.

2) Wrong sign decisions--4 percent of the events in the data have the wrong sign determination due to unfavorable decay configuration or large multiple scattering or a combination of the two. The only effect is to wash out the asymmetry if μ^+ and μ^- scatter identically and the S-counters do not change efficiency with field.

3) Differential absorbtion of μ^+ and μ^- by the lead and aluminum absorber--A one percent difference in dE/dx would produce a .8% asymmetry in the result. A difference in multiple scattering between μ^+ and μ^- would produce a range difference and asymmetry.

4) Some of the muons with large angles and small momentum get around the T counter but multiple scatter and hit the M counters. Then the

associated pions can differentially trigger the T-counter after having scattered from the pole tip. The size of the effect is found from the program and estimates of π^+,π^- differences are made.

B. Calculation of Effect of S-counter Efficiency on the Various Leakages

Figure 18 illustrates in an exaggerated manner what happens to muons which go through a particular S-counter. S1 is picked because it has the most pronounced effect on the leakages. All the muons through S1 are heading upward as well as being 8 inches above the axis of the decay volume. The effects which do not allow collection of all of the muons which pass through S1 are listed.

1) For Atlas up μ^+'s leak out the top of M1 while no μ^-'s leak out of the bottom of M8. For the inside S-counters there are some μ^-'s leaking out the bottom of M8. Muons also leak out the sides of the M counters, but it is the same for μ^+ and μ^- because the vertical focusing of the magnet averages out between μ^+ and μ^-.

2) Muons leak through the spaces between the M counter pairs. There is very little asymmetry in this leakage. A cut is important if it is located at point with a steep gradient in the distribution. So the loss in any one space fluctuates, but considering all the spaces together the effect washes out.

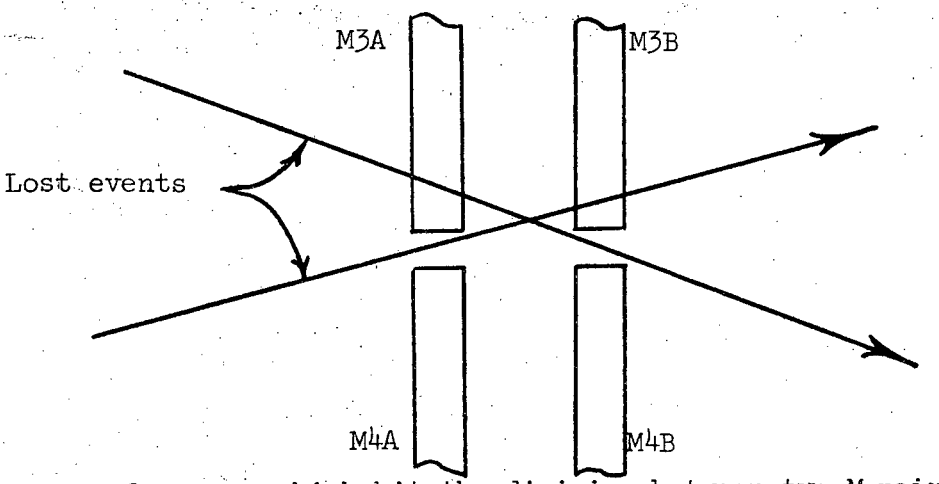

Large angle muons which hit the division between two M pairs are lost because a coincidence is required between the A and B part.

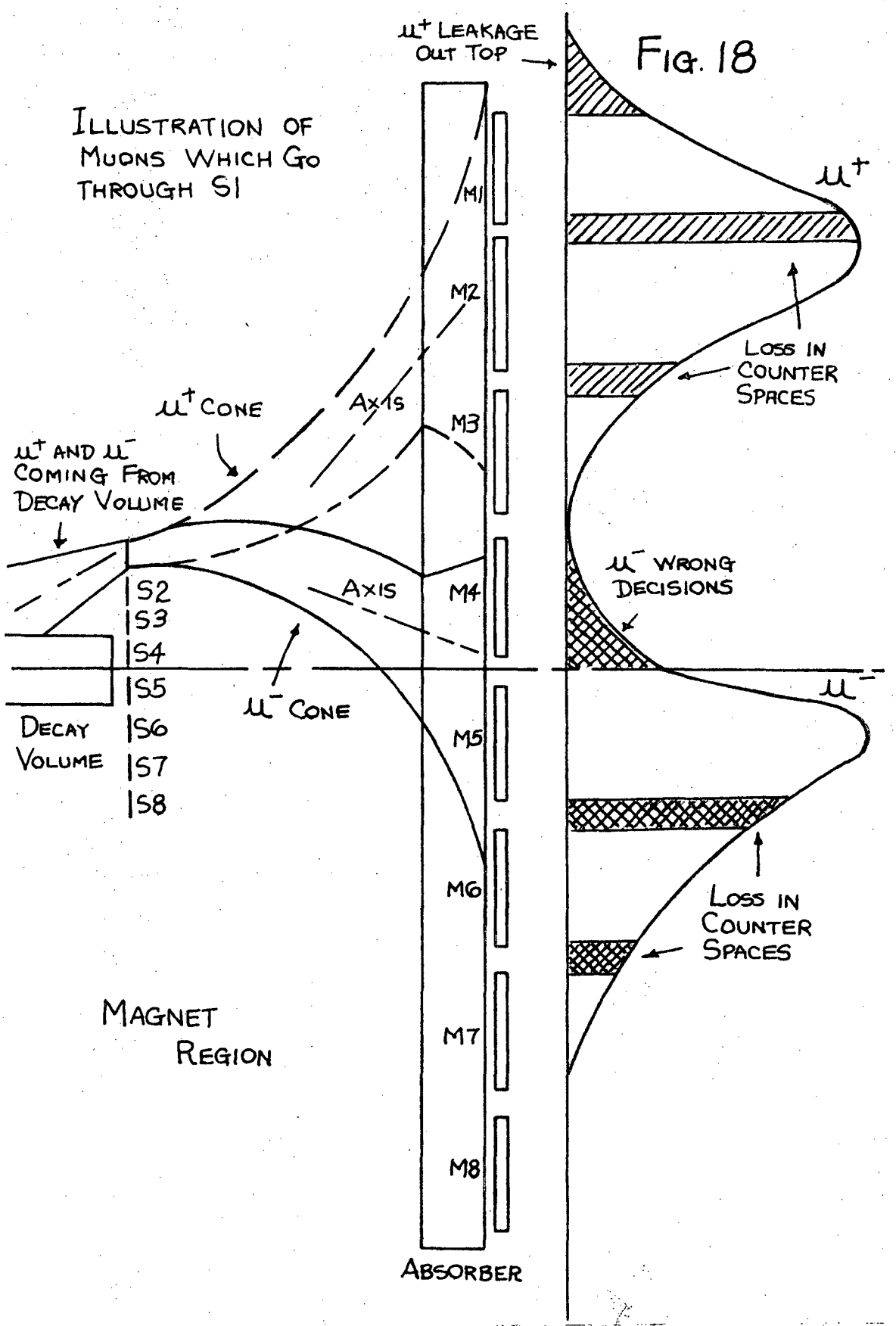
FIG. 18
ILLUSTRATION OF MUONS WHICH GO THROUGH S1
μ+ LEAKAGE OUT TOP
μ+ CONE
AXIS
μ+ AND μ− COMING FROM DECAY VOLUME
S2
S3
S4
S5
S6
S7
S8
DECAY VOLUME
AXIS
μ− CONE
M1
M2
M3
M4
M5
M6
M7
M8
ABSORBER
MAGNET REGION
μ+
LOSS IN COUNTER SPACES
μ− WRONG DECISIONS
μ−
LOSS IN COUNTER SPACES

3) The lead absorber will stop more μ^+ than μ^- if the μ^+'s enter the lead at a steeper angle. All the S1 muons are initially heading upward so the axis of the μ^+ cone heads into the lead at a sharper angle than the μ^- cone. In order to calculate this correlation with the Monte Carlo all events above 1400 MeV/c are allowed to go through the energy loss subroutine. Thus all muons which could conceivably stop are included.

4) The asymmetry in the wrong decisions for muons which go through S1 is almost 100%. That is no μ^+ hitting S1 can ever get into the lower M bank for Atlas bends μ^+ up. The other S-counters have less asymmetry for wrong decisions.

Table III has the Monte Carlo numbers for the losses and the asymmetry in the losses for π or μ hitting each S. All asymmetries reverse and cancel out with the magnetic field if the S-efficiency does not change with the field. A small inefficiency for one sign of the field allows a residual asymmetry to remain. A major point is that the pion is complementary to the muon. This term means that at least half the time the π hits S1 instead of the muon, while the muon usually goes to a down S-counter.

Not shown on the table are the losses out of the sides of the M bank and the spaces. They show no variation in asymmetry as a function of S counter. So for all the S counters together

540 Kg-in	Spaces	$\mu^+/\mu^- = 1.0 \pm .1$	(3.6%)
468 Kg-in	Spaces	$\mu^+/\mu^- = .96 \pm .1$	(3.8%)
540 Kg-in	Side Loss	$\mu^+/\mu^- = 1.16 \pm .16$	(2.2%)
468 Kg-in	Side Loss	$\mu^+/\mu^- = .91 \pm .12$	(2.3%) .

Table III. Percent loss and asymmetry in lost or stopped muons, $\left(\frac{\mu^+ \text{ lost}}{\mu^- \text{ lost}}\right)$ when π or μ hits a particular S-counter. Amount of loss is relative to good events.

	Top and bottom of M's		Stopped in Pb or Al		Wrong Decisions	
	% Loss	$\frac{\mu^+}{\mu^-}\Big\vert_{\text{lost}}$	% Loss	$\frac{\mu^+}{\mu^-}\Big\vert_{\text{lost}}$	% Loss	$\frac{\mu^+}{\mu^-}\Big\vert_{\text{lost}}$
			540 Kg-in. Data			
S1	.25%	2.4 ± .7	1.6%	1.10 ± .09	.13%	.17 ± .14
S2	.43%	1.7 ± .4	3.3%	1.02 ± .09	.18%	.36 ± .20
S3	.5%	1.7 ± .4	5.3%	1.04 ± .06	.17%	.87 ± .40
S4	.33%	1.2 ± .2	7.3%	1.03 ± .06	.15%	.88 ± .40
			468 Kg-in. Data			
S1	.15%	2.4 ± 1.0	1.5%	1.13 ± .13	.22%	.45 ± .14
S2	.23%	1.9 ± .6	3.1%	.94 ± .09	.38%	.41 ± .10
S3	.3%	1.3 ± .3	5.1%	1.02 ± .06	.45%	.80 ± .17
S4	.3%	1.2 ± .3	6.9%	.97 ± .06	.4%	.80 ± .18

The numbers in the Table are used to find the correction to the result if the counter was turned off for one polarity of field. If S1 is turned off for Atlas up and turned on for Atlas down, the correction to the data is -(amount lost, from table) x(asymmetry from table). A factor 1/2 is needed for stops or misses because the asymmetry is present only half the time.

The losses are lumped together for the 4 counters S1 to S4. The wrong decisions are handled separately since they are not strictly a loss; moreover the wrong decisions have opposite and double correction from stops and misses. S1 to S4 is considered a single counter with an efficiency change with the magnet reversal. Assume S1 → S4 95% efficient with Atlas up and 100% efficient with Atlas down. These corrections need to be applied to data.

	Correction to data for S1→S4 5% efficiency loss for one sign of field
All losses except wrong decisions	
540 Kg-in.	-.04% ± .02%
468 Kg-in.	0% ± .02%
Wrong decisions	
540 Kg-in.	+.016% ± .004%
468 Kg-in.	+.028% ± .004%

All of these numbers could be doubled if the same contribution is added from the down S-counters S5→S8. However the field would have to have the opposite correlation, that is, inefficient for Atlas down and efficient for Atlas up. Considering that the S-counters were run at least 150 volts above the knee of the plateau curve which does not change position with Atlas reversal it is reasonable to not put any correction in at all for S-counter efficiency.

An empirical check of S-efficiency correlation was made by recording during a phase of the actual running the two S-counters which fired. Record of S counts for muons in up M bank was kept separately from muons in the down M bank. It was done by strobing a set of S-counter scalers with the up event signal; another set of 8 scalers was strobed with the down event pulse. This procedure allows determination of the asymmetry measured when either the π or the μ hits a particular S counter. The same thing is done in the Monte Carlo except that it looks at the lost events instead of the good events since the sensitivity is so much greater. Figure 19 shows the asymmetry found for μ or π in each S-counter minus the combined asymmetry for other 7 S-counters. The test is not as sensitive as the calculation but it is a check that contribution to the final result is uniformly

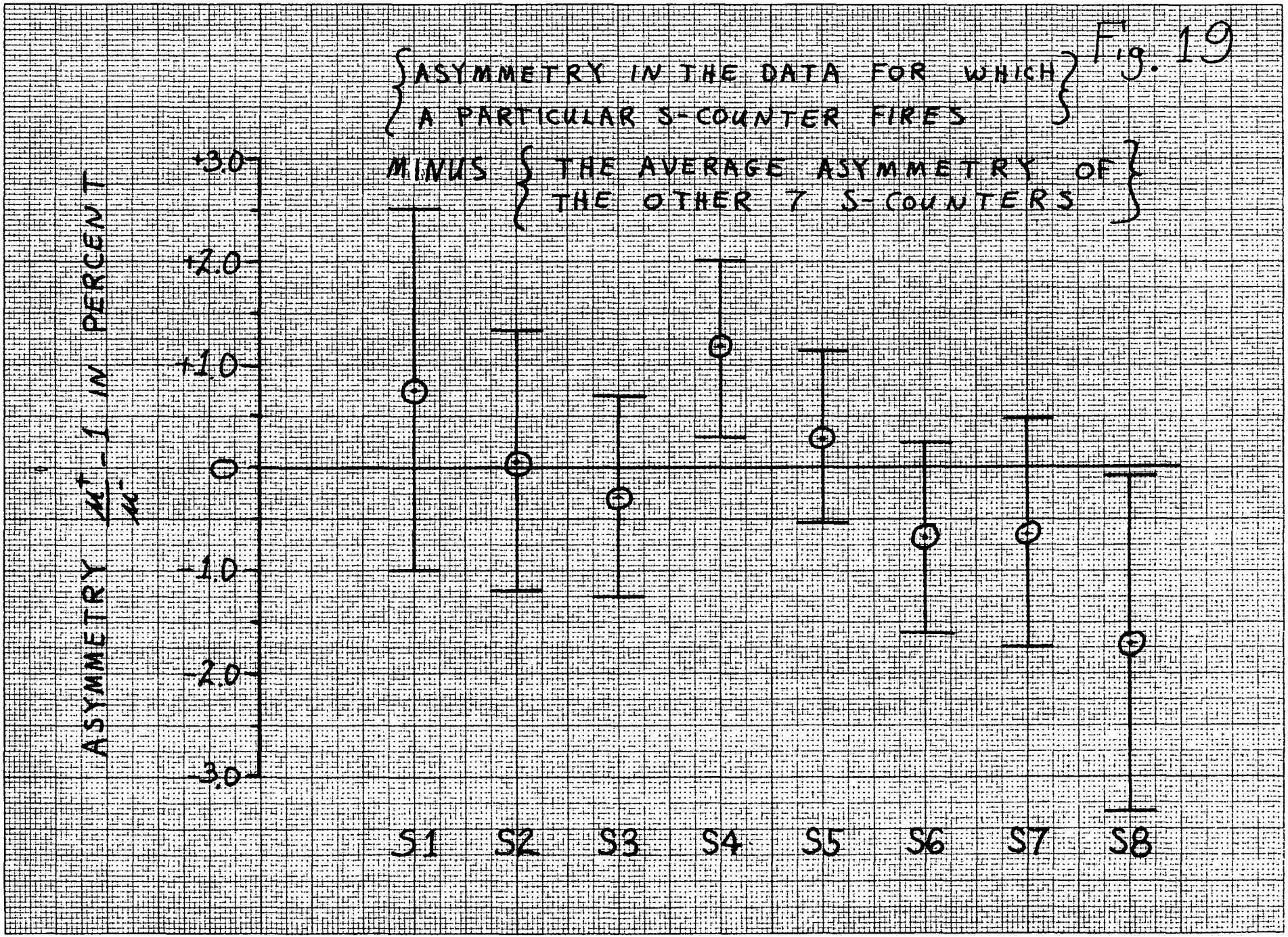
ASYMMETRY IN THE DATA FOR WHICH A PARTICULAR S-COUNTER FIRES
MINUS
THE AVERAGE ASYMMETRY OF THE OTHER 7 S-COUNTERS
ASYMMETRY $\frac{\mu^+ - \mu^-}{\mu^+ + \mu^-}$ IN PERCENT
+3.0
+2.0
+1.0
0
-1.0
-2.0
-3.0
S1
S2
S3
S4
S5
S6
S7
S8

Fig. 19

distributed over the S bank.

C. μ Misses T Counter Fires M

The 468 Kg-in. Data, which was taken with a T counter 30" in the beam bending direction, is considered. A number of muons equal to 3.6% of the event rate miss the top or bottom of the T counter due to large bend by the magnet coupled with extreme initial angle; these muons then go on to fire the M due to large multiple scattering. Of the 3.6%, 60% of them count as good events because the pion hits the T counter directly and completes the trigger. These pions have a very small asymmetry due to passage through the S-counter bank and the two thin plate chambers. The problem is not with these triggers, but in the triggers caused by the other 40% pions which have such wide angles that they miss the T. This group of pions can potentially trigger 40% x 3.6% or 1.4% of the real event rate. Roughly 3/4 of these pions will either hit the pole tip or the coils of the magnet, and some fraction of these different for π^+ and π^-, scatter and trigger T.

Since the entering angles are symmetrical, as many particles of one sign are focused as are defocused by the vertical focusing of the magnet. But since there are more pions in the middle of the magnet gap, the net effect is to push more toward the pole tips. Ignoring that complication, assume that 1% of the muon misses have the associated pion strike the magnet and .4% of the mu misses go into the aluminum thick plate chamber surrounding the edges of the T counter. The fraction of the 540 Kg-in. Data where the muon misses T and fires M is only 0.3% due to a 41 inch high T counter intercepting wide muons. So only half of the data has this problem, and the 1% becomes .5% of the triggers involved.

The momentum of pole tip hits is below.

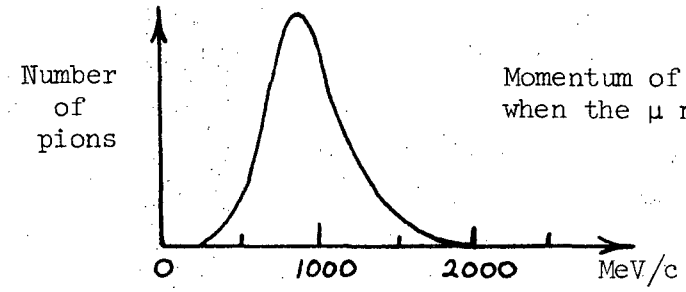

With iron having nearly equal neutrons and protons, the chief asymmetry in T triggers is due to loss from the neutral final state of $\pi^- p$ charge exchange as opposed to $\pi^+ n$ charge exchange. The charge exchange cross section averages 15% of the total $\pi^- p$ cross section over the momentum region above.

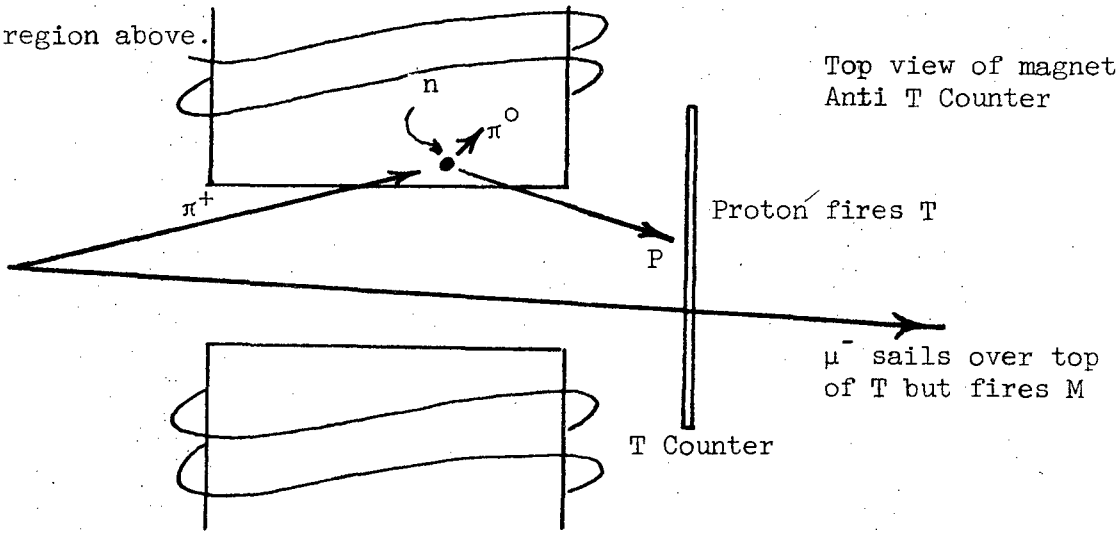

The probability that a charge exchange trigger the T counter is certainly less than 20%.

Correction to result < (.5% pion pole tip hits)

x (15% charge exchange probability)

x (20% chance for T trigger)

< + .015%

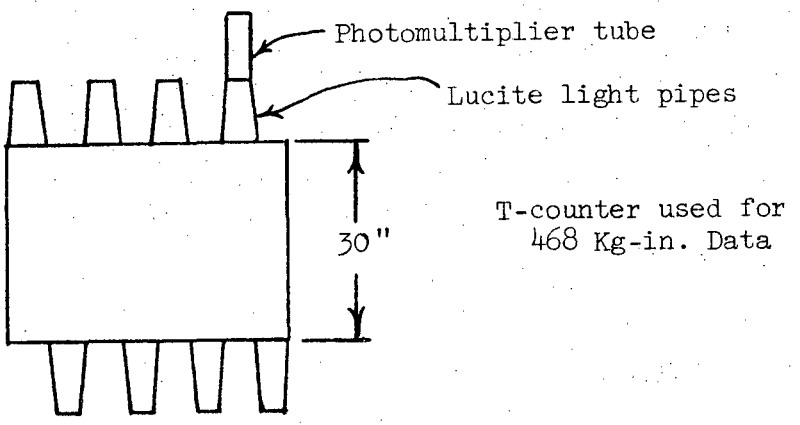

The lucite light pipes on this T counter intercept 1/2 of the troublesome muons whose pions differentially trigger the T. Chrenkov light in the lucite should have enough intensity to trigger the discriminator since the voltages were well above plateau on all the tubes. Hence any correction calculated can be knocked down by another factor of 2.

D. Examination of T Efficiency on Final Result

The sign of μ^+ is 90% correlated with incidence on the upper half of the T-counter. At the S position, turning off a counter removes as many μ plus as μ minus as candidates for events. At the T counter, reducing efficiency can directly affect one sign particles only.

For 70% of the events the π also strikes the T-counter, almost doubling the pulse height and assuring detection. Allowing a uniform, constant with field, 1% inefficiency in the T counter is like adding .3% to the fraction of events where the muon misses the T but fires M. Addition of .3% to the miss rate does not change the conclusion of the previous section.

An inefficiency occurring on the top or bottom of the counter for one sign of the field is possible. In order to find the correlation of this effect with the final result, first assume the pions have lost their

strong interaction. The point is to find out about the muons whose associated pions geometrically miss the T counter. The real situation will give a smaller asymmetry correlation with field.

Assume that the top half of the T is 1% inefficient for Atlas bending plus up but 100% efficient for Atlas reversed. The fraction of μ^+ lost is

$$1/2 \times 30\% \times 1\% = .15\% \ .$$

The muons in question are fairly uniformly distributed over the upper part of the T counter. For a more reasonable model, the upper 1/4 of the T counter lost 1% efficiency for Atlas up, the correction to the data would be +.08%.

This correlation with T efficiency deals only with muons in the upper half of the T counter. The effect would double if the bottom part of the T also had a 1% inefficiency but with the opposite field correlation. The T counter used for the 540 Kg-in. Data had one 5" phototube looking at the entire counter through a twist light pipe. A muon striking near the joint between scintillator and the twist pipe would have its light preferentially travel down one or two of the twist sections. But the majority of events away from the edge use all of the sections for transmitting light and therefore use all of the photocathode surface. Therefore it is impossible to have a nonuniformity over the surface away from the light pipe joint, assuming no defects in the counter. In fact the maximum variation in the singles rate of a Sr90 source over the entire surface of the 540 Kg-in. T counter is less than 20%.

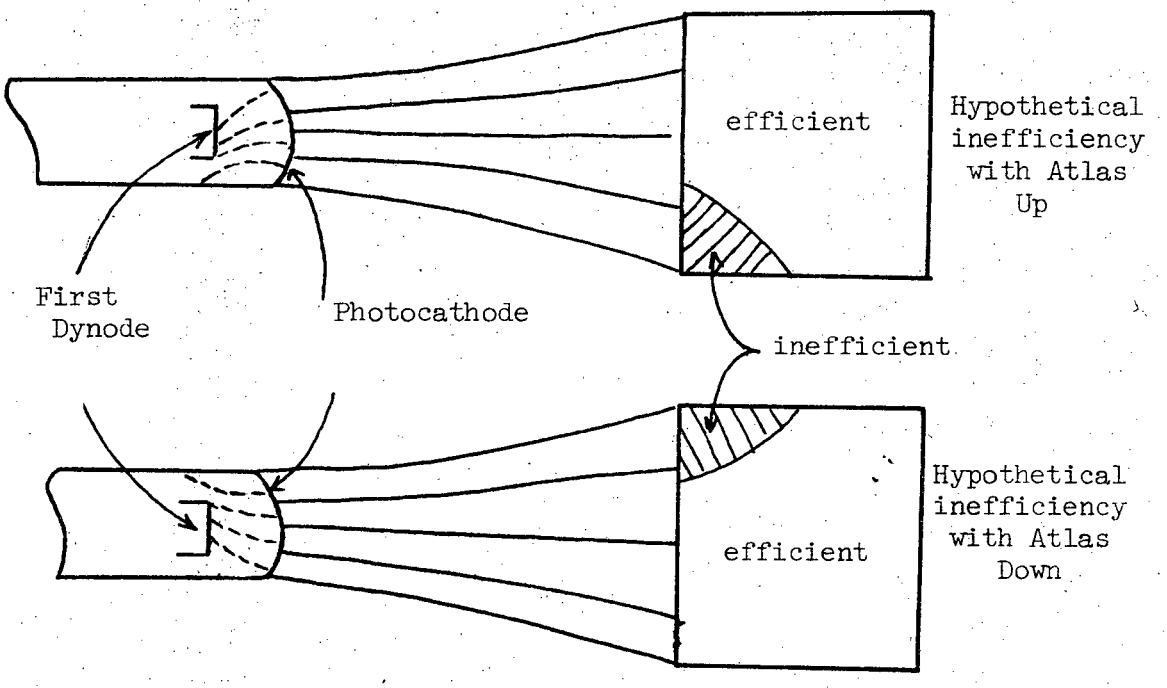

It is easy to see how the affected portion of the counter pictured would be small in the event of an efficiency shift. For the 468 Kg-in. Data the T-counter had eight 2-inch phototubes, 4 on the upper edge and 4 on the lower edge. This arrangement minimizes any non-uniformity in the up and down, beam bending direction.

Accidentals in the T counter are no problem so that both T counters were run at least 150 volts over the knee in the plateau curves. The conclusion is that the T counters cause no bias.

E. $\mu^+\mu^-$ Scattering and Range Differences

If μ^+, for example, scatter more in the lead absorber than μ^-, negative asymmetry results due to more μ^+

1) stopping in the absorber,

2) being lost out the top and sides of M bank,

3) and making wrong decisions by falling into the μ^- side.

Both experimental and theoretical work has been done on μ^+ and μ^-

scattering differences. Goldemberg, Pine, and Yount[25] have measured the quantity

$$R = \frac{\sigma_{e^-}(\theta) - \sigma_{e^+}(\theta)}{\sigma_{e^-}(\theta) + \sigma_{e^+}(\theta)}$$

for elastic scattering of electrons at 300 MeV on bismuth and cobalt. Herman, Clark, and Ravenhall[26] have made partial-wave calculations of the same parameter R for 300 MeV electrons on bismuth and cobalt. The experiment and theory are in good agreement, and some of the calculated parameters are used here. Various charge distributions are used in the calculations, but none of the detailed results in the paper are necessary here.

The qualitative appearance of the asymmetry R is shown below.

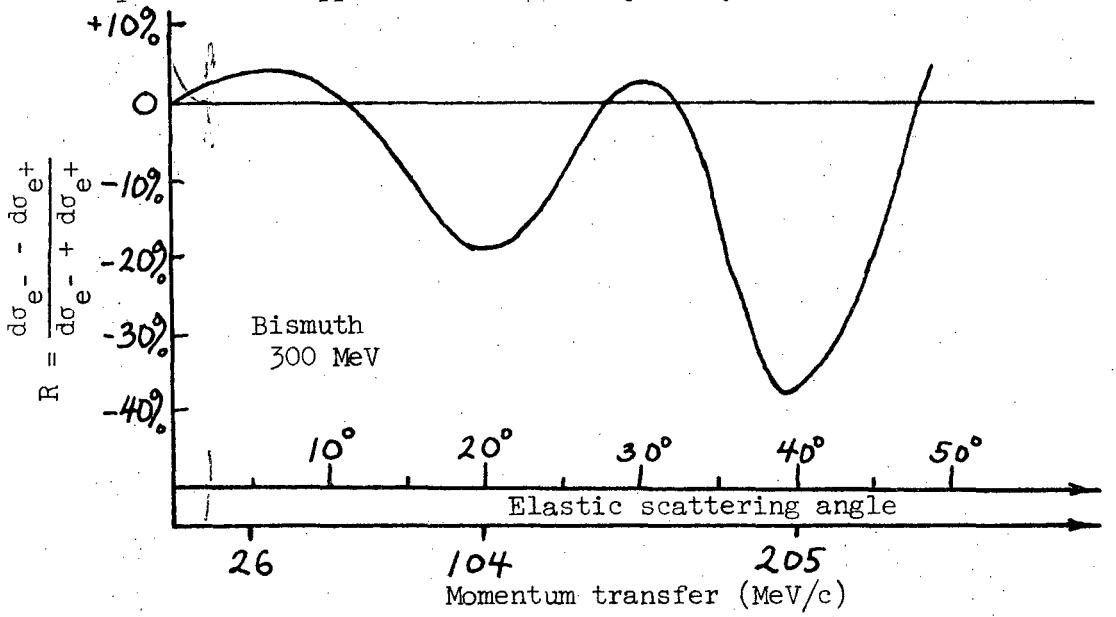

The Monte Carlo is used to see how the scattering differences reflect into the measured charge asymmetry. A rather crude technique is used; however, the effect is small, and no correction is necessary. The procedure is to put, for example, 104 MeV/c momentum tranfer scattering into the program for μ^+ and see what asymmetry results. A manyfold amplification of the real differential cross-section is needed to observe a finite asymmetry. The large angle scattering is folded in with the gaussian multiple scattering at each step through the lead. For the muon momentum

P at each step the scattering angle θ is found.

$$+q^2 = -(104 \text{ MeV/c})^2 = -2P^2(1-\cos\theta) \text{ (cm and lab frames almost same).}$$

It is something of a problem to know how to scale the 300 MeV data to another momentum. Drell and Pratt[27] give an approximate scaling formula for high energy.

$$d\sigma = d\sigma_{\text{Mott}} \, |F(q^2)|^2 \, (1 + \frac{Ze^2 G(q^2)}{P})$$

$$R = \frac{d\sigma_{e^-} - d\sigma_{e^+}}{d\sigma_{e^-} + d\sigma_{e^+}} = \frac{Ze^2 G(q^2)}{P}$$

The other term in $d\sigma$ is a second Born contribution. For purposes here it is only necessary to know that G is only a function of q^2, and the only other explicit P dependence is in $d\sigma_{\text{Mott}}$. The differential cross section at 300 MeV for $\sqrt{q} = -104$ MeV/c is scaled by the factor $(\frac{P}{300})^2$ which is the P dependence in $d\sigma_{\text{Mott}}$ assuming that the energy transfer to the lead nucleus is small. The approximate inverse P dependence of R is also put into the scattering probability as (300/P). The scattering probability for 104 MeV/c at each step through the lead is obtained from the cross section

$$d\sigma = A \times \frac{P^2}{300^2} \times \frac{300}{P} \times \left.\frac{d\sigma(q_o^2)}{d\Omega}\right|_{300 \text{ MeV } e^+} \times 2\pi \int_{\theta(80 \text{ MeV/c})}^{\theta(130 \text{ MeV/c})} \sin\theta \, d\theta$$

μ e universality is assumed.

The angular internal is taken as $20^\circ \pm 5^\circ$ to cover the entire region of the $\frac{(e^- - e^+)}{e^- + e^+}$ dip at 104 MeV/c. ($5^\circ \pm 3^\circ$ at 26 MeV/c and $40^\circ \pm 5^\circ$ at 207 MeV/c are used as approximate angular intervals.) A is the amplification factor used to make the asymmetry visible. The steps through the lead are fine enough so that the scattering probability is always small in a given step. In this way A is a true amplification of scattering probability and should represent a reasonably accurate amplification of induced asymmetry.

The theoretical paper also gives differential cross-sections on bismuth at 300 MeV for a Fermi shaped charge distribution.

θ	$\frac{d\sigma}{d\Omega}$ 300 MeV e^+ on bismuth
10°	$.437 \times 10^4$ mb/sr } from paper
20°	$.446 \times 10^2$ mb/sr } from paper
40°	$.666 \times 10^{-1}$ mb/sr } from paper
5°	5×10^4 mb/sr (extrapolated from above data)

For the parameters of the charge distribution, the reader is referred to the paper.

Angle at 300 MeV	Momentum transfer to μ^+	Induced asymmetry μ^+/μ^- (gaussian scattering for μ^-, (R = -100%))	A	Total Amplification =A x 100%/R(θ)
5°	26 MeV/c	$1.12 \pm .04$	50	1000
20°	104 MeV/c	$.92 \pm .03$	450	2250
40°	207 MeV/c	$.96 \pm .02$	3000	7500

The total amplification factor is an increase over A due to the ratio $R = \frac{\sigma e^- - \sigma e^+}{\sigma e^- + \sigma e^+}$ at 300 MeV. At 5° R = +5%, at 20° R = -20%, and at 40° R = -40%, reducing the asymmetry by factors of 20, 5, and 2.5.

The 26 MeV/c scattering is mostly washed out by the multiple scattering, and for even lower q^2 where the cross sections soar, the scattering is gaussian multiple scattering. Also, the phase space factor is so small that such an enormous cross section (2500 b/sr) is needed to see any effect on charge asymmetry. At the larger $\sqrt{q^2}$ = -207 MeV/c the real differential cross section is so small that too few muons are involved to cause trouble. The R ocillations continue at larger angles, but the cross section falls exponentially and even 100% differences between μ^+

and μ^- could cause no effect on the measured asymmetry.

No correction to the asymmetry is indicated by the above numbers. Even using the differential cross section at 15° which is ten times higher than at 20° leaves a substantial reduction factor.

$$\frac{\mu^+}{\mu^-} = \frac{-8\% \pm 3\%}{225} = -.04\% \pm .02\%$$

Also notice that the 26 and 104 MeV points go in the opposite direction and tend to cancel out.

About 2/3 of the induced asymmetry is due to stops in the absorber, and 1/3 is due to wrong decisions. The experimental data of Goldemberg, Pine and Yount indicate with large errors that the asymmetries R in the inelastic electron scattering on cobalt and bismuth are much smaller than for the elastic data.

The measured charge asymmetry is very sensitive to μ^+, μ^- range differences. A 1% less average dE/dx for μ^+ creates a positive asymmetry .7% ± .4%. A 1% more average dE/dx for μ^+ creates a negative asymmetry -.8% ± .4%.

Bellamy et al.[28], have measured dE/dx (in a .245" thick NaI(Tl) crystal) for muons from .5 GeV/c to 10.5 GeV/c, with an accuracy of ±1%. μ^+ and μ^- data points occur together at 3 GeV/c and 5 GeV/c. The difference between μ^+ and μ^- is known to better than the absolute 1% because most of the corrections are independent of sign. Assuming that systematics between μ^+ and μ^- observations are small, the data shows that at each of the points 3 GeV/c and 5 GeV/c, dE/dx for μ^+ and μ^- is the same with ±.5% error or better. The data however was not analysed as a $\mu^+\mu^-$ comparison and one should be a little cautious. Crispin and Hayman[29] find that the energy loss in plastic scintillator for μ^+ and μ^- is the same within 1%. The momentum range of the muons is 0.4 GeV/c to 100 GeV/c.

The effects of μ capture at end of range are small. The number of muons stopping within 25g/cm^2 from the last M counter is 5% of the real event rate. The μ decay electrons (maximum of 53 MeV/c) can travel up to 25g/cm^2. Only 1% decay in the 22 ns resolution of the (2ST)(M) coincidence. The decay e^+,e^- trigger differently due to positron annihilation.

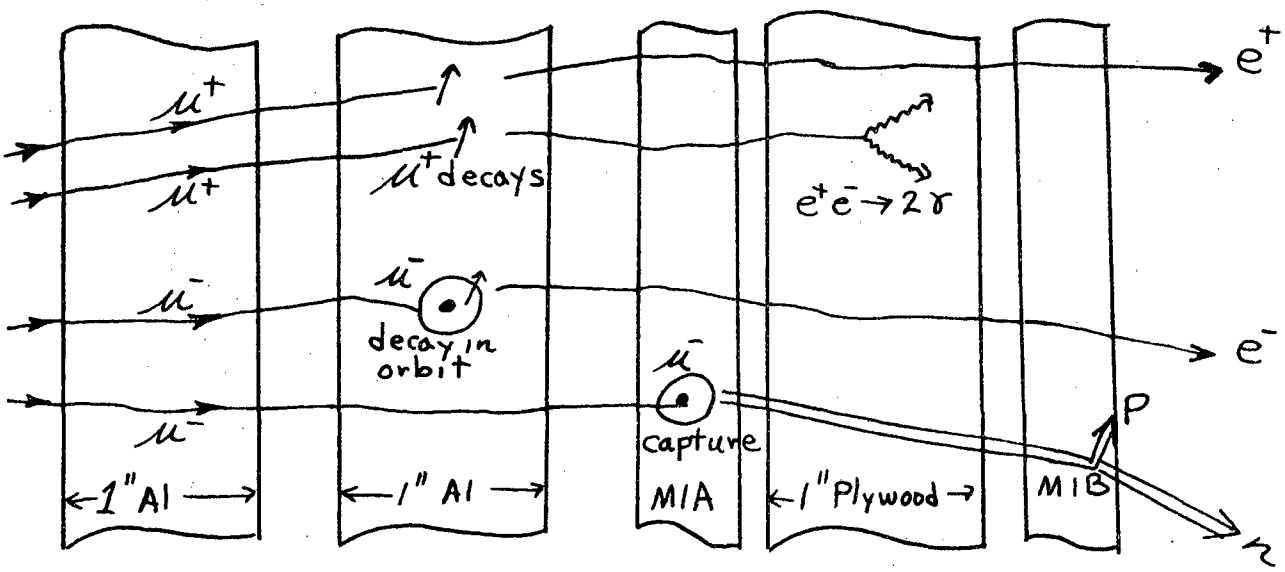

The μ^- capture times are 880 ms in aluminum and 2040 ms in carbon[30]. So only 2.5% of the μ^- capture in the 22 ns gate. The μ^- decay time is also suppressed in a bound state, but the effect is small for low Z materials. In aluminum the μ^- decay time is within 90% of the μ^+ time[31]. The correction is

(5% of event rate) x (1% decay) x (solid angle) x (energy spectrum)
x (asymmetry = Σ all effects = 20% max).

The positron annihilation is opposite the other effects and of same order. μ^- capture effects where a neutron is emitted are not important because capture would have to occur in the first M or the wood which is only 4 grams/cm^2. The carbon capture time is longer and recoil proton probability in last M is small. In the few percent cases where charged particles come out they have very short range. It is concluded that decay

effects are unimportant.

Barkas, Osborne, Simon, and Smith[32] observe a range difference $\langle R_{\pi^-} - R_{\pi^+} \rangle = 3.10 \pm 1.12\mu$ out of a range $\langle R \rangle = 95.7\mu$ in Ilford K-5 emulsion. The π's are in an energy region around 1.6 MeV or initial β about 0.15. The effect is also believed to account for a .1% $\pi^+\pi^-$ mass difference observed by range difference for initial β of .27[33]. The effect also explains an unaccounted for range difference between Σ^+ and Σ^- at initial velocity $\beta = 0.14$[34]. Σ^- looses less energy than Σ^+ at the same velocity. Heckman and Lindstrom[35] studied the effect by measuring dE/dx for π^+ and π^- in emulsion as a function of velocity in the region $.051 < v/c < .178$. Most of the range difference comes at the lowest velocities. It was also concluded that beyond $v/c = .14$ dE/dx difference between π^+ and π^- was less than 1%.

The effect can be explained at low momentum transfer where the electron does not sense the charge distribution of π or Σ. Classically it is just

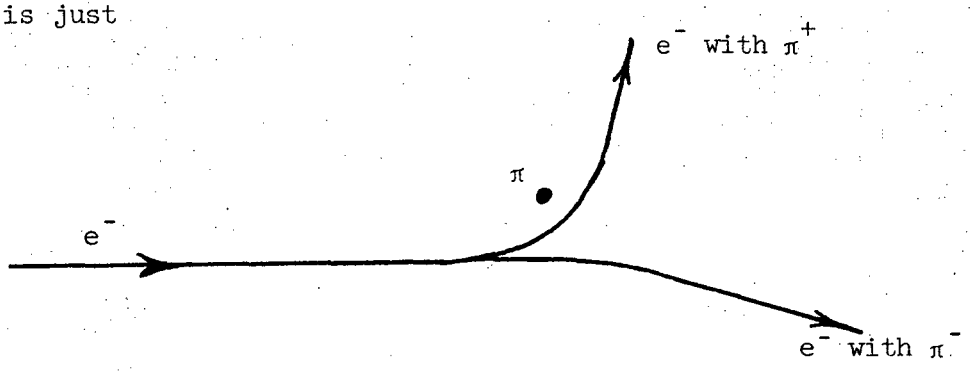

There is greater momentum transfer to the electron from π^+ than π^-. It is a 2 or more photon exchange and the difference is neglected in the usual first Born approximation dE/dx calculations. A less likely explanation for the observed range difference is the following. When the velocity of the muons becomes comparable to the inner electron orbits possible sign differences could arise. At the low velocities the inner shells are ionized by only large momentum transfers and are ineffective for stopping

the muons. If the μ^- saw more K shell electrons than μ^+ due to Coulomb scattering the μ^- would lose energy more slowly.

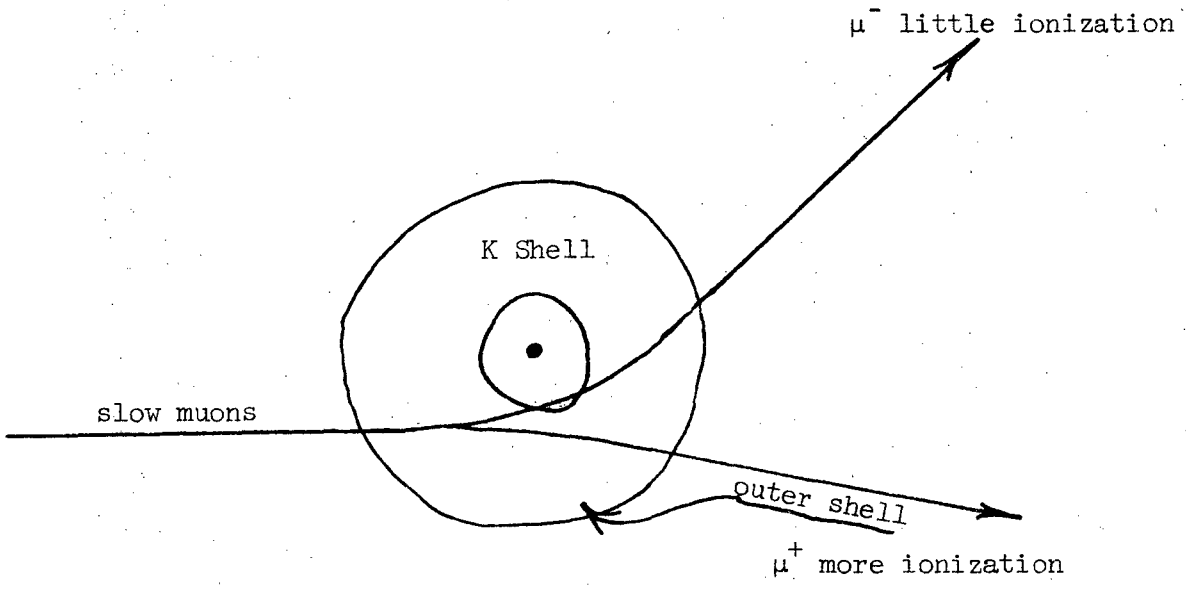

Both explanations predict indentical behavior for muons. For μ^+,μ^- and e^- some initial rise in $\sigma_{(e^-\mu^+)}$ over $\sigma_{(e^-\mu^-)}$ is expected. Using the π data, the asymmetry (μ^+/μ^-) is only .1% for the last 4.3 MeV of distance. The correction equals (.2% of real rate/gram/cm^2) x ($\frac{.2 \text{ grams}}{\text{cm}^2}$ range) x (.1% asymmetry), and is minute. The important thing is that the effect is 3% of the range at β = .15 and falls to .1% of range at β = .27.

Several authors[36,37,38] have calculated radiative corrections to μ e scattering. Two photon exchange and photon emissions must be considered to obtain differences between μ^+ and μ^-. Photon emissions must be considered due to interference between emission from the muon and emission from the electron. The calculations however cannot be used directly to

find dE/dx differences between μ^- and μ^-; for this purpose the calculations are incomplete in two respects. Firstly the momentum transfers in the regions numerically evaluated in the papers are higher than the low momentum transfers in the regions where the bulk of the ionizations occur. One paper[38] gives radiative corrections for scattering from 30° to 180° in the center of mass. Secondly only the relatively soft photon radiations which lie within the resolution of an elastic scattering experiment are calculated.

F. Anti-Counter Efficiency

The purpose of the anti-counter is to shield the apparatus from triggers coming from vertices inside the End Station or from the sides of the hole leading out of the End Station. Even though the nominal beam size is much smaller than the hole, the halo created by the collimator in the last magnet could hit the End Station wall. However, most of the single counts in the anti-counter are charged products from K_L° decay, and most of the vertices which might trigger the apparatus are $K_{\mu 3}$ decays.

The potential background that the anti-counter shields out was studied by placing the counter in coincidence instead of anti-coincidence. The trigger rate for the system was 45% of the normal trigger rate monitored with any singles rate, and the asymmetry in those triggers before the anti was $1.02 \pm .02$. The program finds a 50% trigger rate for $K_{\mu 3}$ decays

occurring in the region two decay lengths long upstream from the anti-counter position. The indication is that "events" originating before the anti are good $K_{\mu 3}$ decays.

The efficiency of the anti-counter was measured to be at least 96% with the voltage unintentionally set 300 volts lower than the normal running voltage. Assuming the 4% inefficiency, a correction of -.035% ± .035% would be needed. However, it is believed that the anti was very nearly 100% efficient throughout the run, and no significant correction will be made for anti-counter efficiency.

G. Pion Absorbtion

A fraction of the negative pions from $K_{\mu 3}$ decays are selectively absorbed by charge exchange before firing the S-counter. The effect decreases the measured charge asymmetry μ^+/μ^-. Reacting with free hydrogen atoms in the plastic end of helium bag, tape, or scintillator

$$\pi^- + P \rightarrow \pi^o n$$

are removed cleanly from the beam. The reaction would have to occur in the first 1/4 or less of the S counter thickness; otherwise the π^- ionization would trigger the discriminator.

The total material involved is

.025 g/cm^2	average length of He bag (no free protons)
.05 g/cm^2	polyethylene (CH_2) end of He bag, light shield into hut, tape on one side of S-counter.
.16 g/cm^2	1/4 thickness of scintillator (CH) (number variable depending on high volts on tube).

Another possible reaction is

$$\pi^- + {}_6C^{12} \rightarrow {}_5B^{11} + n + \pi^o$$

where the incoming π^- has reacted with and removed one proton. The boron is stable, and in cases where it stays together the π^- is effectively

eliminated even in scintillator. An absolute upper limit is obtained when all of the protons are considered free.

Kallen[39] has total charge exchange cross sections. Figure 20 gives the momentum spectrum of pions for all good triggers. Very few pions are in the low energy region where σ_T exchange is big. A good average over the pion spectrum would be 8 mb with at most 25% error.

$$N \sigma x = (34 \times 10^{22} \frac{\text{protons}}{\text{cm}^3} \text{ in plastic}) (8 \text{ mb}) (.2\text{cm plastic})$$
$$= .05\%$$

The protons in the He raise this the number less than 10%. The lower limit considering only free hydrogen is .01%. The value .05% is too large because the other six neutrons in the carbon are a shield for the protons, not allowing them to present their full 8 mb to the π^-. Also breakup of the $_5B^{11}$ in the scintillator will make a large pulse and easily count, whereas in the other plastic, fragments might not reach the scintillator.

π^+ and π^- should be equally effective in producing multibody neutral final states so that the much larger (20-30) mb inelastic cross section is no worry.

The conclusion is that a $+.03\% \pm .02\%$ correction be applied to the μ^+/μ^- asymmetry; to cover the incomplete knowledge of the problem an error is included.

H. Conclusion on Wrong Decisions

The asymmetry in wrong decisions is due to S-efficiency change and $\mu^+\mu^-$ scattering differences. Both of these effects are found to produce negligible bias in the final result through asymmetry in wrong decisions. Accordingly the asymmetry in the wrong decisions is taken to be anti-asymmetry, that is minus the measured asymmetry. From Table II page 21 wrong decisions are $3.0\% \pm .16\%$ of the trigger rate after accidentals subtracted.

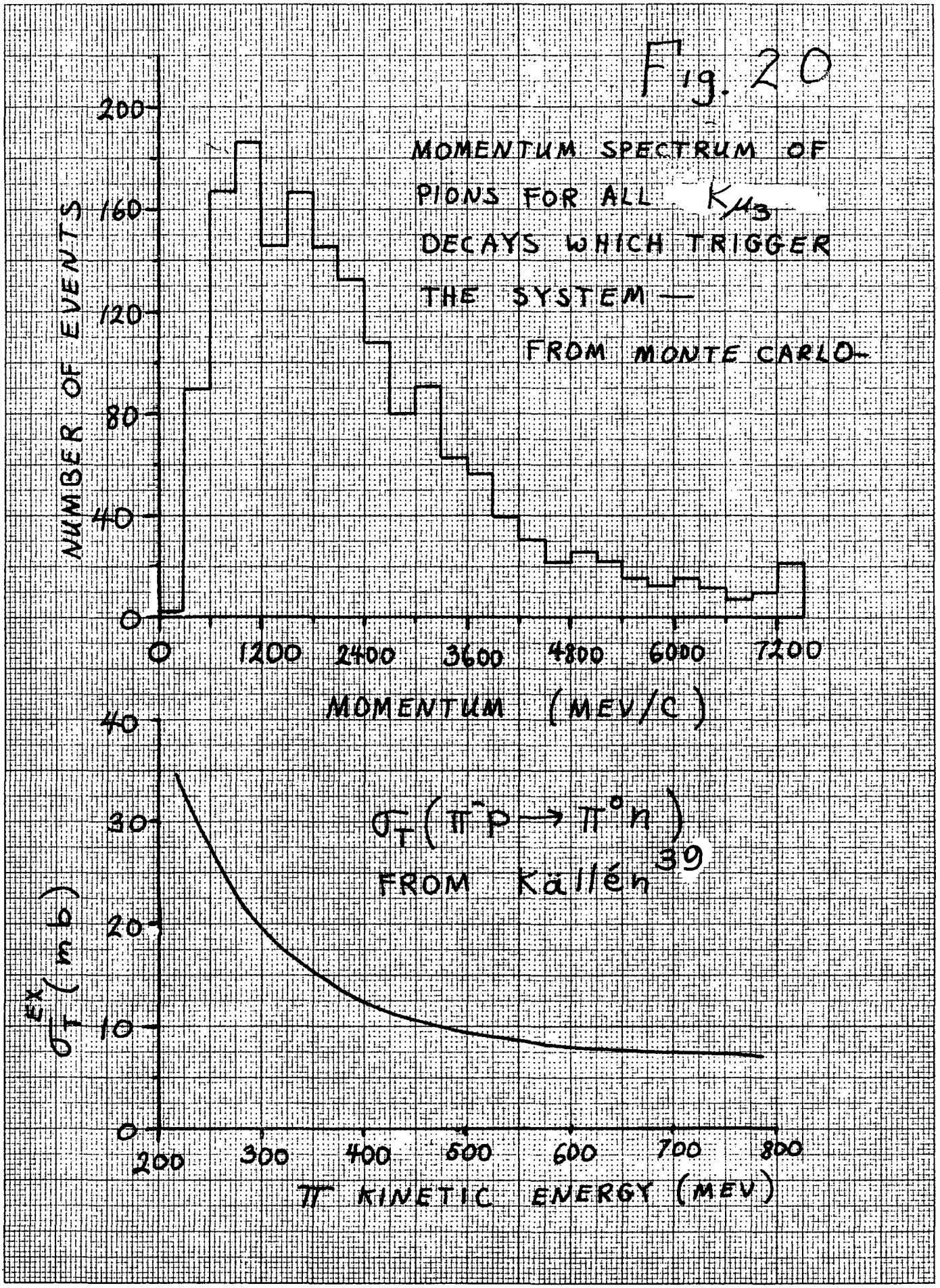
Fig. 20
MOMENTUM SPECTRUM OF PIONS FOR ALL $K_{\mu 3}$ DECAYS WHICH TRIGGER THE SYSTEM — FROM MONTE CARLO
NUMBER OF EVENTS
200
160
120
80
40
0
0
1200
2400
3600
4800
6000
7200
MOMENTUM (MEV/C)
$\sigma_T(\pi^- p \rightarrow \pi^0 n)$ FROM Källén [39]
σ_T^{EX} (mb)
40
30
20
10
0
200
300
400
500
600
700
800
π KINETIC ENERGY (MEV)

VII. BACKGROUND

A. Pion Decay in Flight

The effect of pion decays in flight is primarily a washing out of the charge asymmetry. The modes $K_L^o \to \pi\mu\nu$, $K_L^o \to \pi e\nu$, and $K_L^o \to \pi^+\pi^-\pi^o$ contribute by π decays 6.6% of the event rate.

The matrix elements and phase space have a large effect on the detection efficiency of the S-bank for the different modes.

Mode	Percent of all decays which miss S bank	Percent of all decays which fire same S counter	Detection efficiency of S-bank
$K_{\mu 3}$	32.1	16.3	51.6%
K_{e3}	47.3	10.9	41.8%
$K_{\pi 3}$	13.3	25.4	61.3%

The table is from Monte Carlo. The large transverse momentum available in K_{e3} makes many of the events miss the S bank entirely; although the transverse momentum separates the two particles, and both hit the same S less frequently. The $K_{\pi 3}$ on the other hand with smaller Q value rarely misses the S bank but the π and μ frequently hit the same S-counter.

After the S-bank it is the pion or its decay muon which proceeds on to the M bank to complete the trigger. The first step is to compute the trigger probability assuming all of the pions decay. As a simplification it is assumed that the small momentum in $\pi \to \mu\nu$ of only 29.8 MeV/c does not measurably change the trajectory of the muon from that of the parent pion. For the minimum transmission momentum of the absorber at 1600 MeV/c, 29.8 MeV/c applied transversely amounts to less than 2^o change in direction. A temporary assumption is that the pions all decay forward or that the momentum is not changed in the decay. Another way is to say that the π simply lost its strong interaction. The system has a detection efficiency

for such π triggering "events". This efficiency is the number of such triggers as a percent of the total number of K_L^o decays generated and is listed in second column of Table IV.

Even though K_{e3} has the lowest detection at the S bank, its pion has a higher average momentum, and more pions (or forward decay muons) have enough energy to penetrate the lead. The $K_{\pi 3}$ gets through the S bank easily but the π does not have enough momentum to penetrate the lead as often. Hence it turns out that the detection efficiency for each mode for 100% forward π decay is about equal as indicated in the Table.

Then for each of the "events" the probability that the pion actually decays is found. It is just

$$P = 1 - \exp\left(\frac{\text{travel distance} \times (m_\pi)}{307 \text{ (inches)} \times P_\pi}\right)$$

This probability P must be reduced due to the fact that decay muons have less momentum than the parent pion and sometimes have too little momentum to get through the lead.

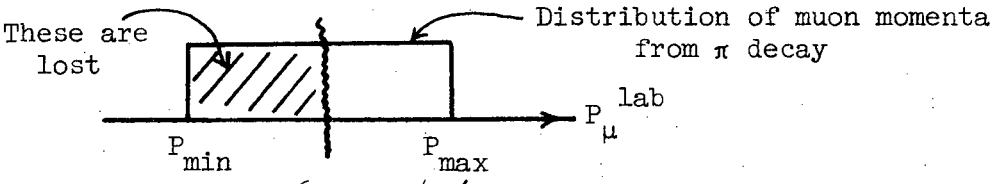

1600 MeV/c (or minimum transmission momentum at a given depth in the absorber)

The P's are summed up for all of the "events" and gives the percent of 100% forward π triggers which are real pion decays, column 3, Table IV. Account is made for absorption by all materials in the system and the travel distance is taken all the way into the absorber until the pion is absorbed by strong interactions.

To get the decay rates relative to real $K_{\mu 3}$ events multiply column 3 in Table IV by the following factor

$$\text{Factor} = \frac{(\text{Detection probability 100\% forward } \pi \text{ decay})(\text{Branching ratio})}{(\text{Detection probability of real } K_{\mu 3})(\text{Branching ratio } K_{\mu 3})}$$

Table IV. Study of pion decay in flight and correction for $\pi^+\pi^-$ cross section differences.

Mode	Branching Ratio	Detection efficiency assuming all pions decay forward	Total decay probability as a fraction of "π triggers"	π^+ cross section in Pb smaller by 20%	Decay probability in percent of muon triggers	Correction for 20% $\pi^+\pi^-$ cross section difference in lead	Comment
$K_L^o \to \pi\mu\nu$	28.1%	19.0%					Real events
$K_L^o \to \pi\mu\nu$	28.1%	25.5%	1.8%	1.01	2.4%	-.025%	π triggers
$K_L^o \to \pi e\nu$	37.7%	21.3%	1.6%	1.01	2.4%	-.025%	π triggers
$K_L^o \to \pi^+\pi^-\pi^o$	12.7%	19.8%	3.9%	1.01	1.8%	-.02%	Detection efficiency for one pion but probabilities doubled for π^+ and π^-
Total decay probability and correction for 20% smaller π^+ cross-section in lead					6.6%	-.07%	

For $K_{\pi 3}$ the probability that the π^+ and the π^- will both decay is very small. However the logic is set up in a way that both will be recorded. That is, the event trigger signal requires (2ST) plus at least one M firing. If more than one M fires, each will be scaled independently. The same effect occurs for $K_{\mu 3}$ where a π decay has a substantial chance of being accompanied by an energetic muon. This chance gives rise to a certain fraction of "doubles" or both pion and muon penetrating events. These events are observed in the sample pictures. As far as the data is concerned, the logic logs them just as if they were independent decays. In the program $K \to \pi\mu\nu$, where the "π triggers," is handled as an independent mode from $K \to \pi\mu\nu$ where μ triggers.

There is asymmetry in the group of decaying pions due to differential absorption of π^+ and π^-. After differential absorption more π^+'s than π^-'s might be present to decay. There is some pion absorption in the S counter bank and the thin plate chambers and with a considerable flight path before reaching the thick aluminum chambers, but the major effect is in the lead where the concentration of pions or their secondaries at a given depth can be different. Little differential absorbtion takes place in the aluminum chambers due to the arguments in the Appendix.

A rough estimate of asymmetry in the pion decay background can be made. The attenuation of pions is computed using the collision lengths found in Rosenfeld table[40]. The correlation between cross section and pion decay probability is obtained by changing the collision length by 20% and watching the change in the number of pion decays. The result for π^+/π^- in column 4 is obtained by putting in 20% less cross section for π^+ in lead. Less cross section means less attenuation and as a result more pion decays. A 1% asymmetry in pion decays is the result.

This 1% asymmetry gets scaled down by the ratio of measured $\pi^+\pi^-$ cross section differences to the 20% difference used in the calculation. Abashian et al.[41], find absorbtion cross section differences in lead.

Pion kinetic energy lab (MeV)	$\frac{\sigma(\pi^-) - \sigma(\pi^+)}{\sigma(\pi^+)}$
700	.050 ± .011
1100	.017 ± .012

1100 MeV or higher is an appropriate energy for pions entering the lead which also have a substantial chance of decay. Hence the asymmetry in π decays becomes

$$\left.\frac{\mu^+}{\mu^-}\right|_{\substack{\pi \text{ decay} \\ \text{in flight}}} = \frac{\pi^+}{\pi^-} = 1\% \times \frac{.017 \pm .012}{.20}$$

$$= .09\% \pm .06\%$$

This is the asymmetry in $K_{\pi 3}$. The $K_{\mu 3}$ will have anti-asymmetry, equal and opposite to the actual charge asymmetry. K_{e3} will also have anti-asymmetry. The $K_{\pi 3}$ contributes exactly as many π^+ as π^-.

In conclusion,

Pion decay in flight	$K_{\mu 3} = 2.4\% \pm 0.3\%$	Asymmetry	$-.89\% \pm .31\%$
	$K_{e3} = 2.4\% \pm 0.3\%$		$-.89\% \pm .31\%$
	$K_{\pi 3} = 1.8\% \pm 0.2\%$		$.09\% \pm .06\%$

B. Pion Penetration of Absorber

The Appendix contains all that is known about π penetration from this experiment. It is concluded that π penetrations leads to a background which is $(2.8 \pm .5\%)$ of the real $K_{\mu 3}$ rate. The number is not directly measured and contains some assumptions about momentum dependence of π penetration probability.

No useful conclusion is reached on the charge bias for the penetrations.

The $\pi^+\pi^-$ bias is a combination of differential penetration probability and asymmetry in π wrong decisions. It is exactly the same situation as for the muons and the muon wrong decisions. The final result includes only anti-asymmetry for the π^+/π^- charge bias. The arguments substantiating this assumption are presented in the Appendix, page **100**.

The only readily calculable penetration mechanism is K^+ associated production with $K_{\mu 2}$ decay, suggested to me by Robert Budnitz. The effect was calculated assuming K^+ production from the initial $\pi^\pm$. A fair fraction of the K^+ are forward, and when the μ^+ is also forward it can have enough energy to penetrate the remainder of the lead. The bias is small because most of the K^+ interact before having a chance to decay. The effect comes to .02% of the real $K_{\mu 3}$ rate and is 100% asymmetrical.

C. Interactions of Beam Particles

1. S-Counter Bank

Beam particles interacting in the S-counter bank can trigger the apparatus in the following way. One of the secondary particles can fire an adjacent S-counter, and another secondary can go on to trigger the M by either strong interaction penetration of the lead or decay to a muon.

The average decay probability in the decay volume for a K_L^o produced at the target and surviving the 12 inch lead γ converter is about 1%. The detection efficiency of the apparatus is 20% requiring 500 K_L/event or 1000 K-zeros transmitted by the 12" lead converter. Using the SLAC Users Handbook for relative K^+ to proton yields, neutral K's and neutrons production are about equal averaged over the neutral beam momentum spectrum. The numbers are crude considering that the beam goes through 12 inches of lead. So roughly 1500 K's and neutrons hit the apparatus for every event. (30% of the K_L's decayed but this amount is smaller than the accuracy of these estimates.)

Substantial asymmetry is possible in these interactions due to K^+ production. Reactions like

$$n + N_{ucleon} \rightarrow K^+ + (\Lambda, \Sigma, Y^*) + N_{ucleon}$$

$$n + C_{arbon} \rightarrow K^+ + (\Lambda, \Sigma, Y^*) + A \text{ final state of 12 Nucleons}$$

have no corresponding K^- reactions without production of additional baryons. Kaon charge exchange produces K^+ more often than K^- due to the extra proton in CH. The K^- has various inelastic channels not open to K^+; hence K^- attenuates faster resulting in more μ^+ than μ^- from $K_{\mu 2}$ decays. It is very unlikely that secondary π^+ and π^- cause much asymmetry either in decays or differential penetration. See Section VII-A.

S-interactions were studied by increasing the interaction probability with additional scintillator placed just upstream from the S-bank. Two inches of scintillator raised the trigger rate by 14% and three inches of scintillator raised the trigger rate 24%. Considering that some of the pions from good events are lost by interactions in the scintillator, it is estimated that the interactions of beam particles are contributing 19% and 32% to the trigger for the two runs. The overall asymmetries are $1.04 \pm .016$ and $1.07 \pm .025$ for 2" and 3" runs. Combining the data gives $1.23 \pm .07$ for the asymmetry in the interactions occurring in scintillator with both 2" and 3" runs together. The selective charge exchange absorbtion of π^- from good events is considered in the combination. See Section VII-G.

The fraction of the $K_{\mu 3}$ triggers caused by S-interactions cannot be found from these two experiments because the solid angle for 2S triggers is much different for vertices originating in front of the S-bank than for vertices inside an S-counter.

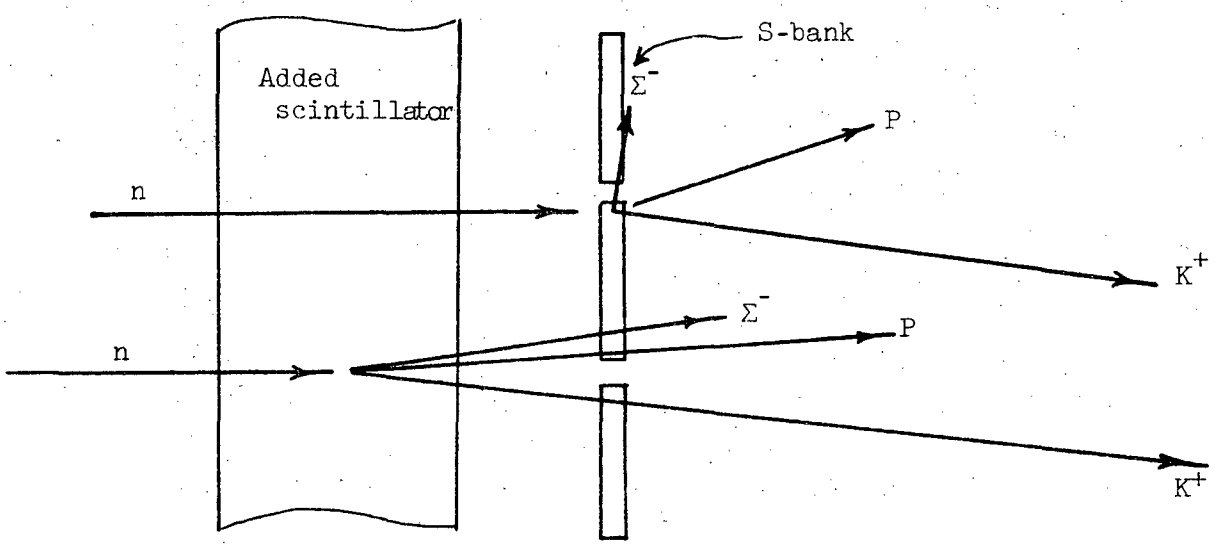

The rate used to make the S-interaction correction is taken from the sample picture analysis which finds 51 positive triggers and 47 negative triggers out of the 14 000 pictures or 0.7% ± .07% of the $K_{\mu 3}$ rate. The interactions are characterized by a vertex just downstream of the chamber with at least one wide angle particle. Most of the interactions are easy to distinguish from $K_{\mu 3}$ decays. It is harder when there are extra decay tracks in the S-chamber, and one has to establish that the "muon" is connected with the interaction (found by projection through the magnet) and not with the good decay.

2. Interactions in the Decay Region

The decay region is 110" long filled with helium. Neutron or Kaon interactions can occur in the He and produce possible bias. Interactions are possible in the last fraction of the anti-counter where the pulse is too small to fire the discriminator and also possible in the associated counter wrapping.

The helium is .055 g/cm^2, 1/4 thickness of anti-counter is .17 g/cm^2, and one side counter wrapping plus the anti-counter end of the helium bag is .044 g/cm^2. The end of the He bag at the S counter position was

included in the previous section.

The effect of interactions in these materials was studied by placing three two-inch slabs of carbon at distances of 30 inches, 48 inches and 64 inches from the S-counter bank. This arrangement produced an overall asymmetry of $\mu^+/\mu^- = 1.029 \pm .030$. The trigger rate did not change from the normal data taking rate, measured with the anti-counter as a monitor. However, the 25 grams/cm^2 of carbon represents attenuation of roughly 35% of the good $K_{\mu 3}$ trigger rate due to interaction of K's or the pion from $K_{\mu 3}$ decays. Therefore, interactions in the carbon are contributing the lost 35% to the trigger rate.

The carbon represents an effective increase of material in the decay volume by a factor of 80. But the anti-counter material is much less effective in producing triggers due to its great distance from S. The carbon produces half as many triggers per gram of material as the extra scintillator placed at the S-position. The effect is a loss of solid angle of the S-bank. The reduction factor is estimated as 200, giving $\frac{1}{200} \times 35\% = (.18 \pm .12)$ percent of the trigger rate as interactions with allowance for error in that reduction factor. The asymmetry in the carbon interactions calculates to be $\left.\frac{\mu^+}{\mu^-}\right|_{\text{carbon interactions}} = 1.07 \pm .10$.

D. Delta Rays

It is possible for a single muon to trigger the S-bank by producing a delta ray which curls around in the magnet fringe field to strike another S-counter.

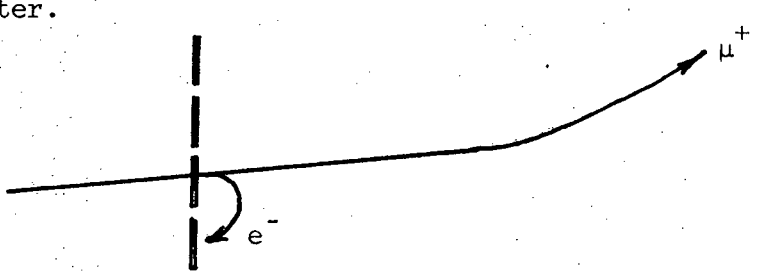

The effect is observed in the first thin plate chamber which records the circular path of the delta. The effect is also seen in the S-counter scalers discussed in Section VI-B. On the average 2.05 S-counters fire per event trigger, giving than 2.5% probability for the single particle process since the π and the μ both contribute to the .05 increase.

The probability is actually larger because 43% of the time the π and μ are in adjacent S-counters.

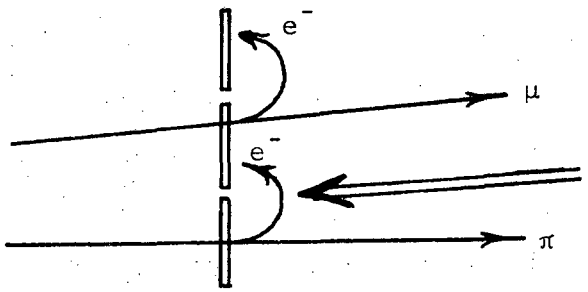

This δ-ray is not scaled

So 20% of the particles make redundent δ-ray counts assuming most of the δ-rays go into the adjacent counter. The δ-ray probability rises to 3.2% for a single particle to make a δ-ray which counts in another counter. In the 14 000 sample pictures, 124 δ-ray candidates are found. They are single muon tracks with 2 S-lights. About half have adjacent S lights and another 20% have the other light one counter away from the muon light. These δ-rays are not visible in the chambers because the chamber is 2.5 inches away from the counters. The remainder of the δ-ray candidates with larger counter separation are not all δ-rays because many of them do not show the δ in the chamber. They could be accidentals with a slow neutron or gamma. The δ-ray candidates, .89%, found by pictures over-estimates δ's in the above sense but also misses events which have a delta ray triggering the 2S requirement but also have an unrelated track within the long time resolution of the chambers. This extra track must roughly verticize and have a rough spatial coincidence with the S-light triggered by the δ-ray. The scanners could miss some of these.

The asymmetry of single muons was measured by requiring only 1S count. It was $\mu^+/\mu^- = 1.009 \pm .014$. It is expected that nearly all of these muons are from $K_{\mu 3}$ decays. So the actual number of δ-rays is unimportant for this correction since the muons have overall asymmetry very near the final answer. 0.89% δ-ray triggers is used for the first δ correction.

δ-rays can cause another effect.

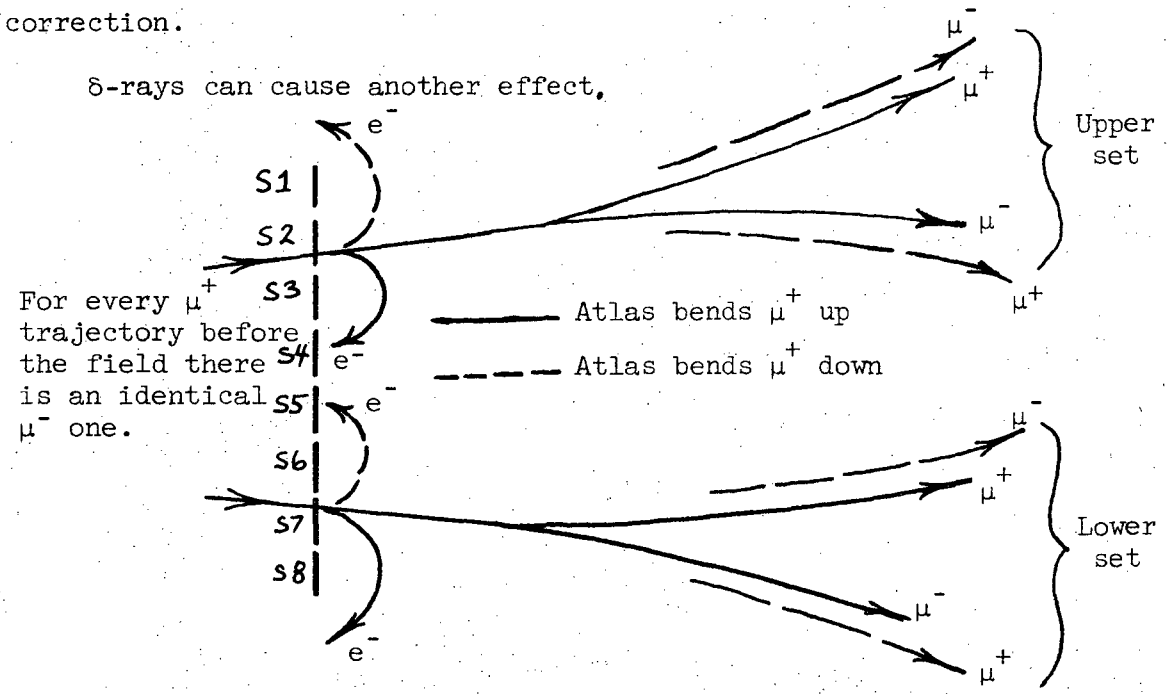

For Atlas Up only the upper set of μ^+,μ^- count since the e^- fires S4. The μ^+ being in an upper S-counter has a large chance of missing the M bank or better chance of stopping than the μ^-. The μ^- has a strong chance for a wrong decision. For Atlas Down only the lower set triggers, and again the μ^+ is lost more often, and the μ^- again makes the wrong decision. The result is a background which will have a net excess of μ^- for this effect.

An additional class of potential δ-ray triggers must be included for this effect.

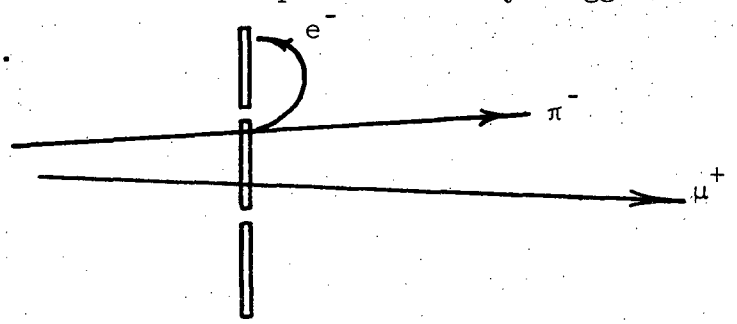

Delta rays can complete the trigger for cases where the π and μ hit the same S-counter. Also the delta ray probability is about doubled. The double $\pi\mu$ hits occur twice as often as the single μ configuration where π misses the S bank entirely. These additional triggers are potentially 50% of the real $K_{\mu 3}$ rate if all had δ-rays looping into another counter.

The analysis of this δ-ray unique sign effect is parallel to Section VI-B, considering a greater than 100% efficiency in S1 and S2 which goes away with field reversed but appears in S7 and S8. The only difference is that the asymmetries for muons through a particular S-counter are smaller than for the δ-ray effect because there is no pion complementation.

The film data showed that only S1, S2, and perhaps a few of the single μ's in S3 are operative in the unique sign mechanism. That is almost no delta rays could fly over the top of S1 from the S4 position. Half of the muon potentials in S2 and 20% of the potentials in S3 are used as well as all the potentials in S1. As with the S-treatment it is only necessary to look at the portion of the background which has asymmetry. Most of the δ-ray triggers produce as many μ^+ counts as μ^- counts and with real $K_{\mu 3}$ asymmetry.

Asymmetrical background due to:	Amount of background as percent of real $K_{\mu 3}$ rate	Asymmetry in background
1) losses of background muons by missing top or bottom of M bank	.95%	-100%
2) background muons making wrong decisions	.5%	+100%
3) background muons stopping in absorber	7%	-7%

These are losses in percent of all real triggers for the potential δ-ray events in the combination of S counters indicated above. The numbers

includes contribution of S6, S7, and S8. The addition of the contributions of the three asymmetrical backgrounds comes to a total .95% of all $K_{\mu 3}$ events with -100% asymmetry, i.e., only μ^- triggering. This would be the correction if all of the .95% muons or the accompanying pion made delta rays which triggered another S-counter. That δ-ray probability was 3.3%. The δ-ray probability must be weighted higher now since most of the potentials (63%) are double S hits; it goes from 3.3% to 5.4%.

A factor of 2 can be taken out of this probability. The δ's which sail over the top simply do not trigger in this analysis so far; whereas the 5.4% probability is mainly central particles which send δ's up or down into neighboring counters. So $.95\% \times \frac{5.4\%}{2} = .026\%$ of the $K_{\mu 3}$ trigger rate is background μ^-, and $\left.\frac{\mu^+}{\mu^-}\right|_{\text{observed}}$ appears smaller by .05%.

The +.05% correction to the measured charge asymmetry is an upper limit because many of the deltas that go over the top (and bottom) make a complete 360° and can still trigger another S-counter. A 1.2 MeV delta has the following trajectory in air.

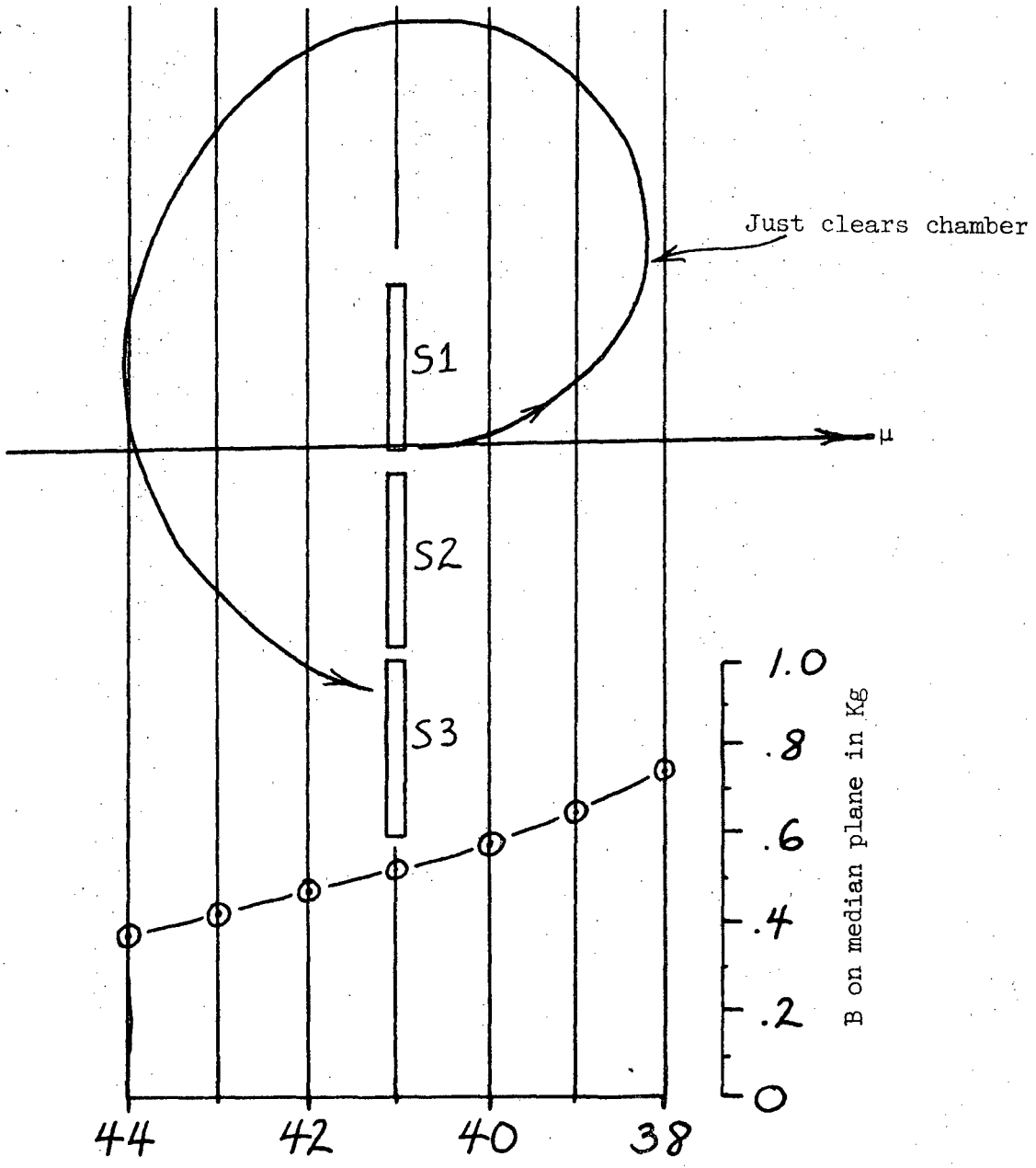

The more common lower momentum delta rays are more circular in shape but can still fire S2 after being produced in S1.

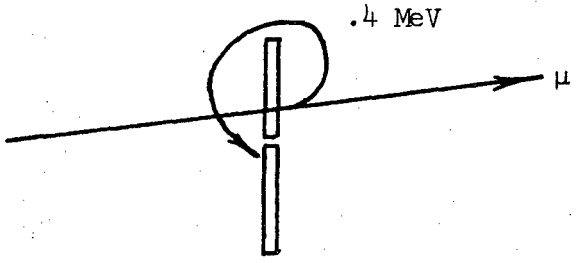

Higher momentum ones get attenuated rather quickly in the thin plate chamber particularly due to the very steep angles through the plates. The inclusion of the circular triggers increases the total number of delta ray triggers but reduces the asymmetry very quickly so that the correction becomes smaller. If all of the delta rays which sail over the top circled around and triggered in the back the correction would be zero.

The complete calculation is difficult to carry out; all that is learned so far is that an estimated correction of $+0.025\% \pm 0.025\%$ is necessarily added to the measured charge asymmetry.

VIII. RESULT

A. Instrumental Asymmetry

The experiment has instrumental asymmetries between opposing M pairs for one sign of field which can be explained by displacement of the S-bank. That is, in Table I consider for either sign of the field the ratios of counts M1/M8, M2/M7, M3/M6, and M4/M5. The 468 Kg-in. Data by itself has even larger instrumental asymmetries and will be used for illustration.

Table V is obtained for each polarity by taking the ratios of counts with the $K_{\mu 3}$ charge asymmetry subtracted out. One observation is that the apparatus is stable with field reversal. These large variations over the M bank can be reasonably explained without resorting to porosity in the lead or M inefficiencies. The section on S-counter efficiency describes how the M distribution is radically changed by the physical position of the muons at the S-bank. The conclusion of that section is that even though the distribution of counts in top and bottom M banks may be significantly different, very little asymmetry with all the M's together is generated for one sign of field.

The evidence for an S-counter effect producing the instrumental asymmetries is good. The 540 Kg-in. Data shows different apparatus asymmetry, indicating for example that there are no holes in front of M4. (M4/M5, 540 Kg-in Data is slightly negative). To have a nearly 8% difference between adjacent counters as in 468 Kg-in. Data means a hole would have to occur very near M4, in which case the 540 Kg-in. Data would have the same correlation. The overall Up and Down symmetry of the M bank is demonstrated by the number

$$\frac{\Sigma\ \text{M1}\rightarrow\text{M4 (both polarities)}}{\Sigma\ \text{M5}\rightarrow\text{M8 (both polarities)}} = \frac{393,254}{393,217}\ .$$

Table V. 468 Kg-in. Data, instrumental asymmetries between opposing pairs. $K_{\mu 3}$ charge asymmetry subtracted out.

Pair	Atlas Up	Atlas Down
M1/M8	1.008 ± .020	1.008 ± .020
M2/M7	.950 ± .011	.943 ± .011
M3/M6	.976 ± .009	.975 ± .009
M4/M5	1.054 ± .009	1.059 ± .009

Table VI. 468 Kg-in. Monte Carlo, apparatus asymmetry between opposing pairs.

Pair	Asymmetry μ^+/μ^-	Systematic error in $(1-\mu^+/\mu^-)$
M1/M8	1.032 ± .013	± 50%
M2/M7	.973 ± .005	± 50%
M3/M6	.991 ± .003	± 50%
M4/M5	1.026 ± .005	± 50%

The S-bank was measured to be displaced in the upward direction by one inch with respect to the beam vertical height projected from the accelerator by transit. The M bank was centered on that line to 1/4 inch. The program produces the large M pair asymmetries with such a displaced S bank. Table VI shows the result. The uncertainty in the program is that the small number of counts in S1 is not represented well by the program, and the amount has to be scaled from the 540 Kg-in. Data where the S distribution was measured. The S explanation is reasonable, and perhaps more importantly S counter effects or any other beam misalignment will produce very little net asymmetry for either sign of the field. Net asymmetry means that all of the Up counters M1 $\rightarrow$ M4 are added together and all of the Down counters M5 $\rightarrow$ M8 are added together as one counter.

If the magnetic field is not reversed, two answers are produced by this experiment.

	Atlas Up	Atlas Down
μ^+/μ^- =	$\frac{M1 \rightarrow M4}{M5 \rightarrow M8} = 1.0095$	$\frac{M5 \rightarrow M8}{M1 \rightarrow M4} = 1.0093$

The field reversed answer is the average of these.

$$\frac{\mu^+}{\mu^-} = 1.0094 \pm .0026$$

This is the answer after accidental substraction only.

B. Corrections Applied to Data

The several backgrounds contributing to the signal in the experiment have been found as a fraction of the raw data or the real data depending on whether they are found from experiment or from the Monte Carlo program. They have all been converted to a fraction of the real data, that is after all backgrounds have been subtracted. The measured or calculated asymmetry is also listed in Table VII. The correction to the charge asymmetry is

Table VII

Background	Amount of background as percent of real rate	Asymmetry in background in percent
M Accidentals	13.06 ± .04	.40 ± .66
S Accidentals	3.04 ± .02	1.00 ± 1.40
Pi Decays $K_{\mu 3}$	2.42 ± .30	-.89 ± .31
Pi Decays K_{e3}	2.36 ± .30	-.89 ± .31
Pi Decays $K_{\pi 3}$	1.82 ± .20	.09 ± .06
Anti Efficiency	.64 ± .38	2.00 ± 2.00
Delta Rays, Single Muon Events	1.03 ± .09	.90 ± 1.40
Decay Volume Interactions	.23 ± .15	7.00 ±10.00
S Interactions	.90 ± .09	23.00 ± 7.00
Pi Penetrations	2.80 ± .50	-.39 ± .12

Background	Correction to μ^+/μ^-
M Accidental	+.00056 ± .00127
S Accidental	-.00002 ± .00069
Pi Decays $K_{\mu 3}$	.00041 ± .00055
Pi Decays K_{e3}	.00042 ± .00056
Pi Decays $K_{\pi 3}$	.00016 ± .00050
Anti Efficiency	-.00006 ± .00033
Delta Rays (includes bias for unique sign effect)	.00026 ± .00049
Decay Volume Interactions	-.00013 ± .00030
S Interactions	-.00176 ± .00078
Pi Penetrations (includes $K^+ \rightarrow \mu^+$)	.00016 ± .00070
Other Biases	**Correction to μ^+/μ^-**
π^- Absorbtion	.00030 ± .00020
Wrong Decisions	.00066 ± .00115

shown for each background.

For an effect such as π decay or penetration which includes anti-asymmetry for the π triggers, the error on that included anti-asymmetry does not include the error on the effect itself.

When a background is subtracted account is made for the fact that the real data sample is reduced. Corrections are made one at a time, in each case reducing the data sample appropriately for the next correction. Hence the order of application has a slight effect on the individual corrections but not on the complete result. Wrong decisions are handled last by a separate formula since they have a doubling property, one wrong decision increases $|\mu^+ - \mu^-|$ by two.

The raw asymmetry

$$\frac{\mu^+}{\mu^-} = 1.0089 \pm .0021$$

is corrected to

$$\frac{\mu^+}{\mu^-} = 1.0098 \pm .0032 \ .$$

C. Conclusions

The parameter Reϵ, the amount $|K_1\rangle$ mixed with $|K_2\rangle$ to form the long lived $|K_L^o\rangle$, has been measured to be

$$\text{Re}\epsilon = (2.6 \pm .8) \times 10^{-3} \ .$$

The number represents further analysis of an earlier paper[42]. The difference from zero indicates the probability that CP is not a conserved symmetry, that is $|K_L^o\rangle$ is not an eigenstate of CP. The correction for the $\Delta S = -\Delta Q$ amplitudes is included in Reϵ[11].

Other interpretations of the charge asymmetry measurement are possible;

the results at SLAC and Brookhaven bear on theories where additional Kaons are introduced or where the usual quantum mechanical interpretation of the K^o-$\bar{K}^o$ system is modified. The Brookhaven number for Reϵ obtained from K_{e3} decays by Bennett, Nygren, Saal, and Steinberger[43] and Saal[44] (Ph.D. thesis) is Reϵ =$(1.16 \pm 0.30) \times 10^{-3}$ (quoted from Saal thesis). The number includes a previous correction for $\Delta S = -\Delta Q$ amplitudes, and the revised correction factor[11] raises Reϵ by 10%.

The extent to which the two values of Reϵ are in agreement is an indication that the charge asymmetry is uncorrelated with initial beam composition. μ e universality is assumed in comparing $K_{\mu 3}$ and K_{e3} charge asymmetry.

The result for μ^+/μ^- has left open the μ^+,μ^- range question to a time when further experimental or theoretical work is done. The ranges are probably equal to a high precision, but any variation found in the future can easily be applied to this result.

The result is given without any correction due to charge bias in pion penetrations. This assumption is based on rather firm arguments involving small (π^+,p) and (π^-,p) absorbtion cross section differences in aluminum above 1500 MeV. When additional experimental evidence is available on pion penetration a more positive statement can be made.

ACKNOWLEDGMENTS

My association with Kenneth M. Crowe through my time in graduate school has been most gratifying and rewarding. I look forward to future years of contact with him.

To all of the people at SLAC, Melvin Schwartz, Stanley Wojcicki, David Dorfan, James Enstrom, and David Raymond I owe a great debt, firstly for the opportunity to do thesis work on the experiment, and secondly for the chance to do physics with a very intuitive and stimulating group of people. They have also had enormous patience with me in the last two years.

I am fortunate to be at LRL where a second $K_{\mu 3}$ charge asymmetry experiment is being conducted at the Bevatron by Donald H. Miller, Robert Budnitz, William Ross, Robert McCarthy, and Jesse Brewer. It would have been very hard to maintain peak interest in the thesis for such an extensive period of time without the added stimulation of a new experiment. How many students are so lucky as to have five people thinking full time about problems directly related to their thesis subject? A new experiment for which ideas are still useful also relieves the frustration that every student feels about things he wishes were done during his experiment.

The contact with Donald Miller, who was also a member of the first experiment, has been a most extraordinary experience. Robert Budnitz has aided me considerably in the electromagnetics problems. Bill Ross has helped me orient myself as to what a thesis should or should not be. Robert McCarthy is the student on the second $K_{\mu 3}$ experiment who has given many useful criticisms, and is incidentally the person who will find the mistakes in this thesis. Jesse Brewer's remarkable sense of humor adds much to my days.

I value highly my acquaintance with Michael E. Zeller, who is always

willing to go with me the very root of any question by throwing aside the pretense of knowledge of things that we are all expected to know. It is at this level and only at this level that the real learning process progresses.

I thank Jim Enstrom for his efforts in helping investigate the muon range question. Special thanks go to Peter Berardo and James Bisterlich for many hours of discussions on errors and related physics questions. Patrick Craig has given insight into the question of what is "education".

Dennis Soon takes full credit for the success of the section on reconstructed events, for without his unique talent for unbiased, unparalled accuracy in measuring events the section would have honestly not been attempted. He also did many fine drawings.

My wife Sandy is waiting patiently to type this section as I finish. Having been a secretary to another physics group until two months ago she is far more aware than I am how to put unrelated thoughts in rough draft into a signed thesis. Among other sacrifices, she spent the first six months of our marriage alone, while I was off at SLAC, only seeing me on weekends. What I really want to say I can only say to her.

This research is supported in part by Air Force Office of Scientific Research and U. S. Atomic Energy Commission.

Appendix. SECONDARY EXPERIMENT WITH PION PENETRATION

The penetration of positive and negative pions has been checked with a charged particle beam which was introduced into the apparatus by inserting a third 18" x 72" magnet into the system shown on Fig. 4.

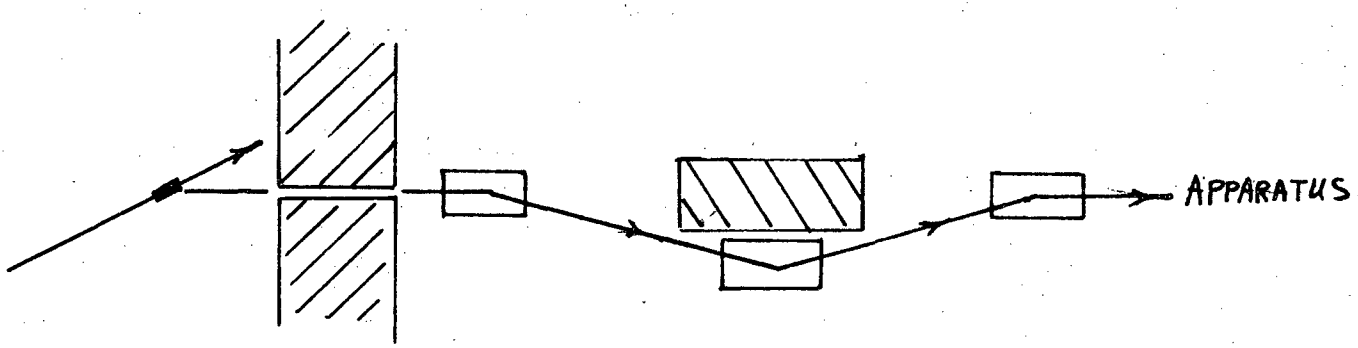

A beam was defined in the vertical direction by a pair of 2-inch counters separated by a distance of 14 feet. The momentum bite was defined by a pair of 6-inch wide counters separated by 10 feet. Thus a 2" by 6" charged particle beam is determined by a four-fold coincidence termed "π'incident". The momentum spectrum accepted by the "π-incident" telescope was measured by firing the spark chambers on "π-incident" trigger. The momentum of a beam particle is obtained by measuring the angle of bend in the Atlas magnet which was set at 540 Kg-inches. Figure 21, page 92 shows a broad spectrum peaked at 4.5 BeV/c with a $\Delta P/P$ of $\pm 10\%$ and a long low momentum tail. The positively and negatively charged spectra are lumped together but do not differ within the large statistical errors.

The muon component which is about 20% of the incident beam is identified with the following arrangement. The upper set of M-counters, M1, M2, M3, M4, were used as muon-anti counters and were placed behind an additional 18 inches of steel just in back of the lower set of M's. The range cutoff for muons is now increased from 1.55 BeV/c to about 2.4 BeV/c for straight through tracks. A "penetration" is a "π-incident" which made it through

the absorber, fired an M-counter but failed to penetrate the steel. A large bend in the magnet plus a net downward multiple scattering can cause a considerable number of muons in the low momentum tail of the input momentum spectrum to be stopped before reaching the muon anti and thus be counted as pion penetrations. Some events of this type can be seen in the pictures. So it is important that the composition of the beam does not change from plus to minus particles. That the overall composition is constant can be seen from the following numbers taken from the counter data.

$$\mu^+/\text{"}\pi^+\text{-incident"} = 0.1931 \pm .0016$$

$$\mu^-/\text{"}\pi^-\text{-incident"} = 0.1948 \pm .0016$$

Penetrations due to pion decay in flight within the lead are not measured in this supplementary experiment, and the effect is calculated in Section VII-A. Correcting the number of "π-incident" for the 20% muon component the pion penetration is as follows:

$$\gamma^+ \equiv \pi^+ \text{ penetrations}/\text{"}\pi^+\text{-incident"} = .01616 \pm .00045$$

$$\gamma^- \equiv \pi^- \text{ penetrations}/\text{"}\pi^-\text{-incident"} = .01614 \pm .00045$$

The thick plate spark chambers are used to find μ contamination in the π penetrations. The chambers were triggered on "π penetration" events; 535 unambiguous events of both sign particles are available for study. Out of this group 143 events show clear strong interactions in one of the three thick plate spark chambers. These events now serve as a calibration since the incident particles are definitely pions. 58 out of the 143 pions have one or more extra sparks in one of the two chambers not containing the visible strong interaction. Hence there is a probability of 61% ± 11% for seeing extra sparks due to strong interactions in any one of the three chambers. (61% = 58/143 x 3/2).

The extra spark technique is a strong handle in identifying incident

pions. To see this fact the delta ray probability must be found. A sample of known muons is available from the scanned and measured decays. In this group 23% ± 2.5% have one or more extra sparks in the last chamber. This situation gives a representative probability for production of delta rays in the chambers. So the probability is 23% ± 2.5% for extra sparks due to a delta in any one of the 3 chambers. It should be noted that the 61% ± 11% probability for incident pions contains the 23% delta ray probability and that the difference of these numbers is the strong interaction effect.

The analysis of the film data follows:

535 Total pictures with an unambiguous single entrace track, triggered on "π penetration".

17 Clear accidentals between the initial track and the M counter which fired --

143 Definite incident pions identified by a strong interaction in one of the three chambers --

20 Possible incident pions as seen by a possible vertex or strong interaction--

58 Out of the 143 pions, 58 contain one or more extra sparks along the track in one of the other two chambers.

2 The 58 is uncertain by +2 due to questionable sparks.

171 Out of the complement of the 143 pions, 171 show one or more extra sparks in one of the three chambers. The number includes the 20 possible pions.

11 Show questionable extra sparks.

Define

$N_0 = 535 - 17 = 518$

$N_R = 143 \pm 12 \, {}^{+20}_{-0}$ is number of definite incident pions.

$N_X = 171 \pm 13 \,^{+11}_{-0}\,^{+0}_{-20}$ is the number of pictures, not considered definite incident pions, with extra sparks. The 20 possible pions go into N_R or N_X.

$f_\pi = \left(\frac{58 \pm 7.6 \,^{+2}_{-0}}{143 \pm 12}\right) \times 3/2 = (61 \pm 11 \,^{+3}_{-0})\%$ is the probability that a pion will make an appearance somewhere in the chambers.

$f_\mu = (23 \pm 2.5)\%$ is the probability that a muon will make an appearance in the chambers.

These quantities are all independent except for the uncertain 20 possible pions. The identity of 143 of the 518 incident particles is established. The remainder are pions (N_π) and muons (N_μ).

$$N_0 - N_R = N_\pi + N_\mu$$

$$N_X = f_\pi N_\pi + f_\mu N_\mu$$

Total pions, $P = N_\pi + N_R$. $P = 366 \pm 65 \,^{+30}_{-35}$, or the fraction of pions in trigger is $F = (70.7 \pm 12 \,^{+5.5}_{-6.5})\%$. No correction is made for the 3% accidentals in the film data since the accidentals have already been subtracted out in the counter data. The reason that the accidental rate in the pictures is low is that pictures were selected to have only one entrance track.

So the π penetration number which is of interest is

$$\beta \equiv (70.7 \pm 12 \,^{+5.5}_{-6.5})\% \frac{\pi\text{-penetrations}}{\text{Picture (excluding accidentals)}}$$

$$\times \ (.016) \frac{\text{Triggers or pictures (excluding accidentals)}}{"\pi_{inc}"}$$

$$\times \ \left(\frac{1}{.806}\right) \frac{"\pi_{inc}"}{\text{Actual pions in beam}}$$

$$\beta = .014 \pm .0025 \,^{+.0010}_{-.0015}$$

A similar number α is the fraction of the muons in the beam which does not fire the muon anti-counter after the 18" of steel because of inefficiency, spaces in counters, or scattered and stopped in steel.

$$\alpha = .024 \pm 0.010 \begin{matrix} -.005 \\ +.006 \end{matrix} \quad \frac{\mu \text{ "Penetrations"}}{\text{actual muons in beam}}$$

To substantiate this analysis further arguments are made based on the momentum spectrums for the pictures analysed. Figures 21 through 25 are the spectrums under consideration. Figure 23 shows the spectrum of all of the pictures, that is particles which have fired the "π penetration" requirement. The hypothesis is that the right hand peak is made of incident pions with strong interaction penetrations and the left hand peak is composed of incident muons which have triggered "π penetration". The left hand peak penetrated with a high probability. It's momentum region which contains roughly 5% of the incident beam has 23% of the penetrations. Besides, the low momentum tail is nearly all decay muons from pions decaying in the 30 feet path from the last sweeping magnet; the size of the tail and its momentum interval is about right. The lowest momenta in the tail are muons which decayed backward in the center of mass of the pion. Muons in the momentum region from 1550 MeV/c up to 2300 MeV/c nearly all stop in the last 18" of steel. Due to multiple scattering muons extending up to about 2550 MeV/c have substantial chance of stopping in the steel. Moreover the low momentum muons can leak out the bottom of the steel and not hit the muon anti.

So most of the muon peak can be accounted for by pion decays before the apparatus. Another effect is pion decays in the magnet and inside the aluminum chamber before interacting. This process was calculated using the same pion decay programs described in Section VII-A. It accounts for only 20 of the 518 pictures because decay muons are antied out except

Fig. 21

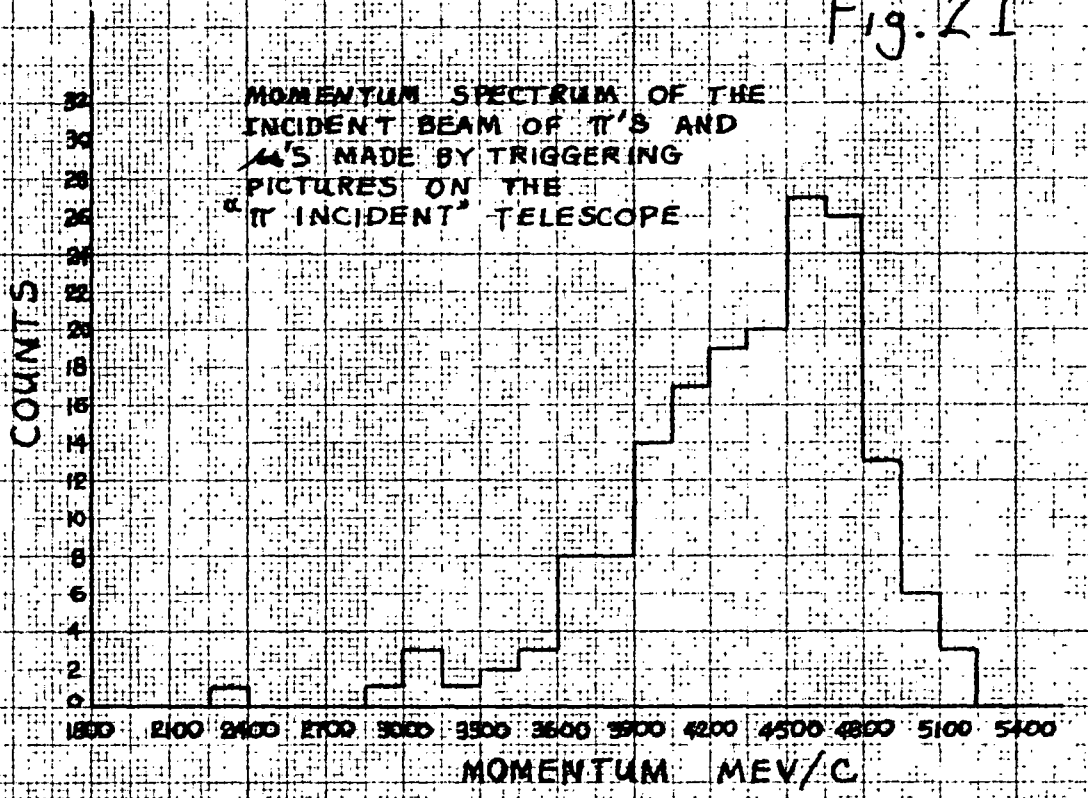
MOMENTUM SPECTRUM OF THE INCIDENT BEAM OF π'S AND μ'S MADE BY TRIGGERING PICTURES ON THE "π INCIDENT" TELESCOPE
COUNTS
0 2 4 6 8 10 12 14 16 18 20 22 24 26 28 30 32
1800 2100 2400 2700 3000 3300 3600 3900 4200 4500 4800 5100 5400
MOMENTUM MEV/C

Fig. 22

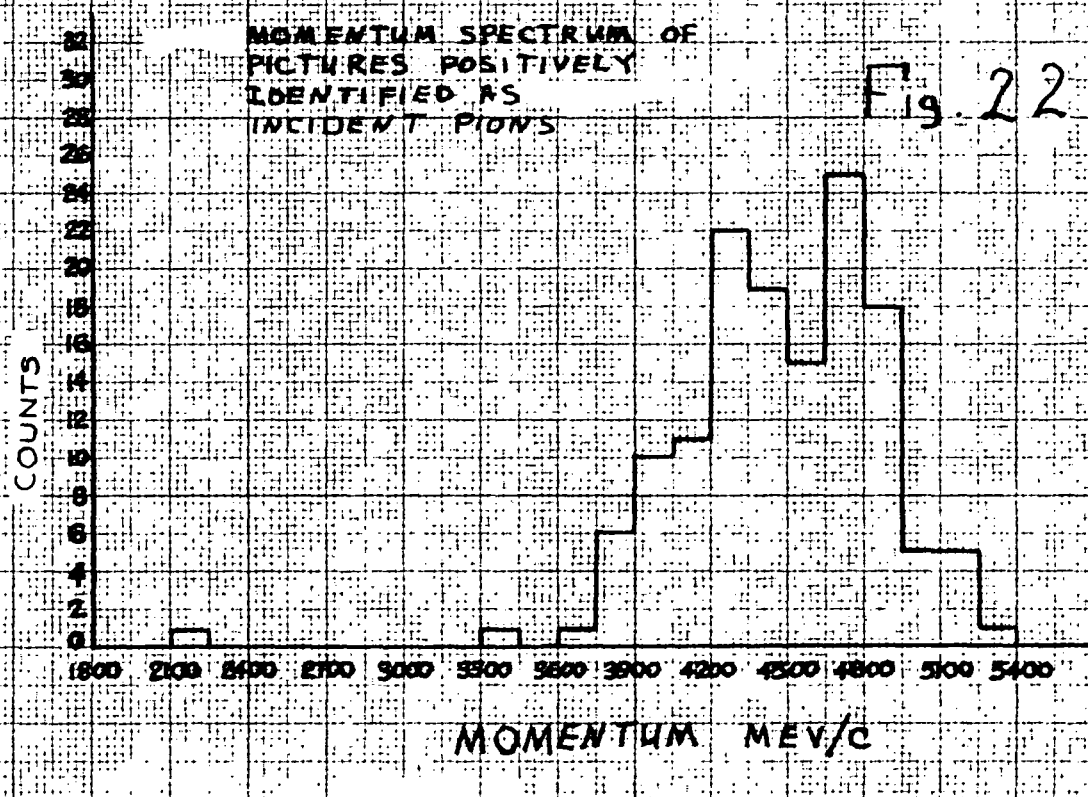
MOMENTUM SPECTRUM OF PICTURES POSITIVELY IDENTIFIED AS INCIDENT PIONS
COUNTS
0 2 4 6 8 10 12 14 16 18 20 22 24 26 28 30 32
1800 2100 2400 2700 3000 3300 3600 3900 4200 4500 4800 5100 5400
MOMENTUM MEV/C

Fig. 23

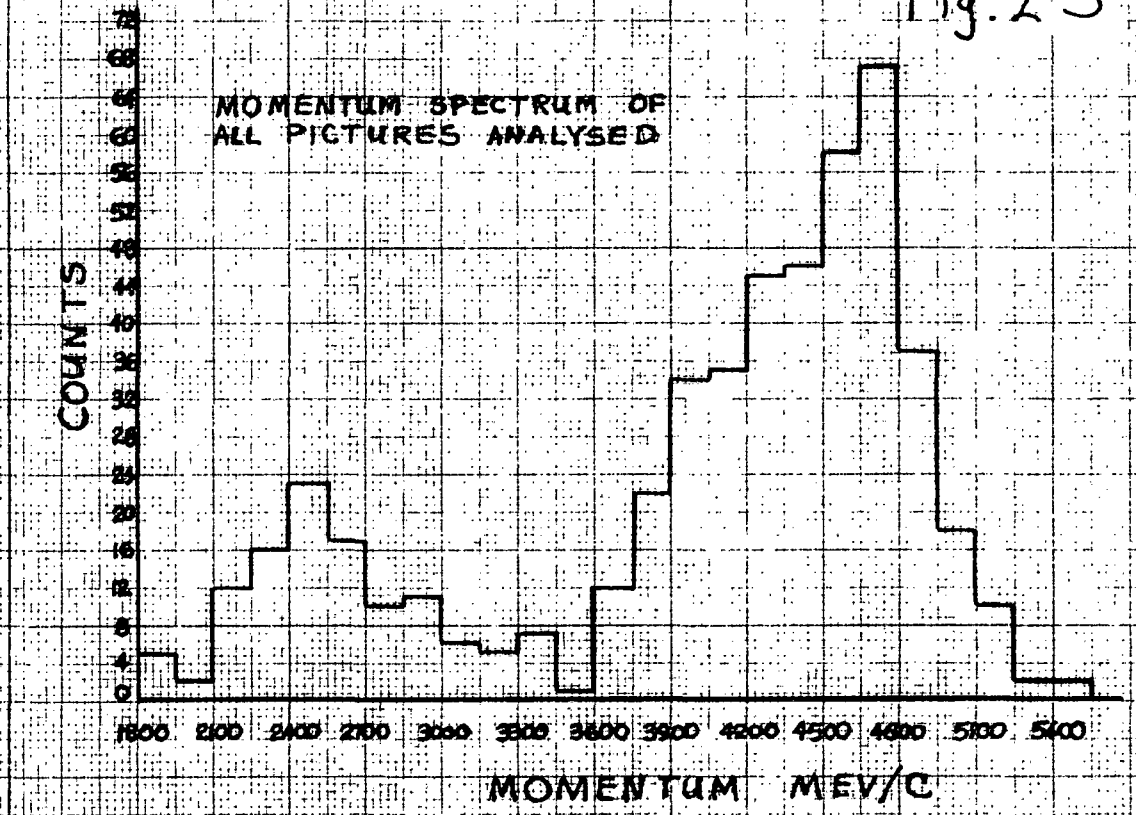
MOMENTUM SPECTRUM OF
ALL PICTURES ANALYSED
COUNTS
0
4
8
12
16
20
24
28
32
36
40
44
48
52
56
60
64
68
72
1800 2100 2400 2700 3000 3300 3600 3900 4200 4500 4800 5100 5400
MOMENTUM MEV/C

Fig. 24

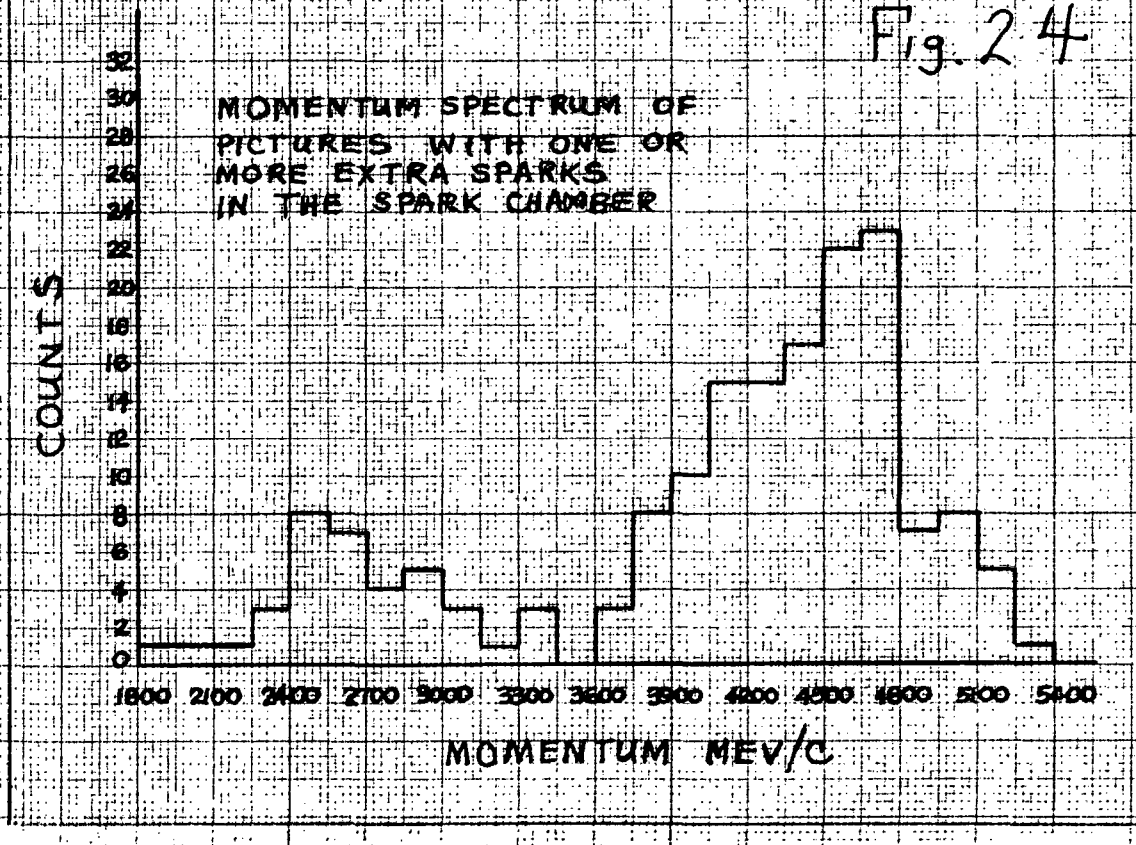
MOMENTUM SPECTRUM OF
PICTURES WITH ONE OR
MORE EXTRA SPARKS
IN THE SPARK CHAMBER
COUNTS
0
2
4
6
8
10
12
14
16
18
20
22
24
26
28
30
32
1800 2100 2400 2700 3000 3300 3600 3900 4200 4500 4800 5100 5400
MOMENTUM MEV/C

Fig. 25

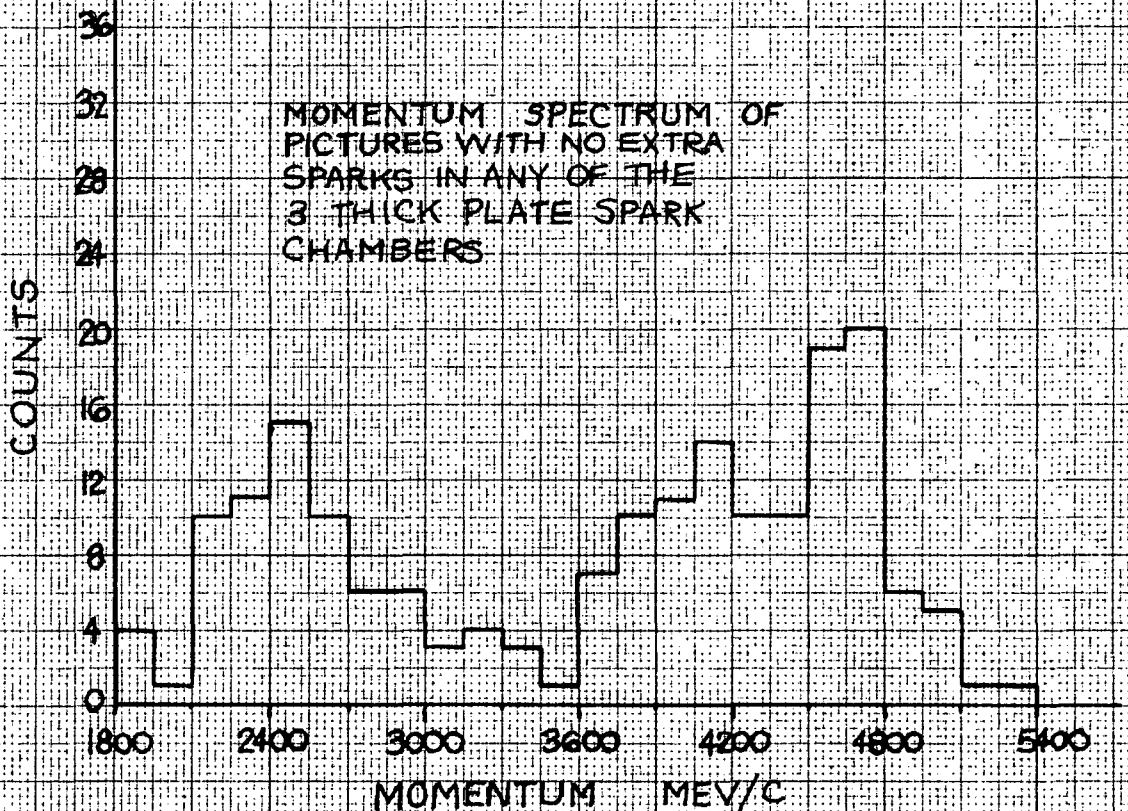
MOMENTUM SPECTRUM OF PICTURES WITH NO EXTRA SPARKS IN ANY OF THE 3 THICK PLATE SPARK CHAMBERS
COUNTS
36
32
28
24
20
16
12
8
4
0
1800
2400
3000
3600
4200
4800
5400
MOMENTUM MEV/C

when backward in cm.

The right hand peak in Fig. 23 could also contain some muon events due to spaces between the antis where high energy muons could pass without detection. A check on this possibility can be made. The film data predict the $\pi/(\pi+\mu)$ ratio for the samples in each of the Figs. 23, 24, and 25. Under the hypothesis that muons and pions are separated on the momentum plots a comparison is made.

Distribution	Film Data $\pi/(\pi+\mu)$	Momentum Plots $\pi/(\pi+\mu)$
All pictures analysed	$\frac{N_\pi+N_R}{N_\pi+N_R+N_\mu} = 0.7\pm.13$	Fig. 23: 0.77
Pictures with one or more extra sparks	$\frac{f_\pi N_\pi}{f_\pi N_\pi + f_\mu N_\mu} = 0.8\pm.1$	Fig. 24: 0.79
Pictures with no extra sparks	$\frac{(1-f_\pi)N_\pi}{(1-f_\pi)N_\pi+(1-f_\mu)N_\mu} = 0.4\pm.2$	Fig. 25: 0.6

The notation on page 90 is used to show the quantity which determines the pion to muon ratio for each distribution. These ratios are the only independent informations not already used in the calculations. The comparison is consistent, but leaves open the possibility of reducing the overall pion penetration by supposing spaces in the muon antis. However under the hypothesis a better upper limit is found for pions/(pions + muons). There is no reason to expect pions at low momentum in the left peak of Fig. 23. Figure 23 gives pions $0.77 \pm .02$ as fraction of pions in the total sample of 518 pictures giving a upper limit for β equals $.015 \pm .0005$).

If it is not clear, the reason there are two such distinct peaks in a momentum spectrum is restated. The idea is that the low momentum side

is backward muon decays making low energy muons which can either stop in the steel or scatter so much that they leak out the sides of the steel. The low edge of the peak cuts off because the lowest momentum pions in the primary beam which are responsible for those low muons are cutting off. The high edge of the muon peak cuts off because they are getting antied out. The high energy muons in the beam, whatever their origin, are another story. They can only be accepted in the trigger by spaces in the muon anti's. Spaces can lead to a substantial rate, but were unfortunately not recorded.

The momentum spectrum of the 143 identified pions is shown in Fig. 22. The event at 2100 MeV/c is of concern. It made a vertex in the second aluminum thick plate chamber before entering the lead; therefore it is conceivable that one of the secondary pions decayed to a muon before traversing the lead. If the vertex occurred in the last chamber after the lead it would be very hard to make a case for π penetration dropping off at low momentum.

A penetration β^+ for positive pions and a β^- for negative pions is defined; the asymmetry β^+/β^- will be found. β is the average of β^+ and β^- since positive and negative muons are taken together in the 535 pictures analysed. Assume that μ^+ and μ^- have the same "penetration" factor.

$$\mu^{\pm}_{\text{"penetrating"}} = \alpha\mu^{\pm}_{\text{Beam}}$$

$$\pi^{+}_{\text{"penetrating"}} = \beta^{+}\pi^{+}_{\text{Beam}}$$

$$\pi^{-}_{\text{"penetrating"}} = \beta^{-}\pi^{-}_{\text{Beam}}$$

The counters measured γ^+ and γ^-, the fraction of the total beam which triggers the π penetrate signal.

$$\gamma^+ = (\mu^{+}_{\text{pen}} + \pi^{+}_{\text{pen}})/(\mu^{+}_{\text{Beam}} + \pi^{+}_{\text{Beam}})$$

$$\gamma^- = (\mu^{-}_{\text{pen}} + \pi^{-}_{\text{pen}})/(\mu^{-}_{\text{Beam}} + \pi^{-}_{\text{Beam}})$$

The composition of the beam was measured and called δ^+, δ^-. It is the fraction of muons in the beam.

$$\delta^+ = \mu^+_{Beam}/(\mu^+_{Beam} + \pi^+_{Beam})$$

$$\delta^- = \mu^-_{Beam}/(\mu^-_{Beam} + \pi^-_{Beam})$$

Putting these things together,

$$\frac{\beta^+}{\beta^-} = \left(\frac{\gamma^+ - \alpha\delta^+}{\gamma^- - \alpha\delta^-}\right)\left(\frac{1 - \delta^-}{1 - \delta^+}\right)$$

The last factor is just the correction for the beam composition before it hits the lead. The $-\alpha\delta$ correction is the triggers from the μ beam; α is the fraction of the μ beam which triggers, and δ accounts for the 20% μ composition of the beam. Putting in the measured values,

$$\frac{\beta^+}{\beta^-} = 1.003 \pm .056 \ .$$

With the penetration probability $\beta = .014 \pm .0024 \ ^{+.0011}_{-.0013}$

$(.015 \pm .0005$ upper limit)

the story is complete for the spectrum in Fig. 21 centered at 4.5 BeV/c.

Figure 26 repeats Fig. 21 (now called curve A) plotted with the momentum spectrum (called curve B) for the pions that must be dealt with in the asymmetry experiment. Curve B is a composite of the three decay modes $K_{\mu 3}$, K_{e3}, and $K_{\pi 3}$ represented in their proper branching ratios. It shows the spectrum of events that would occur via pions triggering the M bank, assuming their strong interaction is turned off. This graph then represents the potential π penetration guys in the actual asymmetry experiment from all of the decay modes yielding pions. It has 3.7 times more events than the corresponding spectrum for good $K_{\mu 3}$ events. At 4.5 BeV/c π penetration is the following fraction of real $K_{\mu 3}$ events

$$3.7 \times \beta = .052 \pm .009 \ ^{+.004}_{-.005}$$

$(.056 \pm .002$ upper limit) .

A somewhat arbitrary procedure is used to find the average penetration over the complete pion spectrum (curve B). On Fig. 26 upper (curve C) and lower (curve D) limits are estimated with the boundary conditions that the penetration goes to zero at the ionization limit, that the upper limit hits the value 5.6% and at 4.5 BeV/c the lower hits 4.0% at 4.5 BeV/c, and that the penetration does not rise indefinitely at higher energy. There is no more justification for the last condition other than the idea that the multiplicity of secondary pions increases thereby dividing up the energy. When this estimated penetration probability is integrated over the pion spectrum (curve B) the average fraction of penetration in the data equals 2.8% ± .5%.

At this point information from the 14 000 sample pictures is introduced. 176 pion penetrations were found. These penetrations come from events with a good vertex in the S-chamber when a clear strong interaction occurred along the pion track somewhere in the thick plate chambers. These easily visible pions correspond to the positively identified pions in the secondary pion experiment. On page 90, the certain pions were 143 out of a total of 366 certain plus inferred pions, or 40%. 40% of (2.8% ± .5%) is roughly the same fraction which is observed in the sample pictures.

The interactions produce large momentum transfer compared to multiple scattering, and naturally mess up the sign determination (or anti-sign determination in this case). From the limited numbers the wrong decision rate in the observable pion cases is 30% ± 5% with 30% error on zero asymmetry in those wrong decisions. It is now clear that the purely measured correction for π penetration is inconclusive. The asymmetry for π penetrations goes from .3% ± 5.6% to .3% ± 18% due to the 30% error on π wrong decisions. For 2.8% penetration, the correction to the final answer would be 0 ± .5%.

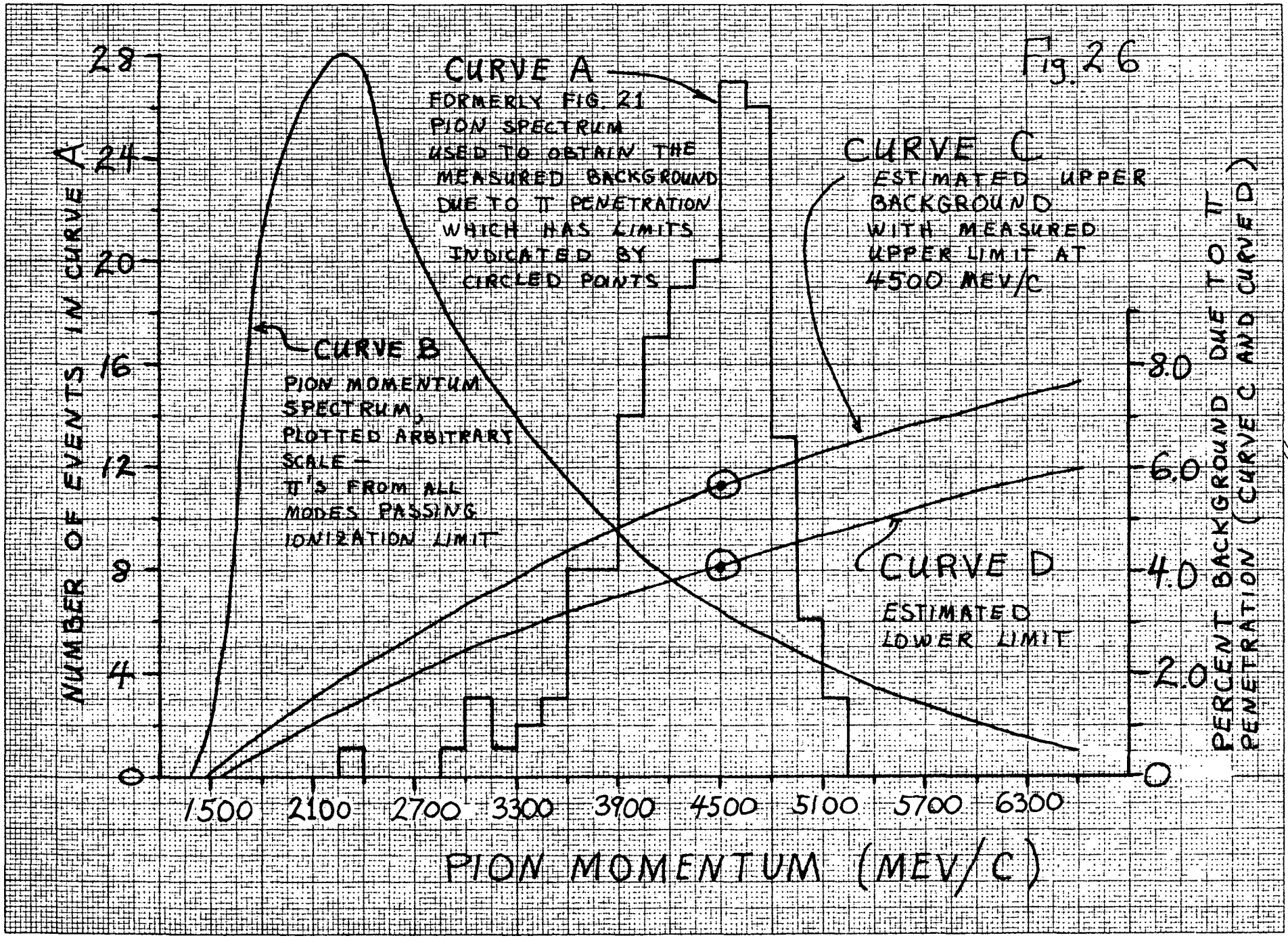
Fig. 26
CURVE A
FORMERLY FIG. 21
PION SPECTRUM
USED TO OBTAIN THE
MEASURED BACKGROUND
DUE TO π PENETRATION
WHICH HAS LIMITS
INDICATED BY
CIRCLED POINTS
CURVE B
PION MOMENTUM
SPECTRUM,
PLOTTED ARBITRARY
SCALE —
π'S FROM ALL
MODES PASSING
IONIZATION LIMIT
CURVE C
ESTIMATED UPPER
BACKGROUND
WITH MEASURED
UPPER LIMIT AT
4500 MEV/C
CURVE D
ESTIMATED
LOWER LIMIT
NUMBER OF EVENTS IN CURVE A
0
4
8
12
16
20
24
28
PERCENT BACKGROUND DUE TO π
PENETRATION (CURVE C AND CURVE D)
0
2.0
4.0
6.0
8.0
1500
2100
2700
3300
3900
4500
5100
5700
6300
PION MOMENTUM (MEV/C)

The $(2.8 \pm .5)$ percent π penetration background is used in calculating the final charge asymmetry. However the asymmetry in the penetrations is assumed zero on the following grounds:

1) Any asymmetry in penetration probability or in wrong decisions must be generated in the first few interaction lengths of absorber before the initial sign of the pion is forgotten. The first two interaction lengths of the absorber are traversed in aluminum. Judging from absorbtion cross differences in lead (see page 68 under π decays), it is certain that $\pi^+\pi^-$ differences in aluminum with nearly equal protons and neutrons is less than a percent averaged over all the pion momenta.

The point is that

$$\sigma(\pi^- p) \neq \sigma(\pi^+ p)$$

implies $\sigma(\pi^+ n) \neq \sigma(\pi^- n)$

but $\left.\begin{aligned}\sigma(\pi^- p) &= \sigma(\pi^+ n)\\ \sigma(\pi^+ p) &= \sigma(\pi^- n)\end{aligned}\right\}$ charge symmetry

So the extra neutrons have different π^+,π^- reactions. It is the relative density at the surface which produces transmission differences because the core absorbs nearly all the π's. The strongest evidence for zero asymmetry is the fact that the $(\pi^+ p)$, $(\pi^- p)$ differences get smaller as the energy goes up, and the largest differences have already subsided at the minimum transmission momentum of the absorber.

2) $\pi^+\pi^-$ can differ in the frequency of scatter, but the momentum transfer to the incident pion or to a secondary is relatively independent of sign. The spatial distribution of secondaries, which determines asymmetry in π wrong decisions, should therefore have the same shape for π^+ incident as for π^- incident. Additional absorbtion scatters for one sign pion (or its secondaries as long as the sign is remembered) changes the transmission probability to first order but changes the final spatial

distribution to second order. It is fortunate that the asymmetry in wrong decisions is less correlated with π sign than the overall transmission because the asymmetry in wrongs is very sensitive to changes in spatial distribution. The large gradient at the sign decision line times a large value of the distribution there can produce big fluctuations.

It is chosen to present the data without π asymmetry with the provision that if any significant pion penetration bias is found during subsequent $K_{\mu 3}$ asymmetry experiments, this result can easily be re-evaluated. The identical approach is taken for the muon range question where the data is also insufficient to make a conclusion.

REFERENCES

1. M. Gell-Mann and A. Pais, Behavior of Neutral Particles under Charge Conjugation, Phys. Rev. 97, 1387 (1955).
2. J. H. Christenson, J. W. Cronin, V. L. Fitch, and R. Turlay, Evidence for the 2π Decay of the K_2^o Meson, Phys. Rev. Letters 13, 138 (1964).
3. T. T. Wu and C. N. Yang, Phenomenological Analysis of Violation of CP Invariance in Decay of K^o and $\bar{K}^o$, Phys. Rev. Letters 13, 380 (1964).
4. J. S. Bell, J. Steinberger, Weak Interactions of Kaons, in Proceedings of the International Conference on Elementary Particles, Oxford 1965, p. 195.
5. T. D. Lee and C. S. Wu, Chapter 9: Decays of Neutral K Mesons, in Annual Review of Nuclear Science, Palo Alto, 1966, Vol. 16, p. 511.
6. H. A. Tolhoek, Status of Fundamental Symmetries and Weak Interactions, in Proceedings of the 1966 CERN School of Physics, Geneva, 1967, Vol. III, p. 1.
7. L. Caneschi and L. Van Hove, Selected Topics on Violation of CP Invariance, (Extended Version of Lectures for the Academic Training Programme May-June 1967, Geneva, 1967), Sept. 22, 1967.
8. See reference 4, p. 198.
9. L. J. Verhey, B. M. K. Nefkens, A. Abashian, R. J. Abrams, D. W. Carpenter, R. E. Mischke, J. H. Smith, R. C. Thatcher, and A. Wattenberg, Experimental Investigation of CP Violation in K_{e3}^o Decays, Phys. Rev. Letters 17, 669 (1966).
10. T. D. Lee, R. Oehme, and C. N. Yang, Remarks on Possible Noninvariance under Time Reversal and Charge Conjugation, Phys. Rev. 106, 340 (1957).
11. S. Bennett, D. Nygren, H. Saal, J. Steinberger, and J. Sunderland, K_S-K_L Regeneration Amplitude in Copper at 2.5 GeV/c and Phase of η_{+-}, Phys. Letters 29B, 317 (1969).

12. H. J. Lipkin and A. Abashian, A Possible Explanation for $K \rightarrow 2\pi$ Decays Without CP Violation, Phys. Letters 14, 151 (1965).

13. J. L. Uretsky, A Speculation Concerning the Apparent CP Violation in K^{o} Decay, Phys. Letters 14, 154 (1965).

14. H. J. Lipkin, Additional Experimental Proof of CP Nonconservation? Who Needs It?, Phys. Rev. Letters 22, 213 (1969).

15. D. I. Lalović, Is CP Invariance Violated?, Phys. Rev. Letters 21, 1662 (1968).

16. A. M. Boyarski, F. Bulos, W. Busza, R. Diebold, S. D. Ecklund, G. E. Fischer, J. R. Rees, and B. Richter, Yields of Secondary Particles from 18-GeV Electrons, SLAC Users Handbook, Stanford University, Stanford, California, (unpublished).

17. See SLAC Users Handbook, Section D.3, Estimates of Secondary-Beam Yields at SLAC, p. D.3-19, Stanford University, Stanford, California.

18. See reference 17, p. D.3-36.

19. A. D. Brody, W. B. Johnson, D. W. G. S. Leith, G. Loew, J. S. Loos, G. Luste, R. Miller, K. Moriyasu, B. C. Shen, W. M. Smart, and R. Yamartino, Production of K_2^{o} Mesons and Neutrons by 10-GeV and 16-GeV Electrons on Beryllium, Phys. Rev. Letters 22, 966 (1969).

20. M. Schwartz, The Strong Interaction of Strange Particles (Experimental), in Proceedings of the Annual International Conference on High Energy Physics, Rochester, 1960, p. 685.

21. G. Danby, J-M. Gaillard, K. Goulianos, L. M. Lederman, N. Mistry, M. Schwartz, and J. Steinberger, Observation of High-Energy Neutrino Reactions and the Existence of two Kinds of Neutrinos, Phys. Rev. Letters 9, 36 (1962).

22. L. Okun', in Annual Review of Nuclear Science, Palo Alto, 1959, Vol. 9, p. 89.

23. W. H. Barkas and M. J. Berger, Tables of Energy Losses and Ranges of Heavy Charged Particles, NASA SP-3013 (1964).

24. Bruno Rossi, High-Energy Particles (Prentice-Hall Inc., New Jersey, 1952), p. 31.

25. J. Goldemberg, J. Pine, and D. Yount, Scattering of 300-MeV Positrons from Cobalt and Bismuth, Phys. Rev. 132, 406 (1963).

26. R. Herman, B. C. Clark, and D. G. Ravenhall, Scattering of Electrons and Positrons by Cobalt and Bismuth: Calculations, Phys. Rev. 132, 414 (1963).

27. S. D. Drell and R. H. Pratt, Extrapolation to Cuts and the Scattering of Electrons and Positrons, Phys. Rev. 125, 1394 (1962).

28. E. H. Bellamy, R. Hofstadter, W. Lakin, J. Cox, M. Perl, W. Toner, and T. F. Zipf, Energy Loss and Straggling of High Energy Muons in NaI(Tl), Phys. Rev. 164, 417 (1967).

29. A. Crispin and P. J. Hayman, Ionization Loss of Muons in a Plastic Scintillator, Proc. Phys. Soc. 83, 1051 (1964).

30. A. O. Weissenberg, Muons (North-Holland Publishing Co., Amsterdam, 1967), Chap. III, p. 160.

31. See reference 30, Chapter III, p. 174.

32. W. H. Barkas, W. Z. Osborne, W. G. Simon, and F. M. Smith, Range Difference Between Positive and Negative Pions in Emulsion, UCRL-11518, June 1964.

33. W. H. Barkas, W. Birnbaum, and F. M. Smith, Mass-Ratio Method Applied to the Measurement of L-Meson Masses and the Energy Balance in Pion Decay, Phys. Rev. 101, 778 (1956).

34. W. H. Barkas, J. N. Dyer, and H. H. Heckman, Resolution of the Σ^- Mass Anomaly, Phys. Rev. Letters 11, 26 (1963).

35. H. H. Heckman and P. J. Lindstrom, Stopping-Power Differences Between Positive and Negative Pions at Low Velocities, Phys. Rev. Letters 22, 871 (1969).

36. K. E. Eriksson, Radiative Corrections to Muon-Electron Scattering, Nuovo Cimento 19, 1029 (1961).

37. A. I. Nikishov, Radiative Corrections to the Scattering of μ Mesons on Electrons, Soviet Physics JEPT 12, 529 (1961).

38. K. E. Eriksson, B. Larsson, and G. A. Rinander, Radiative Corrections to Muon-Electron Scattering, Nuovo Cimento 30, 5992 (1963).

39. Gunnar Källén, Elementary Particle Physics (Addison-Wesley Publishing Co., Inc., Massachusetts, 1964) p. 74.

40. N. Barash-Schmidt, G. Conforto, A. Barbaro-Galtieri, L. R. Price, M. Roos, A. H. Rosenfeld, P. Söding, and C. G. Wohl, Review of Particles Properties, UCRL-8030, January 1969.

41. A. Abashian, R. Cool, and J. W. Cronin, Neutron and Proton Distributions in Pb, Phys. Rev. 104, 855 (1956).

42. D. Dorfan, J. Enstrom, D. Raymond, M. Schwartz, S. Wojcicki, D. H. Miller, and M. Paciotti, Charge Asymmetry in the Muonic Decay of the K_2^o, Phys. Rev. Letters 19, 987 (1967).

43. S. Bennett, D. Nygren, H. Saal, J. Steinberger, and J. Sunderland, Measurement of the Charge Asymmetry in the Decay $K_L^o \to \pi^{\pm} + e^{\mp} + \nu$, Phys. Rev. Letters 19, 993 (1967).

44. H. J. Saal, Charge Asymmetry in K_{e3} Decay, (Ph.D. thesis), Nevis-169, April 1969.

TECHNICAL INFORMATION DIVISION
LAWRENCE RADIATION LABORATORY
UNIVERSITY OF CALIFORNIA
BERKELEY, CALIFORNIA 94720